

Norwegian University of Life Sciences
Faculty of Veterinary Medicine
Department of Preclinical Sciences and Pathology

Philosophiae Doctor (PhD)
Thesis 2022:20

Characterization of teleost pituitary cell types using single-cell transcriptomics (scRNA-seq)

Karakterisering av celletyper i hypofysen
til benfisk ved bruk av enkeltcelle
transkriptomikk (scRNA-seq)

Khadeeja Siddique

Characterization of teleost pituitary cell types using single-cell transcriptomics (scRNA-seq)

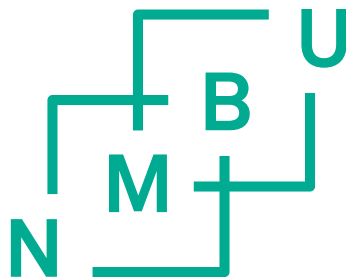
Karakterisering av celletyper i hypofysen til benfisk ved bruk av enkeltcelle transkriptomikk (scRNA-seq)

Philosophiae Doctor (PhD) Thesis

Khadeeja Siddique

Norwegian University of Life Sciences
Faculty of Veterinary Medicine
Department of Preclinical Sciences and Pathology

Ås (2022)



Thesis number 2022:20
ISSN 1894-6402
ISBN 978-82-575-1895-0

“Patience ensures victory”

Hazrat Ali Ibn Abi Talib A.S

**Dedicated to my parents, family and the women in Pakistan who are working hard
for their career.**

Table of Contents

List of figures.....	vii
List of tables.....	viii
Supervisors.....	ix
Acknowledgements.....	x
List of publications	xii
Abstract	xiii
Sammendrag	xiv
1. Introduction.....	1
1.1. General background.....	1
1.2. Model organisms.....	1
1.2.1. Medaka as a model organism.....	2
1.3. The endocrine system	3
1.3.1. The hypothalamus-pituitary-gonad (HPG) axis.....	4
1.3.2. The pituitary gland.....	5
1.3.2.1. Pituitary morphology	6
1.3.2.2. Pituitary cell types.....	7
1.4. Sequencing approaches.....	8
1.4.1. First generation sequencing	8
1.4.2. Second generation sequencing.....	9
1.4.3. Third generation sequencing.....	10
1.4.4. Applications of NGS.....	10
1.5. Transcriptomics.....	10
1.5.1. RNA sequencing (RNA-seq)	10
1.5.2. Single-cell RNA sequencing (scRNA-seq).....	12
1.5.2.1. Timeline of scRNA-seq	12
1.5.2.2. Droplet-based cell capture	14
1.5.2.3. Unique Molecular Identifiers.....	15
1.5.2.4. Technical noise in scRNA-seq.....	16
1.5.2.4.1. Dropouts.....	16
1.5.2.4.2. Batch effects.....	16
1.6. Aims and objectives.....	16
2. Methodological considerations	19

2.1.	Experimental design.....	19
2.1.1.	Medaka.....	19
2.1.2.	Sampling and isolation of cells for single-cell RNA sequencing	19
2.2.	10x Genomics Chromium technology	19
2.2.1.	10x Genomics library preparation	20
2.2.2.	Single-cell sequencing	21
2.3.	Bioinformatic analysis	21
2.3.1.	Cell Ranger	21
2.3.1.1.	Reference genome and annotation	21
2.3.2.	Initial data analysis	23
2.3.3.	Secondary analysis.....	23
2.3.3.1.	Quality control (QC).....	24
2.3.3.2.	Normalization	24
2.3.3.3.	Feature selection	24
2.3.3.4.	Clustering.....	25
2.3.3.4.1.	Principal component analysis (PCA)	25
2.3.3.4.2.	Uniform manifold approximation and projection algorithm (UMAP).....	25
2.3.3.5.	Cell type assignment.....	26
2.3.3.5.1.	Subclustering.....	26
2.3.3.6.	Integration of both datasets.....	26
2.4.	Quantitative polymerase chain reaction.....	26
2.5.	Fluorescence in situ hybridization (FISH).....	28
2.5.1.	RNAscope	29
2.5.2.	Image analysis.....	30
2.5.3.	Volumetric analysis of cell types.....	30
2.5.4.	3D atlas	30
3.	Results – summary of articles	32
3.1.	Paper I: characterization of medaka pituitary cell types.....	32
3.2.	Paper II: medaka pituitary 3D atlas	32
3.3.	Paper III: classification of prolactin populations	32
4.	General discussion and implications.....	35
4.1.	Characterization of the pituitary gland	35
4.1.1.	One cell type-one hormone hypothesis.....	36
4.1.2.	Reproducibility of scRNA-seq data	37
4.2.	Characterization of prolactin populations.....	37
4.3.	3D atlas of the teleost pituitary	38
4.3.1.	Sexual dimorphism	39
5.	General conclusions	41

6. Future perspectives	43
7. References.....	46
8. Appenndix: Paper I-III.....	66

List of figures

Figure 1.1: Phylogenetic tree of medaka and five other model fishes.....	2
Figure 1.2: The hypothalamus-pituitary-gonadal (HPG) axis.	4
Figure 1.3: Teleost pituitary.....	6
Figure 1.4: Representation of the evolution of sequencing technologies.	9
Figure 1.5: Comparison among bulk and single-cell RNA.....	12
Figure 1.6: Timeline of scRNA-seq protocols and advancements in technologies.	14
Figure 2.1: The 10x Genomics platform.....	20

List of tables

Table 1.1: Summary of scRNA-seq methods and their specificity.....	13
Table 2.1: Genome annotation adjustments.....	22
Table 2.2: Statistics of Cell Ranger.	23
Table 2.3: Primer sequences used to analyze the mRNA levels.....	27
Table 2.4: Primer sequences used for making the in situ hybridization (ISH) probes for seven hormone-encoding cell types.	29

Supervisors

Main supervisors

Dr. Christiaan V. Henkel
Department of Preclinical Sciences and Pathology, Faculty of Veterinary Medicine
Norwegian University of Life Sciences
1433 Ås, Norway

Co-supervisors

Prof. Finn-Arne Weltzien
Pro-rector, Norwegian University of Life Sciences
1433 Ås, Norway

Dr. Eirill Ager-Wick
Department of Production Animal Clinical Sciences, Faculty of Veterinary Medicine
Norwegian University of Life Sciences
1433 Ås, Norway

Acknowledgements

This PhD project was completed at the Norwegian University of Life Sciences (NMBU), Faculty of Veterinary Medicine, Department of Preclinical Sciences and Pathology (PREPAT), Physiology Unit and supported by NMBU and the Research Council of Norway, Grants no. 251307, 255601, and 248828. NMBU has been a great place to work, and I am very grateful for my time here. Thanks in advance to the PhD evaluation committee for taking on the task.

First, I would like to thank Allah Almighty for making it possible. My biggest thanks go to my supervisors; **Christiaan V. Henkel, Eirill Ager-Wick and Finn-Arne Weltzien**. Thank you for giving me this opportunity, for sharing your knowledge and for your continued support over a long period of time. **Christiaan**, thank you for your constructive feedback and especially valuable suggestions in bioinformatics part. I learned how to write scientifically and think critically. Thank you for offering coffee, advice, and pep-talks when I needed it. I am very grateful for your constant presence, encouragement, and support. During my PhD I went through a lot physical and mental traumas, but I would like to give special thanks to my supervisors who always motivated me and specially **Eirill**, she always understood my situation and supported me and gave better solutions. Thanks for your understanding and support on a personal level in a professional setting. Because of your arrangements, I was able to keep working. I am very grateful for this. Thank you so much.

Huge and heartfelt thanks go to the group members with whom I have shared both scientific failures and successes, as well as tons of fun experiences. **Rasoul Nourizadeh- Lillabadi** (Nouri), — co-author of one of my thesis papers. Thanks for making me so comfortable in the lab and in group meeting. Since I often work in lab but your welcoming and cherishing behavior always give me good vibes. It was a nice experience to travel with you for a conference and you are a good driver. **Kjetil Hodne** – for always giving me positive and constructive feedback. I appreciate learning about your field the wonders of electrophysiology. **Romain Fontaine** – co-author of all my thesis papers. I remembered when I gave my interview for this position you were the first person whom I meet in group. You are a good group leader and very helpful person in teaching me *in situ* stuffs. **Muhammad Rahmad Royan** – co-author of two thesis papers. Always happy, it seems. Such a hard worker! Thank you for teaching me complicated molecular terms. A good roommate to whom I share ups and downs of my Phd. Apart from scientific discussion we also discussed difficulties to settle with family in Norway. **Lourdes Genove Tan** – thanks so much for taking such good care of all of us and the fish. Also thank you for making yummiest noodles and waffles. Thanks to **Karin Elisabeth Zim, Ida Beitnes Johansen, Marco Vindas, Runa Rørtveit** for their good feedback that helped me to improve my work. **Anthony Peltier** Thanks for all the lovely cakes and for lifting the visual profile of the group in publications! **Guro Sandvik, Gersende Maugars, Elia Ciani and Susann Burow** – not strictly group members anymore. Guro – smiling person ever I met. Though I spent very less time and you left our group. Gersende - Thanks for being nice company both in scientific and non-typical work hours! I learned many pituitary hormones terms from you. Thanks for

giving a present for my son. Elia – I am so impressed by your endless positive outlook. Susaan – thanks for welcoming and positive behavior.

Thanks to my room mates; **Erik Magne Koscielniak Rasmussen, Jorke Kamstra, Tove Nicolaysen, Vilde Arntzen Engdal** for maintaining a good and positive environment in the room. Thanks to **Mariella Güere and Susan Skogtvedt Røed** (a very helpful and good person with beautiful souls)!

Finally, I would like to give huge thanks to my family in Pakistan. I am very happy to fulfill my father's (**M. Siddique**) biggest dream. Due to his unconditional love, support and motivation made it possible. Unfortunately, my **mother** could not see this. But I have faith she can feel my success. Next my husband **Adnan Hashim**, thanks for being someone I can share everything complicated (and easy). It was a bumpy ride but because of you it become possible. I do not know what I would do without you. Thank you so much for your constant support, your warmth, and your wits. My son- **Almeer Hashim** thank you for being in my life (my stress relief). You are such a bonus in my life. Lastly, I would to thanks to my sisters (Saima and Iqra) for their love and motivation. I know this would a proud moment for all family members and for my in-laws.

Oslo, May 18, 2022, Khadeeja Siddique

List of publications

Paper I:

Characterization of hormone-producing cell types in the teleost pituitary gland using single-cell RNA-seq

Khadeeja Siddique, Eirill Ager-Wick, Romain Fontaine, Finn-Arne Weltzien & Christiaan V. Henkel

Scientific Data **volume 8**, article number: 279 (2021)

<https://doi.org/10.1038/s41597-021-01058-8>

Paper II:

3D atlas of the pituitary gland of the model fish medaka (*Oryzias latipes*)

Muhammad Rahmad Royan, Khadeeja Siddique, Gergely Csucs, Maja A. Puchades, Rasoul Nourizadeh-Lillabadi, Jan G. Bjaalie, Christiaan V. Henkel, Finn-Arne Weltzien & Romain Fontaine

Front. Endocrinol **volume 12**, article number: 719843 (2021)

<https://doi.org/10.3389/fendo.2021.719843>

Paper III:

Heterogeneity of pituitary lactotrope populations in the teleost model medaka (*Oryzias latipes*)

Khadeeja Siddique, Muhammad Rahmad Royan, Finn-Arne Weltzien, Romain Fontaine & Christiaan V. Henkel

Manuscript

Abstract

The pituitary gland is an endocrine gland found in vertebrates. It produces and secretes a variety of essential peptide hormones which regulate several physiological functions, such as reproduction, growth, metabolism, homeostasis, and response to stress. It is thought that each hormone is synthesized by a different cell type in teleost fish. The regulation of hormone production and release is complex, involving signals from the hypothalamus, paracrine control by other pituitary cell types, and feedback from downstream target organs. For a complete picture of the regulation of any one peptide hormone, it is therefore important to include the physiological state of many different cell types, as well as their relative positions and contacts. In this study, I have used single-cell transcriptomics (scRNA-seq) and imaging techniques to generate large data sets on gene expression, cell types, and their spatial organization in the pituitary gland of the model fish medaka. I have used these to resolve several open questions in teleost pituitary biology.

First, I used scRNA-seq to profile gene expression in thousands of individual cells from adult medaka. Clustering of these data reveals the female and male pituitary glands to be composed of 15 and 16 distinct cell types, respectively. Ten of these are associated with the production of peptide hormones, showing a clear division of cellular labour: each hormone is produced by a single dedicated cell type, with a few exceptions.

Next, I studied the localization of seven of these cell types within the pituitary. Using *in situ* hybridization with fluorescent probes (FISH) for hormone-encoding genes, we constructed a three-dimensional atlas of the medaka anterior pituitary. The 3D distribution of the cells expressing the hormone-encoding genes *pomca*, *lhb* and *tshba* in adult animals shows evidence of sexual dimorphism. Based on both FISH and scRNA-seq, I identified a few bi-hormonal cells co-expressing *fshb-tshba*, *lhb-sl*, and *lhb-fshb*. However, there is no evidence for a multihormonal population such as the one found in mammals.

In the last paper, I characterize two cellular populations expressing *prl* (encoding the hormone prolactin, which is involved in osmoregulation, among other functions). Based on the scRNA-seq data, these lactotrope populations are clearly distinct, with one similar in expression profile to cells expressing either growth hormone or somatolactin, and the other more similar to stem-cell-like populations. *In situ* hybridization (in other fish species) previously revealed several spatially separated *prl*-expressing clusters: one major cell cluster in the most anterior part of the pituitary, and sometimes additional smaller patches of cells. Under the hypothesis that such lesser patches represent developmentally (and possibly functionally) distinct cell populations, we therefore set out to demonstrate their equivalence to the transcriptomically defined stem cell-like lactotropes. However, to our surprise, the major cluster and the minor patches are indistinguishable at the transcriptomic level and consist of both types of lactotropes.

In summary, these new data firmly support the ‘one cell type – one hormone’ hypothesis of the teleost pituitary. In addition, they form a starting point for new discoveries and hypotheses, as demonstrated by the unexpected finding of lactotrope heterogeneity. In the future, they should provide a rich resource for comparative and functional studies on the teleost pituitary gland.

Sammendrag

Hypofysen er en endokrin kjertel som finnes i vertebrater. Den produserer og skiller ut en rekke viktige peptidhormoner som regulerer ulike fysiologiske funksjoner, som reproduksjon, vekst, metabolisme, homeostase og stressrespons. Man antar at hvert hormon er syntetisert av en spesifikk celletype i teleoster. Reguleringen av hormonproduksjon og -utskillelse er kompleks, og involverer signaler fra hypothalamus, parakrin kontroll fra andre hypofysecelletyper og signaler fra målorganer nedstrøms for hypofysen. For å danne et helhetlig bilde av reguleringen av hvert hypofysehormon er det viktig å inkludere den fysiologiske tilstanden til celletypene, i tillegg til informasjonen om deres relative posisjon.

I dette studiet har jeg benyttet enkeltcelle transkriptomikk (scRNA-seq) og bildebehandlingsteknikker for å generere store datasett med genekspressjon, celletyper og deres romlige organisering i hypofysen til modellfisken medaka. Jeg har benyttet disse for å løse flere ubesvarte spørsmål om biologien til hypofysen hos teleoster.

Først benyttet jeg scRNA-seq for å produsere genekspressionsprofiler til tusenvis av individuelle celler fra hypofysen fra voksen medaka. Gruppering av disse dataene viste at hunn og hann hypofyseceller består av henholdsvis 15 og 16 ulike celletyper. Ti av disse er assosiert med produksjon av peptidhormoner, og gir et tydelig bilde av arbeidsfordelingen: hvert hormon er produsert av en spesifikk celletype, med noen få unntak.

Videre studerte jeg lokaliseringen av syv av disse celletypene i hypofysen. Ved å benytte *in situ* hybridisering med fluorescerende prober (FISH) for hormonkodende gener, laget vi et tredimensjonalt atlas av dem fremre delen av medaka hypofysen. 3D fordelingen av cellene som uttrykker de hormonkodende genene *pomc*, *lhb* and *tshba* i hypofysen hos voksne medaka viser ulikheter mellom kjønnene. Basert på både FISH og scRNA-seq, identifiserte jeg noen hormonproduserende celler som uttrykker både *fshb-tshba*, *lhb-sl* eller *lhb-fshb*. Det var likevel ikke noe bevis for noen multihormonelle cellepopulasjoner, slik som man kan finne hos pattedyr.

I den siste artikkelen karakteriserte jeg to cellulære populasjoner av *prl* (koder for hormonet prolaktin, som blant annet er involvert i osmoregulering). Basert på scRNA-seq data, er disse laktotrope populasjonene tydelig forskjellige, med en populasjon som har en lignende ekspressionsprofil til celler som uttrykker enten veksthormon eller somatolaktin og en annen populasjon som ligner mer på stamceller. *In situ* hybridisering (i andre fiskearter) har tidligere vist flere *prl*-uttrykkende grupper som har vært romlig separert fra hverandre: en hovedgruppe i den mest fremre delen av hypofysen, og noen ganger noen ekstra mindre grupperinger i tillegg. Med bakgrunn i hypotesen at slike mindre grupperinger representerer utviklingsmessige (og mulig funksjonelt) ulike cellepopulasjoner, ønsket vi å demonstrere deres likhet til de stamcelle-liknende laktotropene som ble funnet ved transkriptomanalyse. Til vår overraskelse fant vi ingen forskjeller mellom de store gruppene og de mindre grupperingene på transkriptomnivå, som dermed består av begge typer laktotroper.

Oppsummert støtter disse nye dataene opp om 'en celle – ett hormon' hypotesen om teleost hypofysen. I tillegg danner de utgangspunkt for nye oppdagelser og hypoteser, demonstrert for eksempel ved de uventede funnene av laktotrope cellers heterogenitet. I fremtiden forventes

det at dataene vil være en viktig ressurs for komparative og funksjonelle studier av teleost hypofysen.

Introduction

1

1. Introduction

1.1. General background

Teleost fishes are the world's largest and most diversified class of vertebrates, consisting of around 30,000 species (Nelson, 1994; Wootton, 1990). They comprise approximately half of all vertebrate species and have adapted to a wide range of habitats, which include both freshwater and marine environments. The teleosts exhibit a vast diversity in their physiology, morphology, ecology and behaviour (Nelson, 2012). It is hypothesized that the observed diversity in teleost species is due to the whole-genome duplication in their genomes approximately 300 million years ago (Mya) (Glasauer & Neuhauss, 2014), which resulted in many duplicate gene pairs (Kasahara et al., 2007; Sato et al., 2009).

1.2. Model organisms

A model organism is a non-human species that has been the subject of extensive research in order to get a better understanding of specific biological processes, with the expectation that the study of the model organism will shed light on the mechanisms operating in other organisms that are difficult to study directly. Model organism studies are efficient and effective because they offer various experimental advantages in a laboratory setting, including manageable size, easy maintenance and breeding, ease of observation, and a short generation time. As a result, a diverse spectrum of model organisms spanning from viruses to mammals and plants has been developed. Scientists can choose the most relevant model organism for their research (Sakaguchi et al., 2019).

Using teleosts as models rather than mammals has several advantages (Powers, 1989). The majority of teleosts are egg-laying and embryonic development takes place outside the body. Generally, embryos are transparent throughout their embryonic stages, which provides a significant benefit for studying organ development and facilitates *in vivo* research. Their genome evolution and diversification are critical components for understanding vertebrate evolution because they provide several possibilities to study a variety of physiological processes or adaptations. Finally, comparative studies across species can shed light on previously unknown systems (Naruse et al., 2004).

Amongst teleost model organisms, zebrafish is mostly used for biomedical and developmental research, pigmentation, novel morphological structures and sex determination; stickleback for behaviour; eel for genomic evolution and body elongation; pufferfishes for body plan reduction and genome size reduction; killifish for ageing and pigmentation; and medaka for reproduction, pigmentation, sex determination, diversity and ecology (Braasch et al., 2015).

1.2.1. Medaka as a model organism

Medaka (*Oryzias latipes*), also called Japanese rice fish, is a small (3 cm) freshwater teleost fish native to South-East Asia. The medaka is relatively closely related to stickleback, pufferfish, and fugu (see figure 1.1) (Hashiguchi et al., 2009). A direct comparison of zebrafish, which is a famous model organism for studying the vertebrate genome, and medaka reveals that they diverged approximately 230 Mya from a common ancestor (see figure 1.1) (Hughes et al., 2018; Kumar et al., 2017; Li et al., 2020).

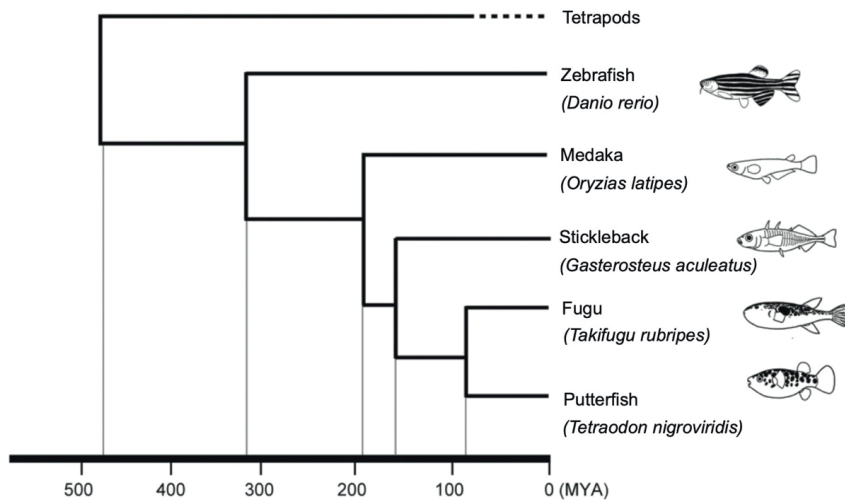


Figure 1.1: Phylogenetic tree of medaka and five other model fishes. Figure adapted and modified from Hashiguchi et al. (2009). Note that current estimates place the zebrafish/medaka split at 230 Mya (Kumar et al., 2017).

Due to its numerous advantages, medaka is frequently used as a model organism (Kasahara et al., 2007; Kirchmaier et al., 2015). For example, medaka is a diurnal species with a short generation period, reproduces daily under favourable environmental and social breeding conditions, and requires little maintenance. Additionally, it is tolerant to temperature, natively living at summer temperatures of up to 40 °C and winter temperatures as low as 4 °C. Also, it has a unique sex determination gene (*dmy*), which is equivalent to the SRY (sex determining region Y) gene found on the mammalian Y chromosome (Kasahara et al., 2007; Matsuda et al., 2002).

The medaka genome is quite small in comparison to other small model fish, and consist of approximately 800 megabasepairs, whereas the zebrafish (*Danio rerio*) genome is about 1700 megabasepairs, approximately double the size of the medaka genome. The medaka genome is around one-quarter the size of the human genome (Naruse et al., 2004). Additionally, several inbred strains have been produced, as medaka appears tolerant to inbreeding

(Kirchmaier et al., 2015). Currently, over 600 different populations of medaka strains, including mutant, wild-type, transgenic and inbred lines, are established at the Medaka Resource Center of the Japan National BioResources Project (NBRP). This is beneficial for genetic mapping and mutagenesis screening. Among the available inbred strains is Hd-rR, which was developed in 1980 at Nagoya University in Japan from the progeny of a single d-rR animal utilized in the medaka genome sequencing effort (Kinoshita, 2009). Sexual dimorphism in body colour distinguishes the d-rR strain, making it particularly well-suited for studies involving sex determination and differentiation.

The medaka genome has been sequenced and made publicly available through the medaka genomic database (<http://utgenome.org/medaka/>), as well as through NCBI and Ensembl. However, this medaka genome assembly was rudimentary due to computational limitations and short-read DNA sequencing data. An improved version of the medaka genome has recently been published (Li et al., 2020), based on advanced high-throughput long-read sequencing techniques, which leads to better gene annotation.

For all these reasons, medaka has gained popularity as a vertebrate model organism and now is commonly used in different fields of research, such as endocrinology, developmental, environmental, and biomedical science (Li et al., 2020).

1.3. The endocrine system

The word ‘endocrine’ is a combination of two Greek words, ‘Endo’ meaning inside or within and ‘Crinos’, which means secretion or discharge. The endocrine system is essentially a group of ductless glands that produce hormones and secrete them directly into the extracellular space and from there to the bloodstream, where they can be transported to specific tissues and organs. Hormones produced by the endocrine system regulate the activity of targeted organs and control different physiological processes, such as digestion, growth, metabolism, development, reproduction, and fertility (Kumar & Tembhre, 1996; Melmed, 2016). Endocrine components and mechanisms are extremely conserved in vertebrates, including between fish and mammals (Jakob Biran, 2018; Levavi-Sivan et al., 2010; Zohar et al., 2010).

Various endocrine glands have been discovered throughout the body of fishes, i.e., ovaries in females and testes in males are in the pelvic region, while the hypothalamus and pituitary gland are located in the brain. Sensory information from both the external and internal environment, such as temperature, metabolism, energy reserves, gonadal status, and the presence of a possible partner, are processed and combined by the hypothalamus and brain of fish to regulate and initiate the reproduction process (Biran & Levavi-Sivan, 2018; Weltzien et al., 2004). The key component of the endocrine system that regulates puberty and sexual maturation in vertebrates is the hypothalamic-pituitary-gonadal axis (HPG) (see figure 1.2

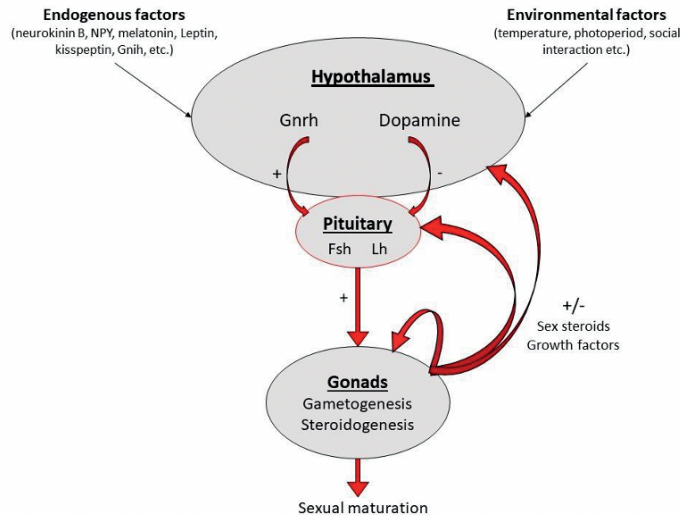


Figure 1.2: The hypothalamus-pituitary-gonadal (HPG) axis. Gnrh production and release can be triggered by a mixture of exogenous and endogenous factors. Gnrh stimulates the pituitary gland through specific Gnrh receptors, resulting in the synthesis of two gonadotropins (Fsh and Lh), whereas dopamine inhibits Gnrh's stimulatory effects. Lh and Fsh are released into the bloodstream, and after binding to their respective gonad receptors trigger the generation of steroid hormones (steroidogenesis) and the production of gametes (gametogenesis). Sex steroids generate a positive and negative feedback effect on all levels of the HPG axis, promoting or inhibiting the production of gonadotropins. (Figure adapted from Weltzien et al. (2004).

1.3.1. The hypothalamus-pituitary-gonad (HPG) axis

The endocrine connections between the hypothalamus, pituitary and the paired gonads constitute the axis that integrates physiological and environmental signals and controls sexual maturation in vertebrates (Biran & Levavi-Sivan, 2018; Schulz et al., 2010; Schulz & Miura, 2002). The HPG-axis is functional and active during early development, but soon enters a quiescent phase until it becomes reactivated at puberty. This reactivation leads to gonad maturation and reproductive capacity (Christensen et al., 2012; Weltzien et al., 2004; F. A. Weltzien et al., 2003; Zohar et al., 2010).

Activity starts with the release of a hormone from the hypothalamus, called gonadotropin-releasing hormone (Gnrh). This interacts to Gnrh receptors located on the plasma membrane of gonadotropes and initiates the intracellular pathways that result in the synthesis and secretion of two gonadotropins: luteinizing hormone (Lh) and follicle-stimulating hormone (Fsh). When Fsh and Lh reach the gonads, they bind to their respective receptors (Fshr and Lhr), triggering the gonads to release sex-specific steroids involved in gametogenesis,

vitellogenesis, and finally maturation of oocytes in females (Patiño & Sullivan, 2002), as well as y spermiogenesis and spermatogenesis in males (Levavi-Sivan et al., 2010; Schulz & Miura, 2002).

Endogenous and exogenous (environmental) factors affect and regulate numerous different neurotransmitters such as GnRH, neuropeptide Y (NPY), neurokinin B, leptin, gonadotropin-inhibitory hormone (GnIH), dopamine, serotonin, pituitary adenylate cyclase-activating peptide (PACAP), and gamma-amino-butyric acid (GABA), among others (Biran & Levavi-Sivan, 2018; Chang et al., 2000; Chang et al., 2009; Nakane & Oka, 2010; Navarro & Tena-Sempere, 2012; Oakley et al., 2009; Trudeau et al., 2000; Yaron et al., 2003). GnRH is required for sexual maturation and was initially isolated in mammals and then in other vertebrates (Sherwood et al., 1983). Many teleost species are subject to a dual control of gonadotropins from the hypothalamus, where stimulatory action of GnRH is countered by the inhibitory effects of dopamine (Dufour et al., 2010). Additionally, gonadotropin inhibitory hormone (GnIH) inhibits gonadotropin secretion in humans and birds, whereas in teleosts it exhibits stimulatory effects (Tsutsui, 2009). Gonadotropin production may also be controlled directly at the pituitary level by a variety of neurotransmitters and hormones via positive and negative feedback processes.

Several studies described the transcriptomes of the HPG-axis at various levels in fish (Harding et al., 2013; Rolland et al., 2013; Sambroni et al., 2013; Takahashi et al., 2016), however information on the complete transcriptomic regulation of the HPG-axis in teleost remains limited. It is therefore important to understand the complex structure of the pituitary, which is a major component of the HPG-axis and the main focus of this thesis.

1.3.2. The pituitary gland

The pituitary is the major endocrine gland of the vertebrates, as it is responsible for regulating a suite of physiological process such as growth, reproduction, and homeostasis maintenance (Kelberman et al., 2009; Ooi et al., 2004; Weltzien et al., 2004). A short neural stalk connects the pituitary gland to the hypothalamus. In fish, the short neural stalk contains neurosecretory fibres which pass from the brain to the pituitary. These are in fact axons of neurons present in the hypothalamus, which spread projections towards the pituitary gland (de Beer, 1924; Schreibman, 1973; Zohar et al., 2010).

The neurohormones that regulate the function of the pituitary gland consist of neuropeptides and neurotransmitters. Both these types of neurohormones are produced by specific neuronal populations and transported to the pituitary gland. In general, tetrapods and fish have similar basic mechanisms but the process of transporting these neurohormones to their target cells in the pituitary gland differs significantly. These neurohormones have particular characteristics, origins and targets that give an essential indication about the way the brain regulates the pituitary gland. Therefore, it is important to elucidate the complex structure of the pituitary gland (Zohar et al., 2010).

1.3.2.1. Pituitary morphology

The pituitary gland consists of two compartments: the adenohypophysis/anterior pituitary (ADH), which originates from Rathke's pouch, an upgrowth of ectodermal tissue from the embryonic oral cavity's anterior roof; and the neurohypophysis/posterior pituitary, which originates from a downgrowth of the diencephalon's floor (Wingstrand, 1966). The term 'hypophysis' is Greek and means 'below', referring to its position in relation to the brain. Recently, Fabian et al. (2020) proposed that both endodermal and ectodermal epithelia are equally capable of producing all endocrine cell types. Additionally, in the absence of ectodermal contributions, endoderm can generate a rudimentary ADH-like structure (Weltzien et al., 2004).

The adenohypophysis of teleosts is separated into a *pars distalis* (PD), located on the anterior side, and a *pars intermedia* (PI), located at the posterior side. In contrast to mammals, fish do not have a clear morphological differentiation between the PD and PI (Pogoda & Hammerschmidt, 2007). The PD is further classified into a *proximal pars distalis* (PPD) and *rostral pars distalis* (RPD) (see figure 1.3) (de Beer, 1924; Pogoda & Hammerschmidt, 2007; Schreibman, 1973; Weltzien et al., 2004). The adenohypophysis contains endocrine cells as well as non-endocrine cells such as folliculostellate cells (FS) (Fauquier et al., 2001; Golan et al., 2016).

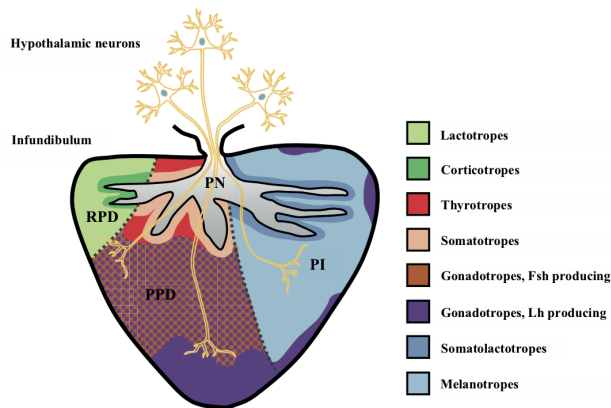


Figure 1.3: Teleost pituitary. This figure represents the organization of the Atlantic halibut (*Hippoglossus hippoglossus*) pituitary through a schematic sagittal section. Endocrine cells in the anterior pituitary are directly innervated by hypothalamic axons. The teleost pituitary is composed of three main compartments and different cell types: PD, pars distalis, further divided into RPD, rostral pars distalis and PPD, proximal pars distalis; PI pars intermedia; and PN, pars nervosa. Each colour indicates an endocrine cell type (Figure adapted from Weltzien et al. (2004)).

The second component, the neurohypophysis, comprises the *pars nervosa* (PN), which mainly consists of nerve terminals from the pre-optic hypothalamic area as well as glia-like

supporting cells (pituicytes) (Ferrandino & Grimaldi, 2008; Pogoda & Hammerschmidt, 2007; Weltzien et al., 2014). In teleosts, the PN secretes vasotocin and isotocin, homologues to the mammalian vasopressin and oxytocin (Feng & Bass, 2017). In most mammals and birds, the neurohypophysis is situated posterior to the ADH, whereas in teleosts, it is normally dorsally situated (Pogoda & Hammerschmidt, 2007). In contrast to mammals, where a hypothalamo-hypophysial portal system is responsible for the delivery of these neurohormonal messages, in teleosts neurons directly connect to the pituitary through the hypophysial stalk and the PN (Ball, 1981; Pogoda & Hammerschmidt, 2007).

1.3.2.2. Pituitary cell types

As explained earlier, the pituitary gland is involved in variety of physiological functions. These processes are controlled by the secretion of various protein hormones, which are synthesized by distinct hormone-encoding cell types of the anterior pituitary (Weltzien et al., 2004). These hormones are chemical messengers that facilitate communication between various cell types that detect them via receptors. Following the binding of the hormone to the receptor, a series of biochemical reactions take place resulting in a variety of biological responses regulating reproduction, metabolism, etc. (Hoga et al., 2018; Reis Filho et al., 2006). The mammalian pituitary contains these hormone-producing cells in a mosaic pattern (Doerr-Schott, 1976; Voss & Rosenfeld, 1992). However, diverse cell types are present in different pituitary compartments in teleosts, retaining the embryogenic arrangement of cell types (Pogoda & Hammerschmidt, 2007; Schreibman, 1973). The PPD hosts gonadotropes (producing Fsh or Lh), thyrotropes (producing thyroid stimulating hormone, Tsh) and somatotropes (producing growth hormone, Gh), whereas the RPD hosts lactotropes (prolactin-producing cells, Prl) and corticotropes (producing adrenocorticotrophic hormone, Acth). The PI represents the position of melanotropes (which produce melanocyte stimulating hormone, α -Msh) (see figure 1.3) (Levavi-Sivan et al., 2010; Sherwood et al., 1983; Weltzien et al., 2004; Weltzien et al., 2014; Zohar et al., 2010). Moreover, in the PI, fish pituitaries have an extra endocrine cell type called the somatolactotropes. These cells produce somatolactin (SI), a hormone related to Prl and Gh that was initially identified from the pituitary of the Atlantic cod (Kaneko, 1996; Rand-Weaver et al., 1991).

Despite widespread acceptance of the one cell – one hormone hypothesis in teleosts, several observations do not fit this hypothesis. For example, numerous teleost species (e.g., Mediterranean yellowtail, tilapia, zebrafish and European hake) have been reported to have gonadotropes generating both gonadotropins (Fontaine et al., 2020). Furthermore Child et al. (1982) and Childs (1983) described that gonadotropes produce only one hormone in mammals. Previously published research indicates that Fsh and Lh cells in fish share a developmental basis that is similar to that found in mammals (Weltzien et al., 2014), implying that Lh and Fsh cells in fish could be indistinguishable from one another and may be more similar to mammalian gonadotropes than previously anticipated.

Numerous teleost species have been studied for their endocrine cell type distribution of the pituitary for the last five decades. Despite their nearly identical structures, the endocrine

cell mapping of the pituitary gland differs in cell types reported. For example, endocrine cell population localisation in dorado fish indicates only four different endocrine cell types throughout the ADH (Honji et al., 2013). In comparison, research on other species has discovered five cell types in Japanese medaka (Aoki & Umeura, 1970), seven in greater weever (Sanchez Cala et al., 2003), dimerus cichlid (Pandolfi et al., 2009) and white seabream (Segura-Noguera et al., 2000), six in fourspine sculpin (Mukai & Oota, 1995), bloodfin tetra and cardinal (Camacho et al., 2020), and eight in Atlantic halibut (F. A. Weltzien et al., 2003) and Nile tilapia (Kasper et al., 2006). As a result, our understanding of the physiology and development of the many pituitary cell types, as well as the regulatory processes underlying hormone synthesis, remains limited. Therefore, the pituitary cell types, their spatial arrangement, and vascularization need to be properly characterized to understand the complexity of pituitary. With advancements in sequencing technologies, it is now possible to analyse the transcriptome, which contains information about the functional, physiological, and biosynthetic states of cells.

1.4. Sequencing approaches

The ability to decode the DNA or RNA sequences of biological samples is of key importance for a variety of scientific applications. For the last five decades, scientists have focused on inventing procedures and techniques that allow the sequencing of DNA and RNA molecules. This period has seen significant advancements, from sequencing a single nucleotide base to millions of bases, from struggling to discover the sequence of a gene to rapidly and extensively sequencing the entire genome. The next section will discuss different generations of sequencing technologies and highlight some of the most significant discoveries (see figure 1.4).

1.4.1. First generation sequencing

Sanger and Coulson invented a first generation sequencing technique in 1975. It is based on DNA polymerases incorporating chain terminating ddNTPs (dideoxynucleotides) during *in vitro* DNA replication. Sanger also sequenced the first-ever genome sequence of bacteriophage ϕ X174/PhiX genome (5368 basepairs, bp) in 1977 (Sanger et al., 1977). Maxam and Gilbert developed another DNA sequencing approach that relies on nucleotide-specific partial chemical alteration of DNA and subsequent breaking of the DNA backbone at sites proximal to the altered nucleotide bases (Maxam & Gilbert, 1977). In comparison to the Sanger method, which required cloning to obtain single-stranded DNA, Maxam–Gilbert sequencing was useful since it allowed for the direct use of pure DNA (Saccone and Pesole, 2003). Sanger’s sequencing method, on the other hand, proved to be relatively easy to scale with subsequent improvements and was broadly applied throughout the next thirty years, including for the initial version of the Human Genome project (Schloss, 2008).

First generation DNA sequencing was able to sequence small fragments, resulting in reads of almost 1000 bp in length, but large mammalian genomes remained challenging to sequence. Therefore, scientists developed the ‘shotgun sequencing’ technique, in which DNA

is randomly broken down into smaller pieces. These small DNA fragments are cloned and sequenced separately (as a sequencing ‘library’), and then assembled into longer sequences (contigs) based on overlapping regions (Anderson, 1981; Staden, 1979). A commonly used type of shotgun sequencing is known as whole-genome shotgun sequencing (WGS), in which the complete genome is broken down into smaller fragments for sequencing. First generation sequencing was widely used by scientists for three decades and the genomes of several organisms were sequenced during this time, such as the nematode roundworm *C. elegans* in 1998, the fruit fly *D. melanogaster* in 2000 (Adams, 2008), the human genome in 2001 (Lander et al., 2001) and also the medaka genome in 2007 (Kasahara et al., 2007). After the first generation, there have been significant advances in sequencing technology (Heather & Chain, 2016), as shown in figure 1.4.

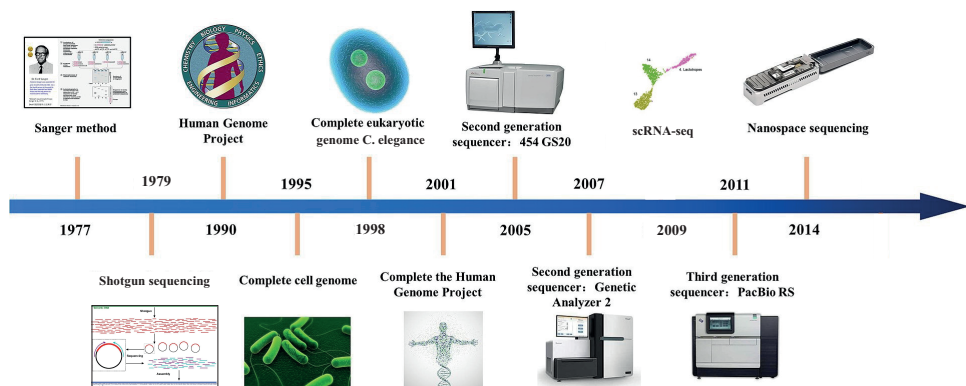


Figure 1.4: Representation of the evolution of sequencing technologies. Figure adapted and modified from Yang et al. (2020).

1.4.2. Second generation sequencing

The first generation of sequencing was a great success, but it was time-consuming and expensive (Kchouk et al., 2017). With the invention of new sequencing methodologies, a new era started in which these limitations of first generation sequencing were overcome. These new sequencing technologies are known as Next Generation Sequencing (NGS) (Mardis, 2011). NGS can sequence multiple samples in parallel, resulting in millions to billions of reads at a time, allowing it to create large sequencing datasets (Churko et al., 2013; Kchouk et al., 2017).

Different sequencing platforms emerged in early 21st century, for example Roche/454 (2005), Solexa/Illumina (2006) and the ABI SOLiD in 2007 (Kchouk et al., 2017). Each platform has different characteristics, which affect accuracy, reproducibility, and usability for specific scientific questions (Li et al., 2014; Su et al., 2014). By 2021, the Illumina platform is the dominant sequencing technology in the scientific community. With time these platforms

improve: in 2005 an Illumina Genome Analyzer could generate almost 1 Gbp of data per run, by 2014 an individual run of HiSeq (Illumina) could generate 1.8 Tbp of sequencing data within a week and with lower costs (Illumina, 2014).

1.4.3. Third generation sequencing

Although NGS (second generation sequencing) is widely used in research, it still has the limitation of short read lengths (100 to 250 bp) and is therefore unable to read the entire DNA sequence of a genome from start to finish. Additionally, NGS generates large amounts of data that require substantial computing resources, as well as sophisticated algorithms to reassemble the short reads, and to identify transcript isoforms, including prediction of splicing sites. To overcome these issues, third generation sequencing has been developed, offering longer read lengths and the capability to capture the isoforms of transcripts and splice sites more efficiently (Schadt et al., 2010). It consists of different platforms like Pacific Biosciences (PacBio) single-molecule real-time (SMRT) sequencing (Eid et al., 2009) and Oxford Nanopore Technologies (ONT) nanopore sequencing (Bayley, 2015).

Currently, scientists are using this approach to make more accurate genome assemblies for many organisms. Recently (2020), an updated and improved version of the medaka genome was published based on a combination of third generation sequencing with older sequencing techniques (Li et al., 2020).

1.4.4. Applications of NGS

NGS approaches have emerged as a significant tool in scientific study in recent years, revolutionizing genetics and genomics by enabling large-scale investigation of the characteristics of biological and cellular processes. It enables genome re-sequencing, *de novo* assembly of the complete genome and transcriptome, transcriptome profiling, DNA-protein interaction analysis, and epigenetics (Barzon et al., 2011).

1.5. Transcriptomics

The transcriptome, the functional complement of the genome, is composed of a variety of RNA molecules, including mRNA, miRNA, ncRNA, rRNA, and tRNA. Each of these RNA molecules is crucial for the physiological response and understanding how they are differently regulated is important for a more complete knowledge of the functional genome (Rodríguez-Ezpeleta et al., 2012).

1.5.1. RNA sequencing (RNA-seq)

RNA-seq is a technique to study mRNA expression at tissue level by using high-throughput sequencing. Before the emergence of NGS, transcriptome profiling was performed by using microarrays, which have many limitations, including low accuracy for lowly

expressed genes and high noise levels due to non-specific hybridization. RNA-seq overcomes these issues by using high-throughput sequencing to identify and count cDNA molecules (Marioni et al., 2008; Reuter et al., 2015).

We can determine which versions of genes are present in a cell by examining its DNA, but we cannot determine which are active or involved in particular processes. This involves an assessment of the dynamically changing components of the system. In an ideal world, we would like to investigate the proteins that are already present, as they are responsible for the majority of the functionality. While this is achievable using technologies such as mass spectrometry, the resulting output is more difficult to interpret, and the encoding is significantly more complex due to the fact that there are 20 different amino acids compared to only four nucleotides. RNA molecules, on the other hand, are far easier to quantify. High-throughput cDNA sequencing (RNA-seq) is a robust technique for determining the quantity of RNA expression in a high-quality manner. RNA is extracted from a biological sample, converted to complementary DNA (cDNA), and supplied into a sequencing machine as an input. An RNA-seq experiment generates millions of short nucleotide sequences derived from the sample's RNA transcripts. In comparison to traditional techniques for detecting RNA, such as probe-based microarrays, RNA-seq does not require prior knowledge of existing sequences and is successful across a far broader range of expression levels (Marioni et al., 2008; Reuter et al., 2015).

In teleosts, RNA-seq has been utilized to evaluate gene expression. For example, He et al. identified global patterns of gene expression in zebrafish pituitaries during the juvenile and sexual maturation stages (He et al., 2014). Ager-Wick and colleagues used RNA sequencing to analyse the pituitary of prepubertal female silver eels and discovered that the most abundant transcript codes for proopiomelanocortin, the precursor to melanocortin system hormones (Ager-Wick et al., 2013). In another study, Ager-Wick et al. sequenced Lh cells sorted by fluorescence-activated cell sorting (FACS) from the Japanese medaka pituitary and reported high levels of other hormone-encoding genes such as Fsh and Pomca (Ager-Wick et al., 2014). Although these studies shed light on how hormone production is regulated, RNA-seq is a high-throughput approach to find average gene expression over a complete tissue sample. Consequently, it is not possible to determine which cells generate particular hormones. The development and physiology of the numerous pituitary cell types, including the regulatory systems that control hormone synthesis, are still poorly known. Recently, single-cell RNA sequencing (scRNA-seq) has become popular for investigating heterogeneity of tissues at the cellular level (Kashima et al., 2019) (see figure 1.5). Therefore, I used this technique in this study to explore the heterogeneity in the teleost pituitary gland.

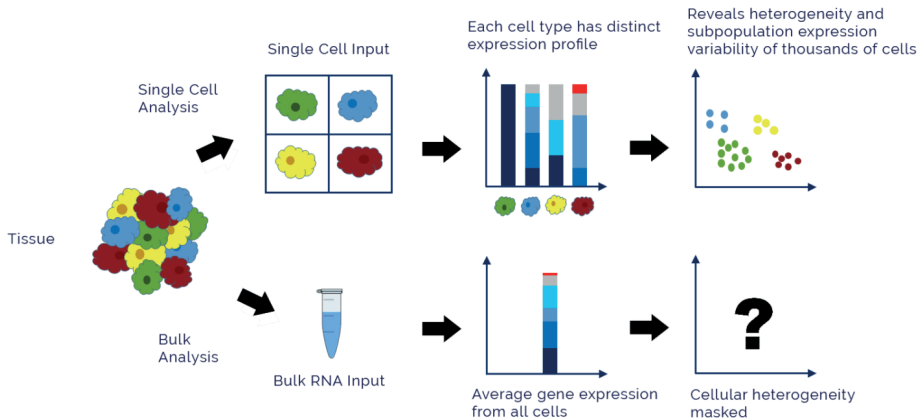


Figure 1.5: Comparison among bulk and single-cell RNA. The scRNA-seq shows cellular heterogeneity that was previously masked by bulk RNA-seq methods. Adapted and modified from Clark (2017).

1.5.2. Single-cell RNA sequencing (scRNA-seq)

Generally, bulk RNA sequencing techniques average the transcriptome across millions of cells in a tissue. Currently, scRNA-seq has made it possible to explore the transcriptome at the single-cell level. Various situations demand an understanding of how specific cell types respond to development or perturbations. It is now feasible to examine the transcriptomes of all cell types in a tissue simultaneously using scRNA-seq methods, which has resulted in better knowledge of different and novel cell types. By detecting transcriptome variation at its most fundamental level, this method enables researchers to (i) investigate how cellular heterogeneity contributes to disease etiology, (ii) identify existing and novel cell populations, and (iii) study the developmental trajectories of cells, etc. (Van den Berge et al., 2018). This section will discuss the current state of scRNA-seq techniques and provide a brief history of scRNA-seq.

1.5.2.1. Timeline of scRNA-seq

The transcriptome of each cell can reveal the dynamics within tissues. This idea was first implemented by Eberwine et al. (1992), who developed a method of unicellular complementary DNA (cDNA) amplification by *in vitro* transcription (IVT), followed by *in situ* and northern blot hybridization. Later in these early years of single-cell gene expression profiling, low throughput methods were frequently employed to profile a target set of genes. These included multiplexed quantitative reverse transcription PCR (RT-qPCR) in single cells, quantitative PCR (qPCR) (Bengtsson et al., 2008; Bengtsson et al., 2005; Peixoto et al., 2004), fluorescent reporter constructs (Chalfie et al., 1994) and single-molecule RNA fluorescence *in situ* hybridization (FISH) (Femino et al., 1998). While these approaches have contributed to some significant discoveries (Wills et al., 2013), they are limited by their ability to detect only

a small number of genes. Researchers eventually developed techniques for untargeted single-cell mRNA (or cDNA) amplification, that enabled them to conduct transcriptomics investigations utilizing microarrays (Kamme et al., 2003; Kurimoto et al., 2006). Tang et al. (2009) modified the technologies to make them compatible with high-throughput DNA sequencing, enabling for the first time to conduct an entirely unbiased transcriptomics analysis of mRNA in a single cell; however, manual manipulation was required, and the study was restricted to a small number of cells.

Guo et al. (2010) followed up with an array-based technique to profile the expression of 48 genes in around 500 cells. While this was not a single-cell RNA sequencing experiment, it had a huge impact on the single-cell community. Moreover, they demonstrated that based on the expression of 48 examined genes, they could distinguish the type of each cell. The concept that the identity of a cell may be derived from the expression of a subset of its genes is important to the theory underlying present scRNA-seq clustering approaches.

During the following years, several scRNA-seq methods have been developed, all with different characteristics in terms of strand specificity, transcript coverage and degree of multiplexing (number of cells assayed). Some of the characteristics are summarized in table 1.1 (Chen et al., 2018; Haque et al., 2017; Kolodziejczyk et al., 2015; Picelli, 2017).

Table 1.1: Summary of scRNA-seq methods and their specificity.

Methods	Transcript coverage	UMI possibility	Strand specific	References
Tang method	Nearly full-length	No	No	(Tang et al., 2009)
Quartz-Seq	Full-length	No	No	(Sasagawa et al., 2013)
SUPeR-seq	Full-length	No	No	(X. Fan et al., 2015)
Smart-seq	Full-length	No	No	(Ramsköld et al., 2012)
Smart-seq2	Full-length	No	No	(Picelli et al., 2013)
MATQ-seq	Full-length	Yes	Yes	(Sheng et al., 2017)
STRT-seq and STRT/C1	5' -only	Yes	Yes	(Islam et al., 2011, 2012)
CEL-seq	3' -only	Yes	Yes	(Hashimshony et al., 2012)
CEL-seq2	3' -only	Yes	Yes	(Hashimshony et al., 2016)
MARS-seq	3' -only	Yes	Yes	(Jaitin et al., 2014)
CytoSeq	3' -only	Yes	Yes	(H. C. Fan et al., 2015)
Drop-seq	3' -only	Yes	Yes	(Macosko et al., 2015)
InDrop	3' -only	Yes	Yes	(Klein et al., 2015)
Chromium	3' -only	Yes	Yes	(Zheng et al., 2017)

Further studies quickly showed that cell types may be recognized without the need for cell sorting, and methods for unbiased capture of the full transcriptome were established. Since then, various scRNA-seq methods have been established, for example, CEL-Seq (Hashimshony et al., 2012), Quartz-Seq (Sasagawa et al., 2013), Smart-seq2 (Picelli et al.,

2013), CEL-Seq2 (Hashimshony et al., 2016) and Quartz-Seq2 (Sasagawa et al., 2018). In addition, the number of cells used in scRNA-seq experiments has significantly increased (see figure 1.6) (Svensson et al., 2018). The Fluidigm C1 was the first commercially available cell capture platform. It uses microfluidics to passively separate cells into individual wells on a plate, where they are lysed, reverse transcribed, and the cDNA collected is PCR amplified. Following this step, the product is removed from the plate and libraries for Illumina sequencing are generated. Although the majority of C1 data has been generated using a 96 well plate, an 800 well plate has recently become available, significantly boosting the number of cells which can be recorded at once. One disadvantage of microfluidic plate-based cell capture systems is that the chips used have a defined size window, limiting the number of cells collected in a single run to a specific size. However, because cells are isolated in individual wells, they can be examined prior to lysis, allowing for the identification of damaged or broken cells, empty wells, or wells containing multiple cells. Multiple cell capture is a well-known issue, since Macosko et al. (2015) discovered that 30% of the generated libraries in an experiment combining human and mouse cells contained transcripts from both species, but only roughly a third of these doublets were visible in microscope images. The Fluidigm Polaris system, which is newer, similarly employs microfluidics to capture cells, but it can also select specific cells based on staining or fluorescent reporter expression and hold them for up to 24 hours while adding various stimuli. During this time period, the cells can be visualized before being lysed and processed for RNA sequencing. This platform enables a variety of studies that would not be performed with other capturing systems (Svensson et al., 2018).

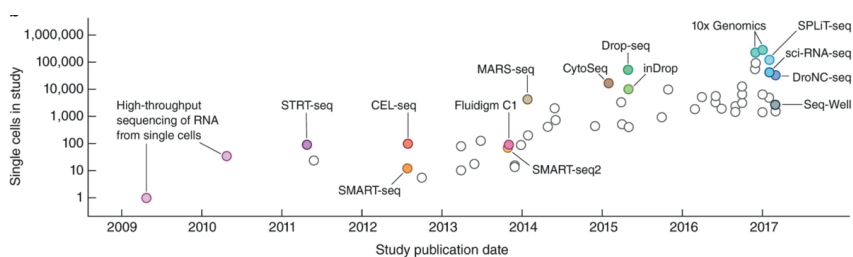


Figure 1.6: Timeline of scRNA-seq protocols and advancements in technologies. Figure adapted from Svensson et al. (2018).

1.5.2.2. Droplet-based cell capture

Rather than using microfluidics to collect cells in wells, they can be collected in nano-droplets. A dissociated cell mixture is delivered into a microfluidic system via one input, while beads coated with primers enter via another. The system is designed to create aqueous droplets inside mineral oil, and the inputs are set in such a way that cells and beads can be caught within a droplet simultaneously. When this occurs, the bead's reagents lyse the cell, and any poly-A-tagged RNA molecules present can bind to the capture probe on the beads. The reverse transcription and PCR amplification process is then initiated, and a separate cDNA library is generated for each cell, tagged with the bead's unique barcode sequence. The primary

advantage of droplet-based capture systems is their capacity to capture tens of thousands of cells at a time. Additionally, these techniques are less selective in terms of cell size and lead to fewer doublets. As a result, they are far less expensive per cell, although studies using droplet-based captures often sequence individual cells at a considerably lower depth due to the fixed sequencing costs.

The Drop-seq (Macosko et al., 2015) and InDrop (Klein et al., 2015) platforms were published in 2015, followed by an improved version of InDrop in 2017 (Zilionis et al., 2017). Both systems differ in terms of how beads are generated, how droplets are broken, and some parts of the chemistry. They can both be built on a lab bench using syringes, automatic plungers, a microscope, and a small custom-built microfluidic chip. The 10x Genomics Chromium device, which automates and simplifies a large portion of the process (see figure 1.6) (Zheng et al., 2017), is a comparable commercially available platform. This device makes use of droplet-based technologies to perform a variety of tasks, including cell capture for scRNA sequencing. Specialized captures, such as those for profiling immune cell receptors, are also accessible, and the company recently launched kits for single-cell Assay for Transposase-Accessible Chromatin utilizing Sequencing (scATAC-seq). According to a recent evaluation, the 10x Chromium is the most ideal droplet-based capture platform for the majority of investigations that are neither cost-sensitive nor require customized methods (Zhang et al., 2019).

1.5.2.3. Unique Molecular Identifiers

In comparison to plate-based capture methods, which typically generate reads along the entire length of RNA transcripts, droplet-based capture techniques generally use protocols that contain short random nucleotide sequences referred to as Unique Molecular Identifiers (UMIs) (Kivioja et al., 2012). Individual cells contain a small quantity of RNA (about 10–30 pg, less than 5% of which is mRNA), requiring a PCR amplification step to generate sufficient cDNA for sequencing. Various transcripts may be amplified at different rates depending on their nucleotide sequence, distorting their relative proportions within a library. UMIs try to improve gene expression measurement by allowing for the elimination of PCR duplicates generated during amplification (Islam et al., 2011, 2012). The nucleotide probes employed in droplet-based capture procedures consist of a poly-dT sequence that binds to mature mRNA molecules, a barcode sequence that is identical for each probe on a bead, and an 8–10 base UMI sequence that is unique to each probe. Due to the length of the UMI sequences, the likelihood of collecting two copies of a transcript on two probes using the same UMI is quite low. De-duplication can be accomplished following reverse transcription, amplification, sequencing, and alignment by detecting reads with the same UMI that align to the same location and hence should be PCR duplicates rather than actually expressed copies of a transcript.

Each scRNA-seq protocol has different features and functional properties, which lead to protocol-specific advantages and disadvantages (Ziegenhain et al., 2017). When doing a single-cell transcriptomic study, it may be required to employ specific scRNA-seq technologies in order to balance the study's goal and sequencing costs (table 1.1).

1.5.2.4. Technical noise in scRNA-seq

The higher precision and resolution provided by the single-cell technique come at a price: single-cell data is significantly noisier than bulk sequencing data. Two particularly significant effects are those referred to as dropouts and batch effects. Dropout is not an issue with bulk RNA-seq data, as these data are created as an average over a collection of cells. While batch effects exist for bulk data as well, their correction is different for scRNA-seq data. The following section discusses these two impacts in detail.

1.5.2.4.1. Dropouts

Current scRNA-seq approaches capture just 10–40% of the transcripts in a particular cell (Zheng et al., 2017). This indicates that the total number of expressed genes in any cell will be underestimated. Lowly expressed genes may be counted as zero, even if they are truly expressed in the given cell. Dropout occurs when a 0 is measured for a gene that is actually expressed. This is referred to as a technical 0, in contrast to a biological 0, in which case a gene is not expressed. This may also occur due to biological reasons. For example, if a mixture of cell types is sequenced and a particular gene is expressed in some but not all cell types, the scRNA-seq data will have biological dropouts (Qiu, 2020). However, it is now commonly recognised that a significant percentage of dropouts in a standard scRNA-seq experiment are technical in character. This indicates that scRNA-seq acts as a sampling technique, and dropout is effectively RNA molecules under sampling. This undercounting obscures numerous biological signals, such as gene-gene interactions (Zhang et al., 2019), making it extremely challenging to work with raw scRNA-seq data.

1.5.2.4.2. Batch effects

Batch effects emerge as a result of technical heterogeneity between samples. Batch effects are not unique to scRNA-seq; they occur frequently in bulk RNA-seq as well (Femino et al., 1998; Femino Andrea et al., 1998). On the other hand, batch effects are more complicated and thus more challenging to account for in scRNA-seq, because each cell might be considered a sample and thus a batch (Tung et al., 2017). Bulk RNA-seq data techniques are based on the assumption that changes in mean gene expression between batches are related to the batch effect, and should therefore be eliminated. This assumption is false for scRNA-seq data, and to address this, new, single cell-specific approaches for dealing with batch effects have been created in well-established bioinformatics tools such as limma (Islam et al., 2014).

1.6. Aims and objectives

The main goal of my thesis is to gain a better understanding of the different cell types (endocrine and non-endocrine) of the medaka pituitary. To investigate this topic, I use both a single-cell transcriptomics approach and fluorescence *in situ* hybridization (FISH) to identify cell types. I will address the overall aim through four sub aims:

1. Identification of different cell types of the medaka pituitary and evaluation of the 'one cell type-one hormone' hypothesis (paper I).
2. A complete description of the methodology including the computational analyses (paper I).
3. Development of a three-dimensional (3D) atlas of endocrine cell types of the medaka pituitary and evaluation of 'one cell type – one hormone' using FISH (paper II).
4. Characterization of the lactotrope populations in the medaka pituitary (paper III).

Methodological Considerations

2

2. Methodological considerations

The purpose of this thesis is to identify and validate the different pituitary cell types in medaka. This chapter explains how the scRNA-seq methodology, together with fluorescent *in situ* hybridization (FISH) and qPCR, was utilized to answer the main scientific questions of my study.

2.1. Experimental design

2.1.1. Medaka

A medaka transgenic line from a d-rR genetic background with the Lh β gene (*lhb*) promoter directing the production of the green fluorescent protein (*hr-gfpII*) gene (Fontaine et al., 2019; Hildahl et al., 2012) was used in the scRNA-seq study (paper I). The fish (approximately 10–12 fish in 3-L tanks) were maintained in the aquarium facilities at the Norwegian University of Life Sciences on a 14:10 h light/dark cycle at 28 °C. Fish were kept in recirculating systems and fed once with artemia (brine-shrimp) and two times with dry feed each day. The animal investigations in this study were in accordance with national regulations for animal welfare and use of experimental animals in science (based on EU directive 2010/63) (paper I, II, III). In paper II and III, wild-type (WT) medaka juveniles (aged two months) and adults (aged six months) were studied (d-rR strain).

2.1.2. Sampling and isolation of cells for single-cell RNA sequencing

Adult medaka pituitaries were extracted from 24 females and 23 males when they were almost 8 months old. On October 20th, 2017, the fish eggs were fertilized, and their pituitaries were sampled on June 6th, 2018. Medaka is sexually dimorphic and fully developed at this age. Fish were sacrificed by hypothermic shock (immersion in ice water) in the morning at 07.30–09.00 h (around spawning time, triggered by the commencement of the artificial light phase) (Kohler et al., 2017). After severing the spinal cord, the pituitary gland was dissected. To minimize the batch effect of sampling time, medaka were handled in alternate groups of 10 males and females of each sex at a time (paper I).

2.2. 10x Genomics Chromium technology

The 10x Genomics Chromium technology was used to prepare sequencing libraries from the pituitary cells. It is based on the microfluidic principles of GemCode technology. The 10x technique isolates a high number of individual cells into nanodrops utilizing an 8-channel microfluidic device and a gel bead in emulsion (GEM) technology. Each gel bead contains oligonucleotide probes that include the following: (1) sequencing primers and adapters; (2) a 14 bp barcode (10x BC) sequence to index GEMs; (3) a 10 bp UMI to index molecules; and

(4) a primer (30 bp oligo-dT) for polyadenylated (poly-A) mRNA capture (see figure 2.1d). After encapsulation, cell lysis occurs. The gel beads disintegrate and reveal their oligos for poly-dT-primed reverse transcription. As a result, each cDNA molecule has a shared barcode for each GEM, a unique molecular identifier (UMI), and a 3' end template switching oligo. Following emulsion disintegration, the pooled barcoded cDNA is amplified using primers complementary to sequencing adapters and the switch oligos. Then, sheared cDNAs are integrated into completed libraries suitable for NGS (short reads). Read 1 contains the cDNA insert, while read 2 contains the UMI (Zheng et al., 2017). Using a UMI has a number of advantages, such as identification of sampling bias, and identification and correction of PCR amplification bias. Therefore, UMI counting is the basis for 10x Genomics quantitative gene expression profiling, which represents the total number of transcripts detected (per gene, cell or sample) (Sena et al., 2018).

Cell lysis, reverse transcription, cDNA amplification, molecular labelling, and library preparation are all done in one step, and up to 10,000 cells can be processed in one Eppendorf tube at once. The 10x system, which is an alternative to the Smart-Seq2 methodology, allows for high throughput, automatic detection of single cells, barcodes, and profiling which allows for control over input and sample cells. Currently, this technology can detect approximately hundreds to thousands of genes per primary cell (see figure 2.1). Due to the platform's low cost and ease of use, 10x is now the dominant player in scRNA-seq (See et al., 2018).

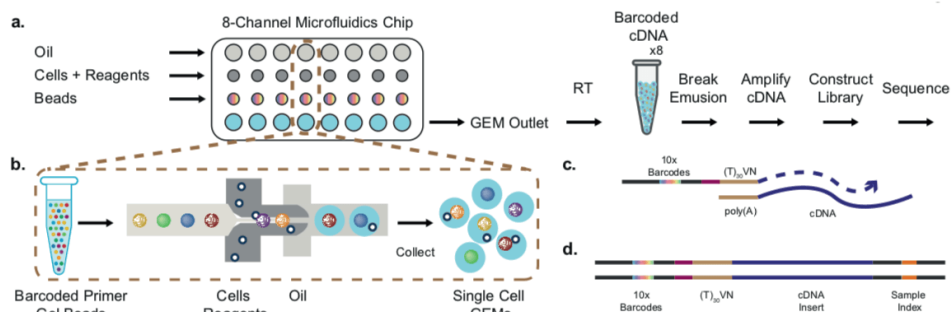


Figure 2.1: The 10x Genomics platform. (a) represents the GEM formation, RT occurs within GEMs, which are subsequently pooled for bulk cDNA amplification and library preparation. (b) indicates the GEM formation for a single cell. (c) shows oligonucleotides with barcodes included within GEMs. (d) shows the molecular structures of the final library of the 10x platform. (Figure adapted from <http://10xgenomics.com/>).

2.2.1. 10x Genomics library preparation

After sample collection, pituitaries from medaka were pooled by sex and immediately cells were isolated in accordance with the technique described in Ager-Wick et al. (2018). In summary, freshly dissected pituitaries were kept on ice until processed inside an Eppendorf tube containing customised phosphate buffered saline (PBS). Pituitaries were treated at 26 °C

for 30 minutes with 0.1 % w/v trypsin type II S, followed by 20 minutes with 0.1 % w/v trypsin inhibitor type I S combined with 2 g/ml DNase I, and then gently mechanically dissociated with repetitive aspiration using a glass pipette.

The solution containing the cells was filtered through a 35 µl cell strainer (BD Pharmingen) to eliminate any remaining leftover of the cells. These dissociated cells were suspended in 90 µl of adjusted PBS again, measured, and visually examined to ensure that the cells were properly dissociated and of acceptable quality. These samples containing female and male cells were maintained on ice for approximately half an hour prior to the library preparation for sequencing. The libraries for scRNA-seq were generated using the 10x Genomics platform at the Radium Hospital, which is part of the Oslo University Hospital Genomics Core Facility. GEMs were synthesized and barcoded in the first step of library preparation; 35 µl suspension of the cells created in the preceding stage comprised roughly 11,000 and 10,000 male and female cells, respectively. Single Cell 3' Reagents Kits (v2) by 10x Genomics were utilized for construction of libraries (cDNA) with a goal of 4,000 cells in accordance with the manufacturer's recommendations.

2.2.2. Single-cell sequencing

At the Genomics Core Facility, an Illumina NextSeq 500 was used to sequence each sample, which consisted of four redundant cDNA sequencing libraries. For read 1, 28 cycles were required (to cover the 26 nucleotides cellular barcode (16 nt) and UMI (10 nt)); for read 2, 96 cycles were required to cover the cDNA sequence. Each sample's generated FASTQ files were collected for downstream analysis.

2.3. Bioinformatic analysis

Despite the challenges discussed above in chapter 1, the technology is advancing at a breakneck pace and new statistical models and bioinformatics tools are continuously being developed. A lot of the tools that previously were developed for bulk RNAseq analysis can also be applied in the context of scRNA-seq data. However, as discussed previously, certain characteristics are unique to the single-cell approach and are inherent in the data generated by this sequencing method. The pipeline below was developed to analyse the single-cell pituitary datasets.

2.3.1. Cell Ranger

2.3.1.1. Reference genome and annotation

As output, the sequencer generates a FASTQ file containing nucleotide reads. For scRNA-seq analysis, an expression matrix is constructed in which each column corresponds to a cell, each row to a feature, and the values correspond to expression levels. To generate this matrix, a series of pre-processing steps are often performed, typically beginning with some quality control of the raw data. After aligning reads to a reference genome, the number of reads

that overlap identified features (genes or transcripts) is calculated. Individual cell quality control is critical since experiments contain low-quality cells that may be uninformative or result in misleading interpretations.

For datasets generated on its Chromium platform, 10x Genomics provides a full suite of tools called Cell Ranger to perform downstream analysis, such as alignment with the reference genome by using STAR (Dobin et al., 2012), filtering of cells, generation of feature barcode matrices, performing clustering, and cluster visualization (Loupe Cell Browser). The FASTQ files were used as input in Cell Ranger (*v 3.0.2*) and alignment was performed using the Hd-rR medaka reference genome (Ensembl release 94) supplemented with the GFP cassette sequence used to generate the transgenic line. During initial analysis, I observed that a large number of reads related to predicted pituitary-specific transcripts were aligned close to, but not within, the 3' boundary of gene annotations. Hence, reads aligned to these genes and also high expressing genes were checked manually using Samtools *v 1.10* (Li et al., 2009) and IGV (Integrative Genomics Viewer) *v 2.3* (Thorvaldsdóttir et al., 2012), and 3' UTR annotations were updated as needed (table 2.1) to improve the accuracy of transcript quantification. Afterward, Cell Ranger was run using the modified annotations (a custom gene transfer file, GTF).

Table 2.1: Genome annotation adjustments.

Gene	Ensembl ID	Feature	Original	Updated
<i>pomca</i>	ENSORLG00000025908	3' exon	2:10971088-10975672 (-)	2:10971088-10971837 (-)
<i>prl</i>	ENSORLG00000016928	3' exon	8:23591803-23592288 (+)	8:23591803-23592634 (+)
<i>smtla</i>	ENSORLG00000013460	3' exon	13:26485894-26486532 (+)	13:26485894-26486136 (+)
<i>gh</i>	ENSORLG00000019556	3' exon	8:75404-76751 (+)	8:75404-75568 (+)
<i>tshba</i>	ENSORLG00000029251	3' exon	5:13105690-13108242 (-)	5:13107640-13108242 (-)
<i>fshb</i>	ENSORLG00000029237	3' exon	3:9888850-9890682 (-)	3:9890408-9890682 (-)
<i>lhb</i>	ENSORLG00000003553	3' exon	15:14339670-14339965 (+)	15:14339670-14340309 (+)
<i>nr5a1</i>	ENSORLG00000013196	3' exon	12:24979868-24980234 (-)	12:24979864-24980234 (-)
<i>cga</i>	ENSORLG00000022598	3' exon	22:10122990-10126745 (-)	22:10126430-10126745 (-)
		alt. transcript	22:10124168-10144948 (-)	removed
<i>mdkb</i>	ENSORLG00000014169	3' exon	6:26806299-26806315 (-)	6:26805916-26806315 (-)
<i>eef1a</i>	ENSORLG00000007614	3' exon	11:17258988-17259109 (-)	11:17258988-17258678 (-)

<i>fh1a</i>	ENSORL00000005872	3' exon	3:17888694-17888835(-)	3:17888418-17888835(-)
		3' exon	3:17888677-17888835 (-)	3:17888418-17888835 (-)
		exon	3:17888057-17888070 (-)	removed
<i>mcee</i>	ENSORL00000022009	3' exon	3:17885682-17890772 (+)	3:17885682-17886310 (+)

2.3.2. Initial data analysis

Cell Ranger was rerun with a customized medaka reference genome and its QC and output are summarized in table 2.2. Additionally, Cell Ranger performed automated clustering of cells based on their similarity in gene expression pattern. The 10x Loupe Cell Browser (v 3.1.1) was used for visualization of the data, which revealed eleven and nine cell clusters for the male and female medaka pituitary, respectively.

Table 2.2: Statistics of Cell Ranger.

Type	Female	Male
Number of reads	165818560	142738097
Q30 bases in barcode	97.5%	97.4%
Q30 bases in RNA read	79.7%	80.3%
Q30 bases in UMI reads	83.4%	81.5%
Reads mapped to genome	84.1%	85.4%
Reads mapped confidently to exonic regions	59.9%	62.5%
Reads mapped uniquely to genome	82.4%	83.8%
Estimated number of cells	2890	4321
Fraction of reads in cells	83.4%	81.5%
Mean reads per cell	57376	33033
Median genes detected per cell	1182	1063
Total genes detected	17321	17775

2.3.3. Secondary analysis

However, traditional pre-processing procedures, such as alignment and cell filtering, may not be optimal for all organisms or tissues (Shainer & Stemmer, 2021). Therefore, I developed a different pipeline to analyse the pituitary data based on dropEst (v 0.8.5) (Petukhov et al., 2018) and the Seurat R toolbox (v 3.1.5) (Butler et al., 2018; Satija et al., 2015). dropEst takes aligned (.bam) files generated by Cell Ranger as an input to determine the molecular counts per cell with high accuracy.

2.3.3.1. Quality control (QC)

Individual cell quality control is essential because experiments may involve low-quality cells that are uninformative or produce misleading results. scRNA-seq data is extremely susceptible to technical artifacts: damaged cells, doublets (several cells collected together), and empty droplets are all examples of cell-like data signatures that are frequently discarded during QC (Brennecke et al., 2013; Hicks et al., 2017; Ilicic et al., 2016; Liu & Trapnell, 2016). To resolve this issue, I began by utilizing dropEst, which by default defines any barcode as a cell that has more than a hundred UMIs. Numerous non-cellular and debris barcodes are probably still included in this more permissive approach (Shainer & Stemmer, 2021). As a result, I used Seurat to analyse these data and generated a new selection process for cell barcodes based on the UMI counts, mitochondrial fraction and globin gene expression. Elevated levels of mitochondrial gene expression have been considered a sign of damaged cells (Ilicic et al., 2016; Luecken & Theis, 2019). Additionally, due to the sensitivity of single cell capture to doublet formation, I used the R package DoubletFinder (*v 2.0.3*) to identify hybrid (mixed) expression patterns in my data. The quantity of true doublets estimated is proportional to the number of cells collected. I set a 2% and 3% doublet rate for the female and male samples, respectively, based on the 10x Genomics criteria.

2.3.3.2. Normalization

Normalization is a critical step in the scRNA-seq process because it accounts for variations during the cell capture, sequencing depth (number of genes or molecules identified per cell), and other technical confounding factors. This supports the validity of subsequent comparisons of relative expression between cells (L. Lun et al., 2016). Normalization used for bulk RNA-seq data sets such as Transcripts Per Million (TPM) or Fragments Per Kilobase per Million (FPKM) scaling can be employed for scRNA-seq data, however the gene length correction is not required for UMI data because reads originate from the 3' end of transcripts. While normalisation methods such as Trimmed mean of M values (TMM) or the DESeq method can be used to discover differential expression between bulk samples, their suitability in the single-cell setting is debatable (Phipson et al., 2017). I used the LogNormalize approach developed by Seurat specifically for scRNA-seq data, which first normalizes the gene expression values for each individual gene by multiplying them with a scale factor (10,000) and then log-transforms the resulting data set.

2.3.3.3. Feature selection

The scRNA-seq is able to quantify the expression of hundreds of thousands of genes in a single cell. Nevertheless, in the majority of cases, only a subset of those shows a response to the biological state being studied, e.g., characterization of different cell types within a tissue. Due to technical noise, the majority of genes identified in a scRNA-seq experiment are detected at different levels. As a result, technical noise and batch effects can obscure the desired biological signal. Thus, feature selection is helpful in order to filter genes that reflect technical noise from downstream analysis. Not only does this correct the signal-to-noise ratio of the data

in general, but it also minimizes the computing complexity of investigations by reducing the overall amount of data to be processed. These features are frequently chosen based on their variability across the dataset. Therefore, I used the variance stabilizing transformation (VST) method to identify genes that were highly variable in male and female data, respectively.

2.3.3.4. Clustering

Clustering of cells is a critical step in the analysis of scRNA-seq data, which is often not required with bulk RNA. This has been incorporated as a key step in the pipeline created for scRNA-seq analysis. Several methods for clustering of cells have been developed, addressing a variety of technical and biological difficulties (Kiselev et al., 2019). All of these approaches aim to cluster cells with identical gene expression profiles, resulting in clusters of cells of a similar type. The most often used methods in this area are principal component analysis (PCA) (Pearson, 1901), t-distributed stochastic neighbourhood embedding (t-SNE) (van der Maaten, 2008) and the uniform manifold approximation and projection algorithm (UMAP) (Becht et al., 2019). Due to its performance, particularly on UMI datasets, the clustering method provided in the Seurat package has gained broad acceptance (Satija et al., 2015). This method begins with the identification of a set of highly variable genes and is followed by PCA. Following that, a set of dimensions is picked that accounts for the majority of the variation in the dataset. To cluster cells, a Louvain optimisation algorithm is applied to the graph, with a resolution parameter dictating the number of clusters generated. Selecting the appropriate parameters is challenging yet critical, as the number of clusters chosen may have an effect on how the results are interpreted.

2.3.3.4.1. Principal component analysis (PCA)

PCA is a statistical method to reduce the dimensionality of big data by identifying a sequence of uncorrelated and ordered projections. These projections are referred to as principal components (PCs), with the first principal component exhibiting the highest variance. By focusing exclusively on the top principal components, the data is projected onto a lower-dimensional space while retaining a significant amount of variance. This contributes to the reduction of the dimensions of our multidimensional data while also removing some noise. This is a critical step before grouping the cells. I have used the jackStraw function to identify important PCs based on the variable genes ($n = 2000$) identified using the VST method in Seurat.

2.3.3.4.2. Uniform manifold approximation and projection algorithm (UMAP)

For both female and male datasets, I selected ten PCA dimensions as the input to project the cells in lower dimensions. I used the UMAP projection in this study to generate comparably accurate representations of the cellular space, particularly when it comes to separate the cell populations defined by subtle differences. Additionally, UMAP preserves more of the global structure and runs faster than t-SNE. As a result, UMAP is widely used and has been integrated

into many scRNA-seq data analysis pipelines (Kiselev et al., 2019). Following the dimension reduction, I used the *FindClusters* function to cluster the cells using a resolution of 0.5 for the female sample and 0.9 for the male sample to identify distinct clusters.

2.3.3.5. Cell type assignment

After clustering the cells, the next step is to interpret what these clusters represent. This is typically accomplished by finding genes that are differentially expressed between clusters or marker genes that are expressed within an individual cluster. For assignment of potential cell type identities to the abovementioned clusters, I applied *FindAllMarkers* to find differentially expressed genes (DEGs) for each cluster with default parameters, and used previously known marker genes (paper I, III).

2.3.3.5.1. Subclustering

Unbiased subpopulation finding is one of the most prominent applications of scRNAseq. Separating these clusters, however, may be difficult in the context of reduced borders between subpopulations, for a variety of reasons, one of which being the constraint of dimensionality. With an increase in the number of genes quantified, the distance between data points (cells) decreases, resulting in poorly defined clusters (Buettner et al., 2015; Kiselev et al., 2019). In this study, I identified multiple clusters that shared common markers. Therefore, I studied their heterogeneity further by iterating on subsets of the data using the clustering algorithms at different resolutions. To underline the differences between each of the sub-clusters, I identified the genes that were differentially expressed between them and eventually established cell-type boundaries for these subclusters.

2.3.3.6. Integration of both datasets

Both datasets were merged by using *FindIntegrationAnchors* and *IntegrateData* functions in Seurat with default parameters (paper I, III) to determine whether the male and female medaka pituitary cells are comparable.

2.4. Quantitative polymerase chain reaction

Gene expression quantification is a critical and frequently used approach that enables the analysis of the state of various biological processes under specified conditions. Among the most popular methods of transcript quantification are Northern blot (Alwine et al., 1977; Pall & Hamilton, 2008), quantitative reverse transcription PCR (RT-qPCR), RNase protection assays (Emery, 2007), serial analysis of gene expression (SAGE) (Velculescu Victor et al., 1995), microarrays, and RNA sequencing (RNA-seq). These techniques vary in terms of their sensitivity, specificity, and throughput. For example, Northern blot is a reasonably sensitive, but imprecise and low-throughput technique. Similarly, RT-qPCR is a highly sensitive, specific, rapid, and reproducible RNA quantification technique (Ginzinger, 2002). RT-qPCR

is the most widely used approach for gene expression analysis, owing to its simple and standardized protocols. Nevertheless, RT-qPCR is a low-throughput technique that allows simultaneous analysis of only a few genes. High-throughput methods such as microarrays and RNA-seq are more suitable for transcriptome-wide gene expression analysis. When comparing RNA-seq to qPCR, the important difference is discovery capability. While both methods are extremely sensitive and reliable for detecting variants, qPCR can detect only known sequences. By contrast, RNA-seq is a hypothesis-free technique which requires no prior knowledge of sequence information. RNA-seq also enables the identification of novel genes and the quantification of uncommon variants and transcripts with increased sensitivity. Nonetheless, RT-qPCR provides a complementary method to validate the candidates identified from RNA-seq analysis.

Therefore, in this study, the qPCR technique was used to quantify mRNA expression levels of seven hormone-encoding genes (*lhb*, *tshb*, *fshb*, *pomca*, *prl*, *gh*, and *sl*) which were found to be differentially expressed after *in silico* analysis. Firstly, the messenger RNAs were extracted from pituitary tissue and reverse transcribed into complementary DNA (cDNA). The cDNA was used to perform qPCR analysis using gene-specific primers (table 2.3) designed for each target. A LightCycler 480 Real-Time PCR System (Roche, Mannheim, Germany) with SYBR Green I Master (Roche) detection (paper II) was used in this study for quantification. Briefly, we first incubated the samples for 10 minutes at 95 °C, followed by 42 cycles of 95 °C for 10 s, 60 °C for 10 s, and 72 °C for 6 s. Each RT-qPCR run was followed by a melting curve analysis to ensure that each sample contained a specific product amplified by RT-qPCR.

Table 2.3: Primer sequences used to analyze the mRNA levels.

Gene Name	Sequence (5' - 3')	Ensembl Gene Name	Accession Number (NCBI/Ensembl)	Amplicon size (bp)	Efficiency
<i>rpl7</i>	F: TGCTTTGGTGGAGAAAGCTC R: TGGCAGGCTTGAAGTTCTTT	<i>rpl7</i>	NM_001104870 ENSORLG00000007967	98	2.03
<i>prl</i>	F: TCAGATGGGAACCAGAGGAC R: GATGTCCACGGCTTTACACA	<i>prl1</i>	XM_004071867.4 ENSORLG00000016928	85	1.987
<i>tshba</i>	F: ATGTGGAGAAGCCAGAATGC R: CTCATGTTGCTGTCCCTGA	<i>tshba</i>	XM_004068796.4 ENSORLG00000029251	88	2
<i>lhb</i>	F: CCACTGCCTTACCAAGGACC R: AGGAAGCTCAAATGTCTTGTAG	<i>lhb</i>	NM_001137653.2 ENSORLG00000003553	100	2
<i>fshb</i>	F: GACGGTGCTACCATGAGGAT R: TCCCACTGCAGATCTTTTC	<i>fshb</i>	NM_001309017.1 ENSORLG00000029237	73	2.03
<i>gh</i>	F: TCGTCTTTGTCTGGGAGTT R: ACATTCTGATTGGCCCTGAT	<i>gh1</i>	XM_004084500.3 ENSORLG00000019556	102	1.94
<i>pomca</i>	F: GTGGTGGTTGTCGGTGGG R: GTGAGGTCAGAGCGGCAG	<i>pomca</i>	XM_004066456.3 ENSORLG00000025908	122	1.956
<i>sl</i>	F: CACCAAAGCATTACCCATCC R: ACCAGCATCAGCACAGAATG	<i>smtla</i>	NM_001104790.1 ENSORLG00000013460	87	1.965

Correct mRNA quantification requires data normalization, which eliminates variations in extraction yield, PCR amplification rate and reverse transcriptase activity (Bustin et al., 2009; Vandesompele et al., 2002). The commonly applied approach of normalization is to compare gene expression data to so-called reference genes. Reference genes should have consistent mRNA expression across a range of experimental settings, tissues, cells, and life cycle stages (Derveaux et al., 2010). As a result, proper selection is critical for the normalization of data. However, there is no general reference gene and numerous studies have demonstrated that regularly used reference genes are not always expressed consistently (Chapman & Waldenström, 2015; Kozera & Rapacz, 2013), indicating that reference genes must be chosen uniquely for every experimental setting and organism (Liang et al., 2014). Additionally, literature search is an ineffective strategy to select them and cannot be applied in the majority of instances. Regardless, new research is using RNA-seq to examine complete transcriptomes in order to uncover novel candidate reference genes (Jureckova et al., 2021). We used the *rpl7* gene as a reference gene to normalize the mRNA level as no significant variation in its expression was observed among the groups (adult, juvenile, females and males).

2.5. Fluorescence *in situ* hybridization (FISH)

In situ hybridization (ISH) is a technique used for identifying nucleotide sequences within single cells, tissue segments, or entire tissue. This approach is based on a nucleotide probe's complementary binding to a specific RNA or DNA target sequence. These probes can be fluorescently or radioactively labelled. PCR-generated double-stranded DNA probes, single-stranded antisense RNA probes (riboprobes) and single-stranded DNA probes all are examples of probes that can be employed. Visualization is accomplished by autoradiography, fluorescence microscopy, or immunohistochemistry, depending on the probe used. *In situ* hybridization was initially used to investigate nucleic acids in 1969 (Bartlett, 2004; John et al., 1969; Langer et al., 1981; Pardue & Gall, 1969). This technique is now an important component of biological research. The spatial information collected through this method has significantly aided researchers in their understanding of a wide variety of research fields, including gene mapping, gene expression, and development.

In this study, fluorescent *in situ* hybridization (FISH) was used to determine the spatial arrangement of hormone-producing cell types in the medaka pituitary gland. Fluorescent protocols have the advantage of being able to work with several colours (Hopman et al., 1998; Speel et al., 1999; Speel et al., 1997), which enables the simultaneous observation of several targets necessary for investigating genes co-expressed in similar cell types, demonstrated in paper II. Previously, the single-labelling techniques and non-species specific antibodies used to examine endocrine cell populations did not provide sufficient detail on either the organization of various endocrine cell populations, nor on the possibility of bi-hormonal cells as reported in mammals (Childs, 1991; Childs, 2002; Frawley & Boockfor, 1991; Fukami et al., 1997). Therefore, a multi-colour FISH approach was used in this study with complementary RNA probes to localize all endocrine cell types of pituitaries (except *pomca*-expressing cells).

Briefly, the tissue was prepared first, followed by the synthesis of the RNA probes. The probes retrieved from NCBI (National Center for Biotechnology Information) are shown in table 2.4. For hormone-encoding genes with multiple paralogs in the genome of medaka, sequences were chosen based on their high expression in the pituitary (*tshba* and *pomca*). Primer3 (<https://primer3.ut.ee/>) was used to design PCR primers to amplify the probe genes from their transcribed sequences (mRNA). The absence of labelling with sense probes was used to verify the specificity of the anti-sense probes. Immunofluorescence (IF) and FISH were employed to identify alpha-melanocyte stimulating hormone (α -Msh) and adrenocorticotrophic-releasing hormone (Acth) cells inside *pomca*-expressing cells.

Table 2.4: Primer sequences used for making the in situ hybridization (ISH) probes for seven hormone-encoding cell types.

Gene Name	Sequence (5' - 3')	Ensembl Gene Name	Accession Number (NCBI/Ensembl)	Amplicon size (bp)
<i>lhb</i>	F: CACAGCCTGCAGATACATGAG R: AGGAAGCTCAAATGTCTTGTAG	<i>lhb</i>	NM_001137653.2 ENSORLG00000003553	318
<i>fshb</i>	F: GAGGAAGCAACACTTTCAGC R: GCACAGTTTCTTTATTCAGTGC	<i>fshb</i>	NM_001309017.1 ENSORLG00000029237	500
<i>pomca</i>	F: ATGTATACCGTTTGGTTGCT R: AAATGCTTCATCTTGTAGGAG	<i>pomca</i>	XM_004066456.3 ENSORLG00000025908	515
<i>sl</i>	F: CCCATCTTTTCACTGTAAGT R: ATACTGGAAGGCACCTTGTT	<i>smtla</i>	NM_001104790.1 ENSORLG00000013460	506
<i>prl</i>	F: GAAAGACCGAGGAGGAACTG R: TTGCAGAGTTGGACAGGACC	<i>prl1</i>	XM_004071867.4 ENSORLG00000016928	381
<i>gh</i>	F: TCTCTGCAGACTGAGGAACA R: AGCCACAGTCAGGTAGGTCT	<i>gh1</i>	XM_004084500.3 ENSORLG00000019556	501
<i>tshba</i>	F: ACAGGCTAAACTCAAGTTAA R: AGGATCATATAGGTGCTCTG	<i>tshba</i>	XM_004068796.4 ENSORLG00000029251	473

2.5.1. RNAscope

In addition, we used multiplexed RNAscope *in situ* hybridization to visualize tissue localization of mRNA expression for selected genes: *prl*, *sox2* and *mala*. This technology employs a novel probe design method that enables simultaneous signal amplification and noise suppression, allowing for single-molecule detection while conserving tissue morphology (paper III) (Wang et al., 2012). RNAscope *in situ* hybridization (Wang et al., 2012), multiplex (v 2), was performed as instructed by Advanced Cell Diagnostics using opal 520, 570 and 690 labels on the adult (six months old) female medaka. An LSM 810 Zeiss confocal microscope with a 25 \times objective was used to take images. The confocal images were processed in Fiji (Schindelin et al., 2012) and combined using Adobe Indesign.

2.5.2. Image analysis

Fluorescent images were obtained using an LSM710 Confocal Microscope (Zeiss) with 25× (for adult pituitary) and 40× (for juvenile pituitary) objectives, which enables the acquisition of high-quality images with a very low background by utilizing spatial pinholes to exclude out of focus light. The microscope progressively captures the fluorescent signal generated by the probes. This is especially beneficial for analysing the expression of many genes from the same cell type in co-localization investigations (paper II, III). ZEN software (*v 2009*, Zeiss) was applied to handle the images acquired with the microscope, while ImageJ (<http://rsbweb.nih.gov/ij/>) was used to handle z projections from confocal image stacks.

2.5.3. Volumetric analysis of cell types

Cell volumes were calculated using ImageJ from pituitary image stacks with $n = 4-8$ in each group. The object volume was calculated by multiplying the slice's area by its depth. By summing the population volumes of each slice, the absolute volume of every population was determined. The relative volume of each population was then calculated as a percentage of the overall pituitary volume (as assessed by DAPI staining) (paper II, III).

2.5.4. 3D atlas

The images of juvenile medaka pituitaries were taken as one block, whereas the images of adult pituitaries were taken utilizing confocal imaging from the ventral and dorsal sides, as previously described, and later these two sides were united using DAPI-stained landmarks. Finally, eight pituitaries identified with different markers were aligned using manually selected landmarks to the same coordinate system. These data were used to generate 3D atlases of the pituitary gland (paper II).

Results - summary of articles

3

3. Results – summary of articles

3.1. Paper I: characterization of medaka pituitary cell types

The major purpose of this study was to characterize the different cell types making up the medaka pituitary gland, and an evaluation of the ‘one cell type-one hormone’ hypothesis. Each hormone is believed to be produced by a distinct cell type in the teleost pituitary. I addressed this question by producing and analysing scRNA-seq data from female and male adult medaka pituitary glands. We characterized 15 and 16 different cell types in the female and male pituitaries, respectively, based on similarity in expression, of which 10 are associated with the production of peptide hormones. These biological function assignments mostly confirmed the ‘one cell type – one hormone’ division of labour, according to which key hormones are synthesized by a single dedicated cell type. There were, however, a few notable exceptions, which I explore in paper II. The data presented in this work serve as a solid foundation for future research on pituitary biology and hormone regulation in fish and other vertebrates.

3.2. Paper II: medaka pituitary 3D atlas

This study provides comparative and precise information about the spatial distribution and localization of several cell types, which is necessary for a comprehensive understanding of their physiological roles. It presents the first three-dimensional (3D) atlas of seven hormone-producing cell types (Fsh and Lh gonadotropes, lactotropes, thyrotropes, *pomca*-expressing melanotropes and corticotropes, and somatotropes) which are located in the anterior part of the medaka pituitary by combining scRNA-seq data and multi-colour fluorescence *in situ* hybridization (FISH). We detected sexual dimorphism by analysing the 3D position of *lhb*, *pomca*, and *tshba*-expressing cells in the fully mature medaka pituitary. Additionally, using *in situ* hybridization and scRNA-seq data, we demonstrated the presence of bi-hormonal cells co-expressing *fshb-tshba*, *lhb-sl*, and *lhb-fshb*. However, unlike in the mammalian pituitary, this study discovered no multi-hormonal cell population, confirming the ‘one cell type – one hormone’ hypothesis in teleosts.

3.3. Paper III: classification of prolactin populations

The focus of this study was the *prl*-expressing (lactotrope) cell populations that we identified from scRNA-seq data (paper I). The cells producing the hormone prolactin are typically localized in the most anterior part of the pituitary (the RPD). However, in several species, smaller satellite populations of *prl*-expressing cells have been described in other parts of the pituitary. Here, we described a similar phenomenon in medaka. We characterized the prolactin populations by using both scRNA-seq data and the *in-situ* technique. Firstly, we discovered two types of *prl*-expressing cells in the scRNA-seq data, which we named primary and secondary lactotropes. Based on the UMAP visualization, the primary lactotropes are

similar in expression profile to cells expressing either growth hormone or somatolactin. In contrast, the secondary lactotropes are similar in expression profile to stem-cell-like populations, which express the *sox2* and *mala* genes. Furthermore, a detailed analysis of the transcriptome data suggests that the secondary lactotropes may be a technical artifact. These cells express more genes and have a larger read count, implying that the secondary population was created by the droplet-based microfluidic devices used to prepare the scRNA-seq libraries. We investigated this hypothesis using RNAscope *in situ* hybridization, using probes for both *prl* and *mala*. Surprisingly, we found that lactotrope cell clusters do, in fact, consist of both primary (*prl*⁺ *mala*⁻) and secondary (*prl*⁺ *mala*⁺) lactotropes. In addition, we found non-RPD lactotrope clusters, which also show this composition. Taken together, the results presented in this paper suggest that prolactin cell clusters are heterogenous and developmentally dynamic.

General discussion and implications

4

4. General discussion and implications

The study described in this thesis provides a characterization of existing and novel pituitary cell types in medaka, and the comprehensive transcriptional profiling of these cell types using scRNA-seq. Additionally, it contains a validation of hormone-producing cell types by *in situ* hybridization (FISH) and subsequent use of these data to develop a three-dimensional (3D) atlas demonstrating the spatial distribution of these cell types in the pituitary.

4.1. Characterization of the pituitary gland

The current understanding of the pituitary gland function is based on the idea that each endocrine cell type is devoted to producing and releasing a single peptide hormone (Cheung et al., 2018; Ho et al., 2020). Each cell type is thought to have a particular function and be regulated by a distinct array of hypothalamic-pituitary regulatory circuits (Ho et al., 2020; Weltzien et al., 2004). Several studies, however, have revealed that the pituitary cell types responsible for producing various hormones may be more structurally and functionally complex than previously known (Cheung et al., 2018; Childs, 2000; Seuntjens et al., 2002). Additionally, the complexity and prevalence of ‘multi-hormone’ cells in teleosts’ adult anterior pituitary have remained unclear on a structural and functional level. Therefore, more research is required to characterize the composition and function of pituitary cells and their relationship to hormone production. In this study, we used medaka because fish (and other vertebrates) share numerous physiological similarities regarding pituitary function, so that the medaka pituitary can be used as a model organism for other species.

The work presented in paper I describes the transcriptomic profiling of the adult medaka pituitary gland at the cellular level using the 10x Genomics platform. The pituitary gene expression profiles of individually isolated female and male cells were sequenced. The female and male pituitaries contained 15 and 16 different cell types, respectively, 10 of which are engaged in peptide hormone synthesis. Apart from the endocrine cell types mentioned above, the anterior pituitary contains many non-endocrine cell types, including progenitor/stem cells, folliculo-stellate (FS) cells and endothelial cells (Denef, 2008; Gleiberman et al., 2008; Ho et al., 2020). We found red blood cell and white blood cell clusters in the scRNA-seq data and showed the vascularization in the 3D atlas (paper II). Such a complex vasculature is crucial for the pituitary’s endocrinological functions, since it enables the effective distribution of generated hormones to peripheral organs. Additionally, this may aid in intra-pituitary signalling. This finding is consistent with previous zebrafish observations indicating a highly vascularized pituitary (Golan et al., 2015; Gutnick et al., 2011). Traditionally, the *s100* gene has been used to identify the FS cells (Inoue et al., 2002; Itakura et al., 2007; Traverso et al., 1999); however, this gene has at least eight homologs in the medaka genome, the majority of which do not exhibit a clear pattern of expression in my scRNA-seq data. Lastly, a cluster of 21 cells is absent from the female data but exists in the male data. According to a recent study

in our group, this cell type is present in younger females but not in adults and has a role in lipid homeostasis or transport (Ager-Wick et al., 2021).

4.1.1. One cell type-one hormone hypothesis

The above functional classifications often favour the hypothesis of ‘one cell type – one hormone’, which states that a single, distinct cell type produces a specific hormone in the pituitary. By contrast, a single cell type in the mammalian pituitary generates and secretes multiple hormones (Cheung et al., 2018; Ho et al., 2020). While scRNA-seq was used to characterize the pituitary of zebrafish, the study did not investigate the presence of multihormonal cells (Fabian et al., 2020). Multihormonal cells have previously been identified in the mouse pituitary using scRNA-seq technology, (Ho et al., 2020), but never in a teleost.

In paper II, a detailed analysis of the medaka scRNA-seq data revealed a small number of bi-hormonal cells and a minimal number of multihormonal cells. By using *in situ* hybridization, we showed the existence of gonadotrope cells co-expressing *fshb* and *lhb*, as previously established in medaka (Fontaine et al., 2020) and other teleost species (Candelma et al., 2017; Golan et al., 2014; Pilar García Hernández et al., 2002). Additionally, I identified cells co-expressing *sl-lhb* and *fshb-tshba*, consistent with earlier immunohistochemistry findings on the pituitary glands of many teleost species, which revealed cross-reactivity among Lh/Fsh and Tsh antibodies (Batten, 1986; Quesada et al., 1988) and between Sl and Lh antibodies (Batten et al., 1975; Batten, 1986; Cambré et al., 1986; Margolis-Kazan et al., 1981). The discrete labelling of *fshb*, *tshba*, *sl*, and *lhb*-expressing cells shown in paper II confirmed the specificity of FISH probes. Thus, the colocalization of *sl-lhb* and *fshb-tshba* confirms the existence of these bi-hormonal cells in the medaka pituitary. Moreover, numerous studies have demonstrated cells co-staining for Prl, Gh, and Sl (García-Hernández et al., 1996; Honji et al., 2013; Ishwar et al., 1998; Naito et al., 1983; Takahiko & Yoshihiko, 1995). Our scRNA-seq results, however, only showed co-expression of *prl* and *gh* in a small number of cells.

In addition, a subset of cells in the pituitary expresses more than two hormone-encoding genes. This is the first time such multihormonal cells have been identified in a teleost pituitary on the transcriptomic level. This contrasts with the mammalian pituitary, which contains a big cluster of multihormonal cells (Cheung et al., 2018; Ho et al., 2020). Because of their low incidence in the scRNA-seq data, we could not validate the existence of these multihormonal cells using FISH. The occurrence of multihormonal cells is likely related to pituitary plasticity, the processes through which the number of cells in the pituitary gland changes in response to physiological demands. It is thought that these multihormonal cells could derive from progenitor cells, in which a partially differentiated transitory state enables the expression of several hormone-encoding genes. The discovery of a multihormonal cell cluster expressing a progenitor cell marker (*pou1f1*) in the mammalian pituitary supports this hypothesis (Ho et al., 2020); however, only very low expression of *pou1f1* (ENSORLG00000015870) was observed in lactotropes and somatotropes in our medaka scRNA-seq data. Since cell cluster identification requires a substantial number of distinct cells, and the data from medaka scRNA-

seq revealed just a few multihormonal expression profiles, this could account for the lack of multihormonal cell cluster identification in teleosts (paper II).

4.1.2. Reproducibility of scRNA-seq data

In order to assess the technical reproducibility of transcriptomics studies on the medaka pituitary, I compared the scRNA-seq data to bulk RNA-seq data for comparable samples (sex and age). On the whole the gene expression profiles remain qualitatively consistent (Spearman rank correlation 0.80 – 0.87). However, the library preparation approaches (3'-specific 10x Genomics versus full transcript Smart-SEQ) obviously have an effect on the quantitative expression levels, which makes a detailed direct comparison challenging.

4.2. Characterization of prolactin populations

During the cell type characterization described in paper I, we detected two clusters with *prl* gene expression (lactotropes) in the adult medaka pituitary using scRNA-seq. Prolactin has been described as the 'freshwater-adapting hormone' in teleost fishes, regulating ion conservation and water secretion mechanisms (Breves et al., 2014; Shu et al., 2016). While *prl* gene expression was found originally in the pituitary's RPD area, numerous fish species contain patches of *prl*-expressing cells in non-RPD locations, for example coho (Farbridge et al., 1990), seabass (Cambré et al., 1986), chum salmon (Naito et al., 1983; Wagner & McKeown, 1983), common barbel (Toubeau et al., 1991), striped bass (Huang & Specker, 1994) and gilt-head seabream (Quesada et al., 1988). In paper III, we described a similar phenomenon in the medaka pituitary and focused on the differences among these prolactin populations using scRNA-seq data and *in situ* hybridization (FISH).

The scRNA-seq data reveal two distinct *prl*-expressing populations, which we called primary and secondary lactotropes. Based on the UMAP visualization, the primary lactotropes are similar in expression profile to cells expressing either growth hormone or somatotactin. In contrast, the secondary lactotropes are similar in expression profile to stem-cell-like populations, as they express *sox2* (SRY-box transcription factor 2: ENSORLG00000001780) and *mala* (encoding MAL, the myelin and lymphocyte T-cell differentiation protein: ENSORLG00000003048) (Andoniadou et al., 2013; Rizzoti et al., 2013). A detailed analysis of the transcriptome data indicates that the secondary lactotropes may be a technical artifact. Their higher gene expression and read counts lead us to hypothesize that they were doublets produced by the droplet-based microfluidics used to prepare the scRNA-seq library. Technical artifacts are undesirable when characterizing populations at the single-cell level. In particular, they may be confused for non-existent transitional populations or transitory periods. The particular doublets we found could conceivably arise as a result of incomplete cell dissociation, or as a result of high and specific *in vitro* affinities between two constituent cell types.

We found co-expression of *mala*, *sox2* and *pit1* (ENSORLG00000001430) in the secondary prolactin population. In mammals, it has been reported that the five hormone-producing

populations in the mature anterior pituitary gland originate from a *sox2*, *prop1*-progenitor cell population and differentiate during development to form separate cell types (Cheung et al., 2018). Together with the trajectory-like placement in the UMAP visualization, this suggests that the secondary lactotropes are developmental intermediates between progenitor cells and primary lactotropes.

To test these alternative hypotheses (artifact or developmental intermediate), RNAscope *in situ* hybridization was used to investigate the spatial distribution patterns of *prl*, *sox2*, and *mala* gene expression. We found *mala* and *prl* to be co-expressed, with *mala* higher expressed in the centre of the RPD prolactin population. Here, *prl* expression was lower, which is consistent with the expression profile of the secondary lactotropes in our transcriptomics data. Due to the co-expression of the markers inside individual cells, this refutes our assumptions about artifactual hybrids and establishes the secondary lactotropes as an actual distinct population of cells in the medaka pituitary.

Using the *in situ* technique, a few *prl* expressing cells were detected in the non-RPD area of the pituitary, consistent with observations in other species. These cell populations have the same composition as the major (RPD) population, with both *mala*⁺ and *mala*⁻ cells. The primary and secondary lactotropes therefore do not correspond to these major and minor populations, respectively.

Next, the RNAscope analysis of *sox2* indicated a high level of expression in the brain, but just a few cells expressing *sox2* in the adult pituitary. These were primarily localized in the dorsal part of the PPD, which agrees with a previous study investigating Sox2 protein location in the medaka pituitary (Fontaine et al., 2019). However, *sox2* labelling was never observed in the *prl*-expressing cells (RPD/non-RPD region), which is in disagreement with our transcriptomics findings. This could be explained by a lower level of *sox2* expression in the *prl/mala*-expressing population than in the brain, which could be below the detection limit with the RNAscope.

This spatial and transcriptional heterogeneity among *prl*-expressing clusters may be consistent with the developmental scenario described previously. Our results therefore suggest that pituitary lactotrope clusters, in general, are plastic and capable of adapting to changing demands – which, however, remain to be elucidated.

4.3. 3D atlas of the teleost pituitary

Spatialization of endocrine cell types in the pituitary of teleosts has been documented in various species during the last five decades. However, these pituitary endocrine cell maps differ in the cell types represented, despite the overall similarity among the pituitaries of different species. While these studies revealed many details about the spatial distribution of hormone-encoding cell populations, they were limited by the methodologies available at the time. Therefore, the study in paper II focused on the spatial distribution (three-dimensional: 3D atlas)

of seven endocrine cell types in the juvenile and adult medaka pituitary after the identification and classification of cell types and their specific markers using scRNA-seq data. This adds to an earlier 3D atlas of pituitary gland development in zebrafish (Chapman et al., 2005). Ours is the first atlas to detail the location and architecture of the various endocrine cell types (thyrotropes, gonadotropes, lactotropes, somatolactotropes, melanotropes, and corticotropes) within the pituitary gland of teleost fish. The endocrine cells of the teleost pituitary are distributed in discrete zones, which is in contrast to mammals. The RPD contains corticotropes and lactotropes, while the PPD contains gonadotropes, somatotropes, and thyrotropes. In addition, somatolactotropes and melanotropes are frequently present in the PI.

Notably, in our atlas, we detected Lh gonadotropes not only in the PPD, but also in the PI (only in adults); no Lh cells were detected in the RPD, as some previous research claimed (Borella et al., 2009; Camacho LR, 2020; Dubourg et al., 1985; Olivereau & Nagahama, 1983; Sánchez Cala et al., 2003). The extra-PPD location of Lh gonadotropes could result from the PPD being extended into the PI (F.-A. Weltzien et al., 2003) or of Lh cells migrating to other zones throughout the adenohypophysis' ontogeny (Nozaki et al., 1990). Other investigations have demonstrated the presence of somatotropes in the RPD (Grandi et al., 2003; Huang & Specker, 1994) and PI, as well as somatolactotropes and melanotropes in the teleost PPD (Camacho LR, 2020; García-Hernández et al., 1996; Honji et al., 2013; Sánchez Cala et al., 2003; Segura-Noguera et al., 2000). However, this was not observed in medaka before. The online 3D atlas platform will enable researchers to better understand the spatial distribution of hormone-producing cell types and vascularization in the pituitary.

4.3.1. Sexual dimorphism

Multiple gender-specific developmental and physiological factors affect the production and secretion of pituitary hormones. These regulatory mechanisms are responsible for essential somatic changes associated with puberty, the reproductive cycle, pregnancy, and (in mammals) breastfeeding. It is unknown to what extent these gender-specific roles are associated with changes in the cellular composition of female and male pituitaries (Lamberts and Macleod, 1990; Nishida et al., 2005). Our scRNA-seq data showed high similarity of female and male pituitary glands at the level of cell types, with some minor differences observed in our 3D atlas. In the 3D atlas, we identified sexual dimorphism in cell populations expressing *tshba*, *pomca*, and *lhb*. For example, we demonstrated for the first time that adult females have the largest *tshba*-expressing cell volumes, while adult males had the largest *pomca*-expressing cell volumes. Our qPCR data further confirmed the *tshba* and *pomca* levels that support past medaka studies on sexual dimorphism (Martin et al., 1999; Ohta et al., 2008). No sexual dimorphism for *tshb* or *pomc* has been found in zebrafish (He et al., 2014).

General conclusions

5

5. General conclusions

The findings in this thesis characterize the medaka pituitary gland using *in silico* and *in vitro* approaches, thereby contributing to deeper understanding of the complexity of the teleost pituitary. We successfully characterized various cell types in the medaka pituitary, each of which produces a distinct hormone in the **paper I**. In this paper we also describe the design choices behind the computational scRNA-seq analysis pipeline. Through a series of in-depth data analyses in **paper I & II**, we confirmed that the teleost pituitary is characterized by a ‘one cell type – one hormone’ division of labour, which is in contrast to the mammalian pituitary. In **paper II** the first 3D atlas of hormone-encoding cell types was developed using the *in situ* technique, providing an online platform for examining the spatial distribution of different cell types of the medaka pituitary. Finally, in **paper III**, we characterized the two different prolactin cell populations by both transcriptomics and *in situ* data. We found that the prolactin populations are heterogenous, which may explain the developmental plasticity of lactotropes.

Future perspectives

6

6. Future perspectives

The discoveries in this study fill many gaps in our knowledge related to pituitary cell type composition and their spatial distribution, but also raised new questions.

We demonstrated the existence of multiple prolactin-producing cell populations, and cellular heterogeneity within these. It is not known what causes or necessitates this diversity. As prolactin is known to regulate adaptation to freshwater, and medaka tolerates a wide range of salinity conditions, it would be interesting to investigate whether lactotrope heterogeneity is affected by changes in salinity. This could be accomplished by conducting a salinity adaptation experiment. From juvenile to adult, fish can be raised under a variety of conditions, including freshwater, isotonic water, and seawater to test the hypotheses that increasing the salinity level would decrease *prl* gene expression or cell number in both prolactin populations.

We employed a single time point (adult fish) to describe different cell types using scRNA-seq. To be able to study developmental dynamics and adaptation in detail, it would be interesting to include additional time points, for example 3, 6 and 8-months old fish. This extended data would be useful for the further characterization of cell types and to establish ‘trajectories,’ i.e., paths through the high-dimensional expression space that pass through cellular states associated with a continuous process such as differentiation (Van den Berge et al., 2020). In paper III, we demonstrated that the secondary lactotropes express *sox2* and *mala* and are in close contact (by UMAP dimensions) with the stem cell populations (which also express these genes). It would be interesting to use data from different time points and conditions to investigate whether this contact corresponds to a developmental path between these populations. In addition, it will help to evaluate the concept that progenitor cells differentiate into endocrine cell types.

In this study we combined the scRNA-seq data and *in situ* hybridization to develop a 3D atlas from juvenile to adult fish pituitary. Because cells are dissociated prior to scRNA-seq, it has been challenging to connect the transcriptomes back to their original positions at single-cell resolution. Over the last decade, technologies have evolved that bridge the gap among traditional techniques that hold spatial information (such as immunofluorescence and *in situ* hybridization) and novel methodology that enables simultaneous querying of the whole transcriptome in individual cells. Until recently, high-throughput approaches could not be employed *in situ*, resulting in the loss of information on the spatial relationships between the documented populations. However, methods for sequencing library preparation on microscope slides have enabled the linking of transcriptomic and spatial data. The advent of this unique approach, known as spatial transcriptomics, has aided in discovering novel mechanisms in various domains ranging from neurology to physiology (Rao et al., 2021). It would be exciting to further develop the medaka pituitary atlas using this advanced technology, which will provide complete cell type characterization and spatial organization together in one platform.

The overall impact of this thesis will be to increase fundamental understanding of the pituitary's complexity. In the longer term, this fundamental knowledge can help the aquaculture industry to address issues related to fish physiology, such as sexual maturation and reproduction, and lead to more sustainable farming.

References

7

7. References

- Adams, J. (2008). Complex genomes: Shotgun sequencing. *Nature Education* 1(1), 186.
- Ager-Wick, E., Dirks, R. P., Burgerhout, E., Nourizadeh-Lillabadi, R., de Wijze, D. L., Spink, H. P., van den Thillart, G. E. E. J. M., Tsukamoto, K., Dufour, S., Weltzien, F. A., & Henkel, C. V. (2013). The Pituitary Gland of the European Eel Reveals Massive Expression of Genes Involved in the Melanocortin System. *PLOS ONE*, 8(10), e77396.
- Ager-Wick, E., Henkel, C. V., Haug, T. M., & Weltzien, F. A. (2014). Using normalization to resolve RNA-Seq biases caused by amplification from minimal input. *Physiol Genomics*, 46(21), 808-820.
- Ager-Wick, E., Hodne, K., Fontaine, R., von Krogh, K., Haug, T. M., & Weltzien, F.-A. (2018). Preparation of a High-quality Primary Cell Culture from Fish Pituitaries. *JoVE*(138), e58159.
- Ager-Wick, E., Maugars, G., von Krogh, K., Fontaine, R., Siddique, K., Nourizadeh-Lillabadi, R., Weltzien, F.-A., & Henkel, C. (2021). Ectopic expression of lipid homeostasis genes in rare cells of the teleost pituitary gland. *bioRxiv*, 2021.2006.2011.448009.
- Alwine, J. C., Kemp, D. J., & Stark, G. R. (1977). Method for detection of specific RNAs in agarose gels by transfer to diazobenzyloxymethyl-paper and hybridization with DNA probes. *Proceedings of the National Academy of Sciences*, 74(12), 5350.
- Anderson, S. (1981). Shotgun DNA sequencing using cloned DNase I-generated fragments. *Nucleic Acids Research*, 9(13), 3015-3027.
- Andoniadou, Cynthia L., Matsushima, D., Mousavy Gharavy, Seyedeh N., Signore, M., Mackintosh, Albert I., Schaeffer, M., Gaston-Massuet, C., Mollard, P., Jacques, Thomas S., Le Tissier, P., Dattani, Mehul T., Pevny, Larysa H., & Martinez-Barbera, Juan P. (2013). Sox2+ Stem/Progenitor Cells in the Adult Mouse Pituitary Support Organ Homeostasis and Have Tumor-Inducing Potential. *Cell Stem Cell*, 13(4), 433-445.
- Aoki, K., & Umeura, H. (1970). Cell types in the pituitary of the medaka, *Oryzias latipes*. *Endocrinol Jpn*, 17(1), 45-55.
- Ball, J. N. (1981). Hypothalamic control of the pars distalis in fishes, amphibians, and reptiles. *Gen Comp Endocrinol*, 44(2), 135-170.
- Bartlett, J. M. S. (2004). Fluorescence In Situ Hybridization. In J. E. Roulston & J. M. S. Bartlett (Eds.), *Molecular Diagnosis of Cancer: Methods and Protocols* (pp. 77-87). Humana Press.
- Barzon, L., Lavezzo, E., Militello, V., Toppo, S., & Palù, G. (2011). Applications of next-generation sequencing technologies to diagnostic virology. *International journal of molecular sciences*, 12(11), 7861-7884.
- Batten, T., Ball, J. N., & Benjamin, M. (1975). Ultrastructure of the adenohypophysis in the teleost *Poecilia latipinna*. *Cell and Tissue Research*, 161(2), 239-261.

- Batten, T. F. C. (1986). Immunocytochemical demonstration of pituitary cell types in the teleost *Poecilia latipinna*, by light and electron microscopy. *General and Comparative Endocrinology*, 63(1), 139-154.
- Bayley, H. (2015). Nanopore sequencing: from imagination to reality. *Clin Chem*, 61(1), 25-31.
- Becht, E., McInnes, L., Healy, J., Dutertre, C.-A., Kwok, I. W. H., Ng, L. G., Ginhoux, F., & Newell, E. W. (2019). Dimensionality reduction for visualizing single-cell data using UMAP. *Nature Biotechnology*, 37(1), 38-44.
- Bengtsson, M., Hemberg, M., Rorsman, P., & Ståhlberg, A. (2008). Quantification of mRNA in single cells and modelling of RT-qPCR induced noise. *BMC Molecular Biology*, 9(1), 63.
- Bengtsson, M., Ståhlberg, A., Rorsman, P., & Kubista, M. (2005). Gene expression profiling in single cells from the pancreatic islets of Langerhans reveals lognormal distribution of mRNA levels. *Genome research*, 15(10), 1388-1392.
- Biran, J., & Levavi-Sivan, B. (2018). Endocrine Control of Reproduction, Fish. In M. K. Skinner (Ed.), *Encyclopedia of Reproduction (Second Edition)* (pp. 362-368). Academic Press.
- Borella, M. I., Venturieri, R., & Mancera, J. M. (2009). Immunocytochemical identification of adenohipophyseal cells in the pirarucu (*Arapaima gigas*), an Amazonian basal teleost. *Fish Physiology and Biochemistry*, 35(1), 3-16.
- Braasch, I., Peterson, S. M., Desvignes, T., McCluskey, B. M., Batzel, P., & Postlethwait, J. H. (2015). A new model army: Emerging fish models to study the genomics of vertebrate Evo-Devo. *J Exp Zool B Mol Dev Evol*, 324(4), 316-341.
- Brennecke, P., Anders, S., Kim, J. K., Kołodziejczyk, A. A., Zhang, X., Proserpio, V., Baying, B., Benes, V., Teichmann, S. A., Marioni, J. C., & Heisler, M. G. (2013). Accounting for technical noise in single-cell RNA-seq experiments. *Nature Methods*, 10(11), 1093-1095.
- Breves, J. P., McCormick, S. D., & Karlstrom, R. O. (2014). Prolactin and teleost ionocytes: new insights into cellular and molecular targets of prolactin in vertebrate epithelia. *General and Comparative Endocrinology*, 203, 21-28.
- Buettner, F., Natarajan, K. N., Casale, F. P., Proserpio, V., Scialdone, A., Theis, F. J., Teichmann, S. A., Marioni, J. C., & Stegle, O. (2015). Computational analysis of cell-to-cell heterogeneity in single-cell RNA-sequencing data reveals hidden subpopulations of cells. *Nature Biotechnology*, 33(2), 155-160.
- Bustin, S. A., Benes, V., Garson, J. A., Hellemans, J., Huggett, J., Kubista, M., Mueller, R., Nolan, T., Pfaffl, M. W., Shipley, G. L., Vandesompele, J., & Wittwer, C. T. (2009). The MIQE Guidelines: Minimum Information for Publication of Quantitative Real-Time PCR Experiments. *Clinical Chemistry*, 55(4), 611-622.

- Butler, A., Hoffman, P., Smibert, P., Papalex, E., & Satija, R. (2018). Integrating single-cell transcriptomic data across different conditions, technologies, and species. *Nature Biotechnology*, *36*(5), 411-420.
- Camacho, L., Pozzi, A., de Freitas, E., Shimizu, A., & Pandolfi, M. (2020). Morphological and immunohistochemical comparison of the pituitary gland between a tropical *Paracheirodon axelrodi* and a subtropical *Aphyocharax anisitsi* characids (Characiformes: Characidae). *Neotropical Ichthyol*, *18*(1).
- Camacho LR, P. A., de Freitas EG, Shimizu A, Pandolfi M. (2020). Morphological and Immunohistochemical Comparison of the Pituitary Gland Between a Tropical *Paracheirodon Axelrodi* and a Subtropical *Aphyocharax Anisitsi* Characids (Characiformes: Characidae). *J Neotropical Ichthyol*, *18*(1).
- Cambré, M. L., Verdonck, W., Ollevier, F., Vandesande, F., Batten, T. F. C., & Kühn, E. R. (1986). Immunocytochemical identification and localization of the different cell types in the pituitary of the seabass (*Dicentrarchus labrax*). *General and Comparative Endocrinology*, *61*(3), 368-375.
- Candelma, M., Fontaine, R., Colella, S., Santojanni, A., Weltzien, F.-A., & Carnevali, O. (2017). Gonadotropin characterization, localization and expression in the European hake (*Merluccius merluccius*). *Reproduction*, *153*(2), 123-132.
- Chalfie, M., Tu, Y., Euskirchen, G., Ward, W. W., & Prasher, D. C. (1994). Green fluorescent protein as a marker for gene expression. *Science*, *263*(5148), 802-805.
- Chang, J. P., Johnson, J. D., Goor, F. V., Wong, C. J., Yunker, W. K., Uretsky, A. D., Taylor, D., Jobin, R. M., Wong, A. O., & Goldberg, J. I. (2000). Signal transduction mechanisms mediating secretion in goldfish gonadotropes and somatotropes. *Biochemistry and Cell Biology*, *78*(3), 139-153.
- Chang, J. P., Johnson, J. D., Sawisky, G. R., Grey, C. L., Mitchell, G., Booth, M., Volk, M. M., Parks, S. K., Thompson, E., Goss, G. G., Klausen, C., & Habibi, H. R. (2009). Signal transduction in multifactorial neuroendocrine control of gonadotropin secretion and synthesis in teleosts—studies on the goldfish model. *General and Comparative Endocrinology*, *161*(1), 42-52.
- Chapman, J. R., & Waldenström, J. (2015). With Reference to Reference Genes: A Systematic Review of Endogenous Controls in Gene Expression Studies. *PLOS ONE*, *10*(11), e0141853.
- Chapman, S. C., Sawitzke, A. L., Campbell, D. S., & Schoenwolf, G. C. (2005). A three-dimensional atlas of pituitary gland development in the zebrafish. *Journal of Comparative Neurology*, *487*(4), 428-440.
- Chen, X., Teichmann, S. A., & Meyer, K. B. (2018). From Tissues to Cell Types and Back: Single-Cell Gene Expression Analysis of Tissue Architecture. *Annual Review of Biomedical Data Science*, *1*(1), 29-51.

- Cheung, L. Y. M., George, A. S., McGee, S. R., Daly, A. Z., Brinkmeier, M. L., Ellsworth, B. S., & Camper, S. A. (2018). Single-Cell RNA Sequencing Reveals Novel Markers of Male Pituitary Stem Cells and Hormone-Producing Cell Types. *Endocrinology*, *159*(12), 3910-3924.
- Childs, G. V. (1983). Application of Dual Pre-Embedding Stains for Gonadotropins to Pituitary Cell Monolayers with Avidin-Biotin (ABC) and Peroxidase-Antiperoxidase (PAP) Complexes: Light Microscopic Studies. *Stain Technology*, *58*(5), 281-289.
- Childs, G. V. (1991). Multipotential pituitary cells that contain adrenocorticotropin (ACTH) and other pituitary hormones. *Trends in Endocrinology & Metabolism*, *2*(3), 112-117.
- Childs, G. V. (2000). Editorial: Green Fluorescent Proteins Light the Way to a Better Understanding of the Function and Regulation of Specific Anterior Pituitary Cells. *Endocrinology*, *141*(12), 4331-4333.
- Childs, G. V. (2002). Development of Gonadotropes May Involve Cyclic Transdifferentiation of Growth Hormone Cells. *Archives of Physiology and Biochemistry*, *110*(1-2), 42-49.
- Childs Moriarty, G. V., Ellison, D. G., Lorenzen, J. R., Collins, T. J., & Schwartz, N. B. (1982). Immunocytochemical Studies of Gonadotropin Storage in Developing Castration Cells*. *Endocrinology*, *111*(4), 1318-1328.
- Christensen, A., Bentley, G. E., Cabrera, R., Ortega, H. H., Perfito, N., Wu, T. J., & Micevych, P. (2012). Hormonal regulation of female reproduction. *Hormone and metabolic research = Hormon- und Stoffwechselforschung = Hormones et metabolisme*, *44*(8), 587-591.
- Churko, J. M., Mantalas, G. L., Snyder, M. P., & Wu, J. C. (2013). Overview of high throughput sequencing technologies to elucidate molecular pathways in cardiovascular diseases. *Circ Res*, *112*(12), 1613-1623.
- Clark, S. (2017). *Single-Cell RNA-Seq: An Introductory Overview and Tools for Getting Started*. 10X Genomics. <https://www.10xgenomics.com/blog/single-cell-rna-seq-an-introductory-overview-and-tools-for-getting-started>
- de Beer, G. R. (1924). The Evolution of the Pituitary. *The Journal of Experimental Biology*, *1*, 271-291.
- Denef, C. (2008). Paracrinicity: The Story of 30 Years of Cellular Pituitary Crosstalk. *Journal of Neuroendocrinology*, *20*(1), 1-70.
- Derveaux, S., Vandesompele, J., & Hellemans, J. (2010). How to do successful gene expression analysis using real-time PCR. *Methods*, *50*(4), 227-230.
- Dobin, A., Davis, C. A., Schlesinger, F., Drenkow, J., Zaleski, C., Jha, S., Batut, P., Chaisson, M., & Gingeras, T. R. (2012). STAR: ultrafast universal RNA-seq aligner. *Bioinformatics*, *29*(1), 15-21.

- Doerr-Schott, J. (1976). Immunohistochemical detection, by light and electron microscopy, of pituitary hormones in cold-blooded vertebrates: II. Reptiles. *General and Comparative Endocrinology*, 28(4), 513-529.
- Dubourg, P., Burzawa-Gerard, E., Chambolle, P., & Kah, O. (1985). Light and electron microscopic identification of gonadotrophic cells in the pituitary gland of the goldfish by means of immunocytochemistry. *General and Comparative Endocrinology*, 59(3), 472-481.
- Dufour, S., Seberty, M. E., Weltzien, F. A., Rousseau, K., & Pasqualini, C. (2010). Neuroendocrine control by dopamine of teleost reproduction. *J Fish Biol*, 76(1), 129-160.
- Eberwine, J., Yeh, H., Miyashiro, K., Cao, Y., Nair, S., Finnell, R., Zettel, M., & Coleman, P. (1992). Analysis of gene expression in single live neurons. *Proceedings of the National Academy of Sciences of the United States of America*, 89(7), 3010-3014.
- Eid, J., Fehr, A., Gray, J., Luong, K., Lyle, J., Otto, G., Peluso, P., Rank, D., Baybayan, P., Bettman, B., Bibillo, A., Bjornson, K., Chaudhuri, B., Christians, F., Cicero, R., Clark, S., Dalal, R., deWinter, A., Dixon, J., Foquet, M., Gaertner, A., Hardenbol, P., Heiner, C., Hester, K., Holden, D., Kearns, G., Kong, X., Kuse, R., Lacroix, Y., Lin, S., Lundquist, P., Ma, C., Marks, P., Maxham, M., Murphy, D., Park, I., Pham, T., Phillips, M., Roy, J., Sebra, R., Shen, G., Sorenson, J., Tomaney, A., Travers, K., Trulson, M., Vieceli, J., Wegener, J., Wu, D., Yang, A., Zaccarin, D., Zhao, P., Zhong, F., Korch, J., & Turner, S. (2009). Real-Time DNA Sequencing from Single Polymerase Molecules. *Science*, 323(5910), 133-138.
- Emery, P. (2007). RNase Protection Assay. In E. Rosato (Ed.), *Circadian Rhythms: Methods and Protocols* (pp. 343-348). Humana Press.
- Fabian, P., Tseng, K.-C., Smeeton, J., Lancman Joseph, J., Dong, P. D. S., Cerny, R., & Crump, J. G. (2020). Lineage analysis reveals an endodermal contribution to the vertebrate pituitary. *Science*, 370(6515), 463-467.
- Fan, H. C., Fu, G. K., & Fodor, S. P. (2015). Expression profiling. Combinatorial labeling of single cells for gene expression cytometry. *Science*, 347(6222), 1258367.
- Fan, X., Zhang, X., Wu, X., Guo, H., Hu, Y., Tang, F., & Huang, Y. (2015). Single-cell RNA-seq transcriptome analysis of linear and circular RNAs in mouse preimplantation embryos. *Genome Biology*, 16(1), 148.
- Farbridge, K. J., McDonald-Jones, G., McLean, C. L., Lowry, P. J., Etches, R. J., & Leatherland, J. F. (1990). The development of monoclonal antibodies against salmon (*Oncorhynchus kisutch* and *O. keta*) pituitary hormones and their immunohistochemical identification. *General and Comparative Endocrinology*, 79(3), 361-374.
- Fauquier, T., Guérineau, N. C., McKinney, R. A., Bauer, K., & Mollard, P. (2001). Folliculostellate cell network: A route for long-distance communication in the anterior pituitary. *Proceedings of the National Academy of Sciences*, 98(15), 8891-8896.
- Femino, A. M., Fay, F. S., Fogarty, K., & Singer, R. H. (1998). Visualization of single RNA transcripts in situ. *Science*, 280(5363), 585-590.

- Femino Andrea, M., Fay Fredric, S., Fogarty, K., & Singer Robert, H. (1998). Visualization of Single RNA Transcripts in Situ. *Science*, 280(5363), 585-590.
- Feng, N. Y., & Bass, A. H. (2017). Neural, Hormonal, and Genetic Mechanisms of Alternative Reproductive Tactics: Vocal Fish as Model Systems. In D. W. Pfaff & M. Joëls (Eds.), *Hormones, Brain and Behavior (Third Edition)* (pp. 47-68). Academic Press.
- Ferrandino, I., & Grimaldi, M. C. (2008). Ultrastructural study of the pituicytes in the pituitary gland of the teleost *Diplodus sargus*. *Brain Res Bull*, 75(1), 133-137.
- Fontaine, R., Ager-Wick, E., Hodne, K., & Weltzien, F.-A. (2019). Plasticity of Lh cells caused by cell proliferation and recruitment of existing cells. *Journal of Endocrinology*, 240(2), 361-377.
- Fontaine, R., Ager-Wick, E., Hodne, K., & Weltzien, F.-A. (2020). Plasticity in medaka gonadotropes via cell proliferation and phenotypic conversion. *Journal of Endocrinology*, 245(1), 21-37.
- Frawley, L. S., & Boockfor, F. R. (1991). Mammosomatotropes: Presence and Functions in Normal and Neoplastic Pituitary Tissue*. *Endocrine Reviews*, 12(4), 337-355.
- Fukami, K., Tasaka, K., Mizuki, J., Kasahara, K., Masumoto, N., Miyake, A., & Murata, Y. (1997). Bihormonal Cells Secreting Both Prolactin and Gonadotropins in Normal Rat Pituitary Cells. *Endocrine Journal*, 44(6), 819-826.
- García-Hernández, M. P., García-Ayala, A., Elbal, M. T., & Agulleiro, B. (1996). The adenohypophysis of Mediterranean yellowtail, *Seriola dumerilii* (Risso, 1810): an immunocytochemical study. *Tissue and Cell*, 28(5), 577-585.
- Ginzinger, D. G. (2002). Gene quantification using real-time quantitative PCR: An emerging technology hits the mainstream. *Experimental Hematology*, 30(6), 503-512.
- Glasauer, S. M. K., & Neuhauss, S. C. F. (2014). Whole-genome duplication in teleost fishes and its evolutionary consequences. *Molecular Genetics and Genomics*, 289(6), 1045-1060.
- Gleiberman, A. S., Michurina, T., Encinas, J. M., Roig, J. L., Krasnov, P., Balordi, F., Fishell, G., Rosenfeld, M. G., & Enikolopov, G. (2008). Genetic approaches identify adult pituitary stem cells. *Proceedings of the National Academy of Sciences*, 105(17), 6332-6337.
- Golan, M., Biran, J., & Levavi-Sivan, B. (2014). A Novel Model for Development, Organization, and Function of Gonadotropes in Fish Pituitary [Original Research]. *Frontiers in Endocrinology*, 5(182).
- Golan, M., Hollander-Cohen, L., & Levavi-Sivan, B. (2016). Stellate Cell Networks in the Teleost Pituitary. *Scientific Reports*, 6(1), 24426.
- Golan, M., Zelinger, E., Zohar, Y., & Levavi-Sivan, B. (2015). Architecture of GnRH-Gonadotrope-Vasculature Reveals a Dual Mode of Gonadotropin Regulation in Fish. *Endocrinology*, 156(11), 4163-4173.

- Grandi, G., Colombo, G., & Chicca, M. (2003). Immunocytochemical studies on the pituitary gland of *Anguilla anguilla* L., in relation to early growth stages and diet-induced sex differentiation. *General and Comparative Endocrinology*, *131*(1), 66-76.
- Guo, G., Huss, M., Tong, G. Q., Wang, C., Li Sun, L., Clarke, N. D., & Robson, P. (2010). Resolution of Cell Fate Decisions Revealed by Single-Cell Gene Expression Analysis from Zygote to Blastocyst. *Developmental Cell*, *18*(4), 675-685.
- Gutnick, A., Blechman, J., Kaslin, J., Herwig, L., Belting, H.-G., Affolter, M., Bonkowsky, Joshua L., & Levkowitz, G. (2011). The Hypothalamic Neuropeptide Oxytocin Is Required for Formation of the Neurovascular Interface of the Pituitary. *Developmental Cell*, *21*(4), 642-654.
- Haque, A., Engel, J., Teichmann, S. A., & Lönnberg, T. (2017). A practical guide to single-cell RNA-sequencing for biomedical research and clinical applications. *Genome Medicine*, *9*(1), 75.
- Harding, L. B., Schultz, I. R., Goetz, G. W., Luckenbach, J. A., Young, G., Goetz, F. W., & Swanson, P. (2013). High-throughput sequencing and pathway analysis reveal alteration of the pituitary transcriptome by 17 α -ethynylestradiol (EE2) in female coho salmon, *Oncorhynchus kisutch*. *Aquatic Toxicology*, *142-143*, 146-163.
- Hashiguchi, Y., Furuta, Y., & Nishida, M. (2009). Evolutionary Patterns and Selective Pressures of Odorant/Pheromone Receptor Gene Families in Teleost Fishes. *PLOS ONE*, *3*(12), e4083.
- Hashimshony, T., Senderovich, N., Avital, G., Klochendler, A., de Leeuw, Y., Anavy, L., Gennert, D., Li, S., Livak, K. J., Rozenblatt-Rosen, O., Dor, Y., Regev, A., & Yanai, I. (2016). CEL-Seq2: sensitive highly-multiplexed single-cell RNA-Seq. *Genome Biology*, *17*(1), 77.
- Hashimshony, T., Wagner, F., Sher, N., & Yanai, I. (2012). CEL-Seq: single-cell RNA-Seq by multiplexed linear amplification. *Cell Rep*, *2*(3), 666-673.
- He, W., Dai, X., Chen, X., He, J., & Yin, Z. (2014). Zebrafish pituitary gene expression before and after sexual maturation. *Journal of Endocrinology*, *221*(3), 429-440.
- Heather, J. M., & Chain, B. (2016). The sequence of sequencers: The history of sequencing DNA. *Genomics*, *107*(1), 1-8.
- Hicks, S. C., Townes, F. W., Teng, M., & Irizarry, R. A. (2017). Missing data and technical variability in single-cell RNA-sequencing experiments. *Biostatistics*, *19*(4), 562-578.
- Hildahl, J., Sandvik, G. K., Lifjeld, R., Hodne, K., Nagahama, Y., Haug, T. M., Okubo, K., & Weltzien, F. A. (2012). Developmental tracing of luteinizing hormone beta-subunit gene expression using green fluorescent protein transgenic medaka (*Oryzias latipes*) reveals a putative novel developmental function. *Dev Dyn*, *241*(11), 1665-1677.
- Ho, Y., Hu, P., Peel, M. T., Chen, S., Camara, P. G., Epstein, D. J., Wu, H., & Liebhaber, S. A. (2020). Single-cell transcriptomic analysis of adult mouse pituitary reveals sexual dimorphism and physiologic demand-induced cellular plasticity. *Protein & Cell*, *11*(8), 565-583.

- Hoga, C. A., Almeida, F. L., & Reyes, F. G. R. (2018). A review on the use of hormones in fish farming: Analytical methods to determine their residues. *CyTA - Journal of Food*, 16(1), 679-691.
- Honji, R. M., Nóbrega, R. H., Pandolfi, M., Shimizu, A., Borella, M. I., & Moreira, R. G. (2013). Immunohistochemical study of pituitary cells in wild and captive *Salminus hilarii* (Characiformes: Characidae) females during the annual reproductive cycle. *SpringerPlus*, 2(1), 460.
- Hopman, A. H. N., Ramaekers, F. C. S., & Speel, E. J. M. (1998). Rapid Synthesis of Biotin-, Digoxigenin-, Trinitrophenyl-, and Fluorochrome-labeled Tyramides and Their Application for In Situ Hybridization Using CARD Amplification. *Journal of Histochemistry & Cytochemistry*, 46(6), 771-777.
- Huang, L., & Specker, J. L. (1994). Growth Hormone- and Prolactin-Producing Cells in the Pituitary Gland of Striped Bass (*Morone saxatilis*): Immunocytochemical Characterization at Different Life Stages. *General and Comparative Endocrinology*, 94(2), 225-236.
- Hughes, L. C., Ortí, G., Huang, Y., Sun, Y., Baldwin, C. C., Thompson, A. W., Arcila, D., Betancur-R., R., Li, C., Becker, L., Bellora, N., Zhao, X., Li, X., Wang, M., Fang, C., Xie, B., Zhou, Z., Huang, H., Chen, S., Venkatesh, B., & Shi, Q. (2018). Comprehensive phylogeny of ray-finned fishes (Actinopterygii) based on transcriptomic and genomic data. *Proceedings of the National Academy of Sciences*, 115(24), 6249-6254.
- Ilicic, T., Kim, J. K., Kolodziejczyk, A. A., Bagger, F. O., McCarthy, D. J., Marioni, J. C., & Teichmann, S. A. (2016). Classification of low quality cells from single-cell RNA-seq data. *Genome Biology*, 17(1), 29.
- Illumina. (2014). *HiSeq X Ten Series of Sequencing Systems*. <https://www.illumina.com/documents/products/datasheets/datasheet-hiseq-x-ten.pdf>
- Inoue, K., Mogi, C., Ogawa, S., Tomida, M., & Miyai, S. (2002). Are Folliculo-Stellate Cells in the Anterior Pituitary Gland Supportive Cells or Organ-Specific Stem Cells? *Archives of Physiology and Biochemistry*, 110(1-2), 50-53.
- Ishwar, S. P., Yoshitaka, N., Grau, E. G., & Robert, M. R. (1998). Immunocytochemical and Ultrastructural Identification of Pituitary Cell Types in the Protogynous *Thalassoma duperrey* during Adult Sexual Ontogeny. *Zoological Science*, 15(2), 263-276.
- Islam, S., Kjallquist, U., Moliner, A., Zajac, P., Fan, J. B., Lonnerberg, P., & Linnarsson, S. (2011). Characterization of the single-cell transcriptional landscape by highly multiplex RNA-seq. *Genome Res*, 21(7), 1160-1167.
- Islam, S., Kjallquist, U., Moliner, A., Zajac, P., Fan, J. B., Lonnerberg, P., & Linnarsson, S. (2012). Highly multiplexed and strand-specific single-cell RNA 5' end sequencing. *Nat Protoc*, 7(5), 813-828.

- Islam, S., Zeisel, A., Joost, S., La Manno, G., Zajac, P., Kasper, M., Lönnerberg, P., & Linnarsson, S. (2014). Quantitative single-cell RNA-seq with unique molecular identifiers. *Nature Methods*, *11*(2), 163-166.
- Itakura, E., Odaira, K., Yokoyama, K., Osuna, M., Hara, T., & Inoue, K. (2007). Generation of Transgenic Rats Expressing Green Fluorescent Protein in S-100 β -Producing Pituitary Folliculo-Stellate Cells and Brain Astrocytes. *Endocrinology*, *148*(4), 1518-1523.
- Jaitin, D. A., Kenigsberg, E., Keren-Shaul, H., Elefant, N., Paul, F., Zaretsky, I., Mildner, A., Cohen, N., Jung, S., Tanay, A., & Amit, I. (2014). Massively parallel single-cell RNA-seq for marker-free decomposition of tissues into cell types. *Science*, *343*(6172), 776-779.
- Jakob Biran, B.-S. (2018). Endocrine Control of Reproduction, Fish. *Encyclopedia of Reproduction (Second Edition)*, *6*, 362-368.
- John, H. A., Birnstiel, M. L., & Jones, K. W. (1969). RNA-DNA Hybrids at the Cytological Level. *Nature*, *223*(5206), 582-587.
- Jureckova, K., Raschmanova, H., Kolek, J., Vasytkivska, M., Branska, B., Patakova, P., Provaznik, I., & Sedlar, K. (2021). Identification and Validation of Reference Genes in *Clostridium beijerinckii* NRRL B-598 for RT-qPCR Using RNA-Seq Data [Original Research]. *Frontiers in Microbiology*, *12*.
- Kamme, F., Salunga, R., Yu, J., Tran, D. T., Zhu, J., Luo, L., Bittner, A., Guo, H. Q., Miller, N., Wan, J., & Erlander, M. (2003). Single-cell microarray analysis in hippocampus CA1: demonstration and validation of cellular heterogeneity. *J Neurosci*, *23*(9), 3607-3615.
- Kaneko, T. (1996). Cell Biology of Somatolactin. In K. W. Jeon (Ed.), *International Review of Cytology* (Vol. 169, pp. 1-24). Academic Press.
- Kasahara, M., Naruse, K., Sasaki, S., Nakatani, Y., Qu, W., Ahsan, B., Yamada, T., Nagayasu, Y., Doi, K., Kasai, Y., Jindo, T., Kobayashi, D., Shimada, A., Toyoda, A., Kuroki, Y., Fujiyama, A., Sasaki, T., Shimizu, A., Asakawa, S., Shimizu, N., Hashimoto, S.-i., Yang, J., Lee, Y., Matsushima, K., Sugano, S., Sakaizumi, M., Narita, T., Ohishi, K., Haga, S., Ohta, F., Nomoto, H., Nogata, K., Morishita, T., Endo, T., Shin-I, T., Takeda, H., Morishita, S., & Kohara, Y. (2007). The medaka draft genome and insights into vertebrate genome evolution. *Nature*, *447*(7145), 714-719.
- Kashima, Y., Suzuki, A., & Suzuki, Y. (2019). An Informative Approach to Single-Cell Sequencing Analysis. *Adv Exp Med Biol*, *1129*, 81-96.
- Kasper, R. S., Shved, N., Takahashi, A., Reinecke, M., & Eppler, E. (2006). A systematic immunohistochemical survey of the distribution patterns of GH, prolactin, somatolactin, β -TSH, β -FSH, β -LH, ACTH, and α -MSH in the adenohypophysis of *Oreochromis niloticus*, the Nile tilapia. *Cell and Tissue Research*, *325*(2), 303-313.
- Kchouk, M., Gibrat, J., & Elloumi, M. (2017). Generations of Sequencing Technologies: From First to Next Generation. *Biology and medicine*, *9*, 1-8.

- Kelberman, D., Rizzoti, K., Lovell-Badge, R., Robinson, I. C., & Dattani, M. T. (2009). Genetic regulation of pituitary gland development in human and mouse. *Endocr Rev*, *30*(7), 790-829.
- Kinoshita, M., Murata, K., Naruse, M., Tanaka. (2009). *Medaka: Biology, Management, and Experimental Protocols* (Vol. 18-19). Wiley-Blackwell.
- Kirchmaier, S., Naruse, K., Wittbrodt, J., & Loosli, F. (2015). The genomic and genetic toolbox of the teleost medaka (*Oryzias latipes*). *Genetics*, *199*(4), 905-918.
- Kiselev, V. Y., Andrews, T. S., & Hemberg, M. (2019). Challenges in unsupervised clustering of single-cell RNA-seq data. *Nature Reviews Genetics*, *20*(5), 273-282.
- Kivioja, T., Vähärautio, A., Karlsson, K., Bonke, M., Enge, M., Linnarsson, S., & Taipale, J. (2012). Counting absolute numbers of molecules using unique molecular identifiers. *Nature Methods*, *9*(1), 72-74.
- Klein, A. M., Mazutis, L., Akartuna, I., Tallapragada, N., Veres, A., Li, V., Peshkin, L., Weitz, D. A., & Kirschner, M. W. (2015). Droplet barcoding for single-cell transcriptomics applied to embryonic stem cells. *Cell*, *161*(5), 1187-1201.
- Kohler, A., Collymore, C., Finger-Baier, K., Geisler, R., Kaufmann, L., Pounder, K. C., Schulte-Merker, S., Valentim, A., Varga, Z. M., Weiss, J., & Strahle, U. (2017). Report of Workshop on Euthanasia for Zebrafish-A Matter of Welfare and Science. *Zebrafish*, *14*(6), 547-551.
- Kolodziejczyk, A. A., Kim, J. K., Svensson, V., Marioni, J. C., & Teichmann, S. A. (2015). The technology and biology of single-cell RNA sequencing. *Mol Cell*, *58*(4), 610-620.
- Kozera, B., & Rapacz, M. (2013). Reference genes in real-time PCR. *Journal of Applied Genetics*, *54*(4), 391-406.
- Kumar, S., Stecher, G., Suleski, M., & Hedges, S. B. (2017). TimeTree: A Resource for Timelines, Timetrees, and Divergence Times. *Molecular Biology and Evolution*, *34*(7), 1812-1819.
- Kumar, S., & Tembhre, M. (1996). *Anatomy and physiology of fishes*. Vikas Pub. House Pvt.
- Kurimoto, K., Yabuta, Y., Ohinata, Y., Ono, Y., Uno, K. D., Yamada, R. G., Ueda, H. R., & Saitou, M. (2006). An improved single-cell cDNA amplification method for efficient high-density oligonucleotide microarray analysis. *Nucleic Acids Res*, *34*(5), e42.
- L. Lun, A. T., Bach, K., & Marioni, J. C. (2016). Pooling across cells to normalize single-cell RNA sequencing data with many zero counts. *Genome Biology*, *17*(1), 75.
- Lander, E. S., Linton, L. M., Birren, B., Nusbaum, C., Zody, M. C., Baldwin, J., Devon, K., Dewar, K., Doyle, M., FitzHugh, W., Funke, R., Gage, D., Harris, K., Heaford, A., Howland, J., Kann, L., Lehoczyk, J., LeVine, R., McEwan, P., McKernan, K., Meldrim, J., Mesirov, J. P., Miranda, C., Morris, W., Naylor, J., Raymond, C., Rosetti, M., Santos, R., Sheridan, A.,

Sougnéz, C., Stange-Thomann, Y., Stojanovic, N., Subramanian, A., Wyman, D., Rogers, J., Sulston, J., Ainscough, R., Beck, S., Bentley, D., Burton, J., Clee, C., Carter, N., Coulson, A., Deadman, R., Deloukas, P., Dunham, A., Dunham, I., Durbin, R., French, L., Grafham, D., Gregory, S., Hubbard, T., Humphray, S., Hunt, A., Jones, M., Lloyd, C., McMurray, A., Matthews, L., Mercer, S., Milne, S., Mullikin, J. C., Mungall, A., Plumb, R., Ross, M., Shownkeen, R., Sims, S., Waterston, R. H., Wilson, R. K., Hillier, L. W., McPherson, J. D., Marra, M. A., Mardis, E. R., Fulton, L. A., Chinwalla, A. T., Pepin, K. H., Gish, W. R., Chissole, S. L., Wendl, M. C., Delehaunty, K. D., Miner, T. L., Delehaunty, A., Kramer, J. B., Cook, L. L., Fulton, R. S., Johnson, D. L., Minx, P. J., Clifton, S. W., Hawkins, T., Branscomb, E., Predki, P., Richardson, P., Wenning, S., Slezak, T., Doggett, N., Cheng, J. F., Olsen, A., Lucas, S., Elkin, C., Uberbacher, E., Frazier, M., Gibbs, R. A., Muzny, D. M., Scherer, S. E., Bouck, J. B., Sodergren, E. J., Worley, K. C., Rives, C. M., Gorrell, J. H., Metzker, M. L., Naylor, S. L., Kucherlapati, R. S., Nelson, D. L., Weinstock, G. M., Sakaki, Y., Fujiyama, A., Hattori, M., Yada, T., Toyoda, A., Itoh, T., Kawagoe, C., Watanabe, H., Totoki, Y., Taylor, T., Weissenbach, J., Heilig, R., Saurin, W., Artiguenave, F., Brottier, P., Bruls, T., Pelletier, E., Robert, C., Wincker, P., Smith, D. R., Doucette-Stamm, L., Rubenfield, M., Weinstock, K., Lee, H. M., Dubois, J., Rosenthal, A., Platzer, M., Nyakatura, G., Taudien, S., Rump, A., Yang, H., Yu, J., Wang, J., Huang, G., Gu, J., Hood, L., Rowen, L., Madan, A., Qin, S., Davis, R. W., Federspiel, N. A., Abola, A. P., Proctor, M. J., Myers, R. M., Schmutz, J., Dickson, M., Grimwood, J., Cox, D. R., Olson, M. V., Kaul, R., Raymond, C., Shimizu, N., Kawasaki, K., Minoshima, S., Evans, G. A., Athanasiou, M., Schultz, R., Roe, B. A., Chen, F., Pan, H., Ramsay, J., Lehrach, H., Reinhardt, R., McCombie, W. R., de la Bastide, M., Dedhia, N., Blocker, H., Hornischer, K., Nordsiek, G., Agarwala, R., Aravind, L., Bailey, J. A., Bateman, A., Batzoglu, S., Birney, E., Bork, P., Brown, D. G., Burge, C. B., Cerutti, L., Chen, H. C., Church, D., Clamp, M., Copley, R. R., Doerks, T., Eddy, S. R., Eichler, E. E., Furey, T. S., Galagan, J., Gilbert, J. G., Harmon, C., Hayashizaki, Y., Haussler, D., Hermjakob, H., Hokamp, K., Jang, W., Johnson, L. S., Jones, T. A., Kasif, S., Kasprzyk, A., Kennedy, S., Kent, W. J., Kitts, P., Koonin, E. V., Korf, I., Kulp, D., Lancet, D., Lowe, T. M., McLysaght, A., Mikkelsen, T., Moran, J. V., Mulder, N., Pollara, V. J., Ponting, C. P., Schuler, G., Schultz, J., Slater, G., Smit, A. F., Stupka, E., Szustakowki, J., Thierry-Mieg, D., Thierry-Mieg, J., Wagner, L., Wallis, J., Wheeler, R., Williams, A., Wolf, Y. I., Wolfe, K. H., Yang, S. P., Yeh, R. F., Collins, F., Guyer, M. S., Peterson, J., Felsenfeld, A., Wetterstrand, K. A., Patrinos, A., Morgan, M. J., de Jong, P., Catanese, J. J., Osoegawa, K., Shizuya, H., Choi, S., Chen, Y. J., Szustakowki, J., & International Human Genome Sequencing, C. (2001). Initial sequencing and analysis of the human genome. *Nature*, 409(6822), 860-921.

Langer, P. R., Waldrop, A. A., & Ward, D. C. (1981). Enzymatic synthesis of biotin-labeled polynucleotides: novel nucleic acid affinity probes. *Proceedings of the National Academy of Sciences*, 78(11), 6633.

Levavi-Sivan, B., Bogerd, J., Mananos, E. L., Gomez, A., & Lareyre, J. J. (2010). Perspectives on fish gonadotropins and their receptors. *Gen Comp Endocrinol*, 165(3), 412-437.

Li, H., Handsaker, B., Wysoker, A., Fennell, T., Ruan, J., Homer, N., Marth, G., Abecasis, G., Durbin, R., & Genome Project Data Processing, S. (2009). The Sequence Alignment/Map format and SAMtools. *Bioinformatics (Oxford, England)*, 25(16), 2078-2079.

Li, S., Tighe, S. W., Nicolet, C. M., Grove, D., Levy, S., Farmerie, W., Viale, A., Wright, C., Schweitzer, P. A., Gao, Y., Kim, D., Boland, J., Hicks, B., Kim, R., Chhangawala, S., Jafari, N., Raghavachari, N., Gandara, J., Garcia-Reyero, N., Hendrickson, C., Roberson, D.,

- Rosenfeld, J., Smith, T., Underwood, J. G., Wang, M., Zumbo, P., Baldwin, D. A., Grills, G. S., & Mason, C. E. (2014). Multi-platform assessment of transcriptome profiling using RNA-seq in the ABRF next-generation sequencing study. *Nat Biotechnol*, *32*(9), 915-925.
- Li, Y., Liu, Y., Yang, H., Zhang, T., Naruse, K., & Tu, Q. (2020). Dynamic transcriptional and chromatin accessibility landscape of medaka embryogenesis. *Genome Res*, *30*(6), 924-937.
- Liang, P., Guo, Y., Zhou, X., & Gao, X. (2014). Expression Profiling in Bemisia tabaci under Insecticide Treatment: Indicating the Necessity for Custom Reference Gene Selection. *PLOS ONE*, *9*(1), e87514.
- Liu, S., & Trapnell, C. (2016). Single-cell transcriptome sequencing: recent advances and remaining challenges. *F1000Research*, *5*, F1000 Faculty Rev-1182.
- Luecken, M. D., & Theis, F. J. (2019). Current best practices in single-cell RNA-seq analysis: a tutorial. *Molecular Systems Biology*, *15*(6), e8746.
- Macosko, E. Z., Basu, A., Satija, R., Nemes, J., Shekhar, K., Goldman, M., Tirosh, I., Bialas, A. R., Kamitaki, N., Martersteck, E. M., Trombetta, J. J., Weitz, D. A., Sanes, J. R., Shalek, A. K., Regev, A., & McCarroll, S. A. (2015). Highly Parallel Genome-wide Expression Profiling of Individual Cells Using Nanoliter Droplets. *Cell*, *161*(5), 1202-1214.
- Mardis, E. R. (2011). A decade's perspective on DNA sequencing technology. *Nature*, *470*(7333), 198-203.
- Margolis-Kazan, H., Peute, J., Schreiber, M. P., & Halpern, L. R. (1981). Ultrastructural localization of gonadotropin and luteinizing hormone releasing hormone in the pituitary gland of a teleost fish (the platyfish). *Journal of Experimental Zoology*, *215*(1), 99-102.
- Marioni, J. C., Mason, C. E., Mane, S. M., Stephens, M., & Gilad, Y. (2008). RNA-seq: an assessment of technical reproducibility and comparison with gene expression arrays. *Genome Res*, *18*(9), 1509-1517.
- Martin, S. A. M., Wallner, W., Youngson, A. F., & Smith, T. (1999). Differential expression of Atlantic salmon thyrotropin β subunit mRNA and its cDNA sequence. *Journal of Fish Biology*, *54*(4), 757-766.
- Matsuda, M., Nagahama, Y., Shinomiya, A., Sato, T., Matsuda, C., Kobayashi, T., Morrey, C. E., Shibata, N., Asakawa, S., Shimizu, N., Hori, H., Hamaguchi, S., & Sakaizumi, M. (2002). DMY is a Y-specific DM-domain gene required for male development in the medaka fish. *Nature*, *417*(6888), 559-563.
- Maxam, A. M., & Gilbert, W. (1977). A new method for sequencing DNA. *Proc Natl Acad Sci U S A*, *74*(2), 560-564.
- Melmed, S., Polonsky, K.S., Larsen, P.R., Kronenberg, H.M. (2016). *Williams textbook of endocrinology*. Elsevier Health Sciences, Philadelphia.

- Mukai, T., & Oota, Y. (1995). Histological Changes in the Pituitary, Thyroid Gland and Gonads of the Fourspine Sculpin (*Cottus kazika*) during Downstream Migration. *Zoolog Sci*, *12*(1), 91-97.
- Naito, N., Takahashi, A., Nakai, Y., Kawauchi, H., & Hirano, T. (1983). Immunocytochemical identification of the prolactin-secreting cells in the teleost pituitary with an antiserum to chum salmon prolactin. *General and Comparative Endocrinology*, *50*(2), 282-291.
- Nakane, R., & Oka, Y. (2010). Excitatory Action of GABA in the Terminal Nerve Gonadotropin-Releasing Hormone Neurons. *Journal of Neurophysiology*, *103*(3), 1375-1384.
- Naruse, K., Hori, H., Shimizu, N., Kohara, Y., & Takeda, H. (2004). Medaka genomics: a bridge between mutant phenotype and gene function. *Mech Dev*, *121*(7-8), 619-628.
- Navarro, V. M., & Tena-Sempere, M. (2012). Neuroendocrine control by kisspeptins: role in metabolic regulation of fertility. *Nature Reviews Endocrinology*, *8*(1), 40-53.
- Nelson, J. S. (1994). *Fishes of the World*. John Wiley & Sons.
- Nelson, J. S. (2012). *Fishes of the World*. New York: John Wiley & Sons.
- Nozaki, M., Naito, N., Swanson, P., Miyata, K., Nakai, Y., Oota, Y., Suzuki, K., & Kawauchi, H. (1990). Salmonid pituitary gonadotrophs I. Distinct cellular distributions of two gonadotropins, GTH I and GTH II. *General and Comparative Endocrinology*, *77*(3), 348-357.
- Oakley, A. E., Clifton, D. K., & Steiner, R. A. (2009). Kisspeptin Signaling in the Brain. *Endocrine Reviews*, *30*(6), 713-743.
- Ohta, K., Mine, T., Yamaguchi, A., & Matsuyama, M. (2008). Sexually dimorphic expression of pituitary glycoprotein hormones in a sex-changing fish (*Pseudolabrus sieboldi*). *Journal of Experimental Zoology Part A: Ecological Genetics and Physiology*, *309A*(9), 534-541.
- Olivereau, M., & Nagahama, Y. (1983). Immunocytochemistry of gonadotropic cells in the pituitary of some teleost species. *General and Comparative Endocrinology*, *50*(2), 252-260.
- Ooi, G. T., Tawadros, N., & Escalona, R. M. (2004). Pituitary cell lines and their endocrine applications. *Mol Cell Endocrinol*, *228*(1-2), 1-21.
- Pall, G. S., & Hamilton, A. J. (2008). Improved northern blot method for enhanced detection of small RNA. *Nature Protocols*, *3*(6), 1077-1084.
- Pandolfi, M., Canepa, M. M., Meijide, F. J., Alonso, F., Vazquez, G. R., Maggese, M. C., & Vissio, P. G. (2009). Studies on the reproductive and developmental biology of *Cichlasoma dimerus* (Perciformes, Cichlidae). *Biocell*, *33*(1), 1-18.
- Pardue, M. L., & Gall, J. G. (1969). Molecular hybridization of radioactive dna to the dna of cytological preparations. *Proceedings of the National Academy of Sciences*, *64*(2), 600.
- Patiño, R., & Sullivan, C. V. (2002). Ovarian follicle growth, maturation, and ovulation in teleost fish. *Fish Physiology and Biochemistry*, *26*(1), 57-70.

- Pearson, K. (1901). LIII. On lines and planes of closest fit to systems of points in space. *The London, Edinburgh, and Dublin Philosophical Magazine and Journal of Science*, 2(11), 559-572.
- Peixoto, A., Monteiro, M., Rocha, B., & Veiga-Fernandes, H. (2004). Quantification of multiple gene expression in individual cells. *Genome research*, 14(10A), 1938-1947.
- Petukhov, V., Guo, J., Baryawno, N., Severe, N., Scadden, D. T., Samsonova, M. G., & Kharchenko, P. V. (2018). dropEst: pipeline for accurate estimation of molecular counts in droplet-based single-cell RNA-seq experiments. *Genome Biology*, 19(1), 78.
- Phipson, B., Zappia, L., & Oshlack, A. (2017). Gene length and detection bias in single cell RNA sequencing protocols. *F1000Research*, 6, 595-595.
- Picelli, S. (2017). Single-cell RNA-sequencing: The future of genome biology is now. *RNA Biol*, 14(5), 637-650.
- Picelli, S., Bjorklund, A. K., Faridani, O. R., Sagasser, S., Winberg, G., & Sandberg, R. (2013). Smart-seq2 for sensitive full-length transcriptome profiling in single cells. *Nat Methods*, 10(11), 1096-1098.
- Pilar García Hernández, M., García Ayala, A., Zandbergen, M. A., & Agulleiro, B. (2002). Investigation into the duality of gonadotropic cells of Mediterranean yellowtail (*Seriola dumerilii*, Risso 1810): immunocytochemical and ultrastructural studies. *General and Comparative Endocrinology*, 128(1), 25-35.
- Pogoda, H. M., & Hammerschmidt, M. (2007). Molecular genetics of pituitary development in zebrafish. *Semin Cell Dev Biol*, 18(4), 543-558.
- Qiu, P. (2020). Embracing the dropouts in single-cell RNA-seq analysis. *Nature Communications*, 11(1), 1169.
- Quesada, J., Lozano, M. T., Ortega, A., & Agulleiro, B. (1988). Immunocytochemical and ultrastructural characterization of the cell types in the adenohypophysis of *Sparus aurata* L. (Teleost). *General and Comparative Endocrinology*, 72(2), 209-225.
- Ramsköld, D., Luo, S., Wang, Y.-C., Li, R., Deng, Q., Faridani, O. R., Daniels, G. A., Khrebtkova, I., Loring, J. F., Laurent, L. C., Schroth, G. P., & Sandberg, R. (2012). Full-length mRNA-Seq from single-cell levels of RNA and individual circulating tumor cells. *Nature Biotechnology*, 30(8), 777-782.
- Rand-Weaver, M., Baker, B. J., & Kawauchi, H. (1991). Cellular localization of somatolactin in the pars intermedia of some teleost fishes. *Cell and Tissue Research*, 263(2), 207-215.
- Rao, A., Barkley, D., França, G. S., & Yanai, I. (2021). Exploring tissue architecture using spatial transcriptomics. *Nature*, 596(7871), 211-220.
- Reis Filho, R. W., Araújo, J. C. d., & Vieira, E. M. (2006). Hormônios sexuais estrógenos: contaminantes bioativos. *Química Nova*, 29, 817-822.

- Reuter, J. A., Spacek, D. V., & Snyder, M. P. (2015). High-throughput sequencing technologies. *Molecular Cell*, 58(4), 586-597.
- Rizzoti, K., Akiyama, H., & Lovell-Badge, R. (2013). Mobilized Adult Pituitary Stem Cells Contribute to Endocrine Regeneration in Response to Physiological Demand. *Cell Stem Cell*, 13(4), 419-432.
- Rodríguez-Ezpeleta, N., Hackenberg, M., & Aransay, A. M. (2012). *"Bioinformatics for High Throughput Sequencing"* (Vol. 1). Springer, New York, NY.
- Rolland, A. D., Lardenois, A., Goupil, A.-S., Lareyre, J.-J., Houlgatte, R., Chalmel, F., & Le Gac, F. (2013). Profiling of Androgen Response in Rainbow Trout Pubertal Testis: Relevance to Male Gonad Development and Spermatogenesis. *PLOS ONE*, 8(1), e53302.
- Sakaguchi, K., Yoneda, M., Sakai, N., Nakashima, K., Kitano, H., & Matsuyama, M. (2019). Comprehensive Experimental System for a Promising Model Organism Candidate for Marine Teleosts. *Scientific Reports*, 9(1), 4948.
- Sambroni, E., Rolland, A. D., Lareyre, J.-J., & Le Gac, F. (2013). Fsh and Lh have common and distinct effects on gene expression in rainbow trout testis. *Journal of Molecular Endocrinology*, 50(1), 1-18.
- Sanchez Cala, F., Portillo, A., Martín del Río, M. P., & Mancera, J. M. (2003). Immunocytochemical characterization of adenohipophyseal cells in the greater weever fish (*Trachinus draco*). *Tissue Cell*, 35(3), 169-178.
- Sánchez Cala, F., Portillo, A., Martín del Río, M. P., & Mancera, J. M. (2003). Immunocytochemical characterization of adenohipophyseal cells in the greater weever fish (*Trachinus draco*). *Tissue and Cell*, 35(3), 169-178.
- Sanger, F., Air, G. M., Barrell, B. G., Brown, N. L., Coulson, A. R., Fiddes, C. A., Hutchison, C. A., Slocombe, P. M., & Smith, M. (1977). Nucleotide sequence of bacteriophage phi X174 DNA. *Nature*, 265(5596), 687-695.
- Sasagawa, Y., Danno, H., Takada, H., Ebisawa, M., Tanaka, K., Hayashi, T., Kurisaki, A., & Nikaido, I. (2018). Quartz-Seq2: a high-throughput single-cell RNA-sequencing method that effectively uses limited sequence reads. *Genome Biology*, 19(1), 29.
- Sasagawa, Y., Nikaido, I., Hayashi, T., Danno, H., Uno, K. D., Imai, T., & Ueda, H. R. (2013). Quartz-Seq: a highly reproducible and sensitive single-cell RNA sequencing method, reveals non-genetic gene-expression heterogeneity. *Genome Biology*, 14(4), 3097.
- Satija, R., Farrell, J. A., Gennert, D., Schier, A. F., & Regev, A. (2015). Spatial reconstruction of single-cell gene expression data. *Nature Biotechnology*, 33(5), 495-502.
- Sato, Y., Hashiguchi, Y., & Nishida, M. (2009). Temporal pattern of loss/persistence of duplicate genes involved in signal transduction and metabolic pathways after teleost-specific genome duplication. *BMC Evol Biol*, 9, 127.

- Schadt, E. E., Turner, S., & Kasarskis, A. (2010). A window into third-generation sequencing. *Hum Mol Genet*, *19*(R2), R227-240.
- Schloss, J. A. (2008). How to get genomes at one ten-thousandth the cost. *Nature Biotechnology*, *26*(10), 1113-1115.
- Schreibman, M. P., J.F. Leatherland, and B.A. McKeown. (1973). Functional Morphology of the Teleost Pituitary Gland. *American Zoologist*(13), 719-742.
- Schulz, R. W., de Franca, L. R., Lareyre, J. J., Le Gac, F., Chiarini-Garcia, H., Nobrega, R. H., & Miura, T. (2010). Spermatogenesis in fish. *Gen Comp Endocrinol*, *165*(3), 390-411.
- Schulz, R. W., & Miura, T. (2002). Spermatogenesis and its endocrine regulation. *Fish Physiology and Biochemistry*, *26*(1), 43-56.
- See, P., Lum, J., Chen, J., & Ginhoux, F. (2018). A Single-Cell Sequencing Guide for Immunologists [10.3389/fimmu.2018.02425]. *Frontiers in Immunology*, *9*, 2425.
- Segura-Noguera, M. M., Laíz-Carrión, R., Martín del Río, M. P., & Mancera, J. M. (2000). An Immunocytochemical Study of the Pituitary Gland of the White Seabream (*Diplodus Sargus*). *The Histochemical Journal*, *32*(12), 733-742.
- Sena, J. A., Galotto, G., Devitt, N. P., Connick, M. C., Jacobi, J. L., Umale, P. E., Vidali, L., & Bell, C. J. (2018). Unique Molecular Identifiers reveal a novel sequencing artefact with implications for RNA-Seq based gene expression analysis. *Scientific Reports*, *8*(1), 13121.
- Seuntjens, E., Hauspie, A., Roudbaraki, M., Vankelecom, H., & Deneff, C. (2002). Combined Expression of Different Hormone Genes in Single Cells of Normal Rat and Mouse Pituitary. *Archives of Physiology and Biochemistry*, *110*(1-2), 12-15.
- Shainer, I., & Stemmer, M. (2021). Choice of pre-processing pipeline influences clustering quality of scRNA-seq datasets. *BMC Genomics*, *22*(1), 661.
- Sheng, K., Cao, W., Niu, Y., Deng, Q., & Zong, C. (2017). Effective detection of variation in single-cell transcriptomes using MATQ-seq. *Nat Methods*, *14*(3), 267-270.
- Sherwood, N., Eiden, L., Brownstein, M., Spiess, J., Rivier, J., & Vale, W. (1983). Characterization of a teleost gonadotropin-releasing hormone. *Proceedings of the National Academy of Sciences*, *80*(9), 2794-2798.
- Shu, Y., Lou, Q., Dai, Z., Dai, X., He, J., Hu, W., & Yin, Z. (2016). The basal function of teleost prolactin as a key regulator on ion uptake identified with zebrafish knockout models. *Scientific Reports*, *6*(1), 18597.
- Speel, E. J. M., Hopman, A. H. N., & Komminoth, P. (1999). Amplification Methods to Increase the Sensitivity of In Situ Hybridization: Play CARD(S). *Journal of Histochemistry & Cytochemistry*, *47*(3), 281-288.

Speel, E. J. M., Ramaekers, F. C. S., & Hopman, A. H. N. (1997). Sensitive Multicolor Fluorescence In Situ Hybridization Using Catalyzed Reporter Deposition (CARD) Amplification. *Journal of Histochemistry & Cytochemistry*, 45(10), 1439-1446.

Staden, R. (1979). A strategy of DNA sequencing employing computer programs. *Nucleic Acids Research*, 6(7), 2601-2610.

Su, Z., Łabaj, P. P., Li, S., Thierry-Mieg, J., Thierry-Mieg, D., Shi, W., Wang, C., Schroth, G. P., Setterquist, R. A., Thompson, J. F., Jones, W. D., Xiao, W., Xu, W., Jensen, R. V., Kelly, R., Xu, J., Conesa, A., Furlanello, C., Gao, H., Hong, H., Jafari, N., Letovsky, S., Liao, Y., Lu, F., Oakeley, E. J., Peng, Z., Praul, C. A., Santoyo-Lopez, J., Scherer, A., Shi, T., Smyth, G. K., Staedtler, F., Sykacek, P., Tan, X.-X., Thompson, E. A., Vandesompele, J., Wang, M. D., Wang, J., Wolfinger, R. D., Zavadil, J., Auerbach, S. S., Bao, W., Binder, H., Blomquist, T., Brilliant, M. H., Bushel, P. R., Cai, W., Catalano, J. G., Chang, C.-W., Chen, T., Chen, G., Chen, R., Chierici, M., Chu, T.-M., Clevert, D.-A., Deng, Y., Derti, A., Devanarayan, V., Dong, Z., Dopazo, J., Du, T., Fang, H., Fang, Y., Fasold, M., Fernandez, A., Fischer, M., Furió-Tari, P., Fuscoe, J. C., Caimet, F., Gaj, S., Gandara, J., Gao, H., Ge, W., Gondo, Y., Gong, B., Gong, M., Gong, Z., Green, B., Guo, C., Guo, L., Guo, L.-W., Hadfield, J., Hellemans, J., Hochreiter, S., Jia, M., Jian, M., Johnson, C. D., Kay, S., Kleinjans, J., Lababidi, S., Levy, S., Li, Q.-Z., Li, L., Li, L., Li, P., Li, Y., Li, H., Li, J., Li, S., Lin, S. M., López, F. J., Lu, X., Luo, H., Ma, X., Meehan, J., Megherbi, D. B., Mei, N., Mu, B., Ning, B., Pandey, A., Pérez-Florido, J., Perkins, R. G., Peters, R., Phan, J. H., Pirooznia, M., Qian, F., Qing, T., Rainbow, L., Rocca-Serra, P., Sambourg, L., Sansone, S.-A., Schwartz, S., Shah, R., Shen, J., Smith, T. M., Stegle, O., Stralis-Pavese, N., Stupka, E., Suzuki, Y., Szkotnicki, L. T., Tinning, M., Tu, B., van Delft, J., Vela-Boza, A., Venturini, E., Walker, S. J., Wan, L., Wang, W., Wang, J., Wang, J., Wieben, E. D., Willey, J. C., Wu, P.-Y., Xuan, J., Yang, Y., Ye, Z., Yin, Y., Yu, Y., Yuan, Y.-C., Zhang, J., Zhang, K. K., Zhang, W., Zhang, W., Zhang, Y., Zhao, C., Zheng, Y., Zhou, Y., Zumbo, P., Tong, W., Kreil, D. P., Mason, C. E., Shi, L., & Consortium, S. M.-I. (2014). A comprehensive assessment of RNA-seq accuracy, reproducibility and information content by the Sequencing Quality Control Consortium. *Nature Biotechnology*, 32(9), 903-914.

Svensson, V., Vento-Tormo, R., & Teichmann, S. A. (2018). Exponential scaling of single-cell RNA-seq in the past decade. *Nature Protocols*, 13(4), 599-604.

Takahashi, A., Kanda, S., Abe, T., & Oka, Y. (2016). Evolution of the Hypothalamic-Pituitary-Gonadal Axis Regulation in Vertebrates Revealed by Knockout Medaka. *Endocrinology*, 157(10), 3994-4002.

Takahiko, M., & Yoshihiko, O. (1995). Histological Changes in the Pituitary, Thyroid Gland and Gonads of the Fourspine Sculpin *Cottus kazika* during Downstream Migration. *Zoological Science*, 12(1), 91-97.

Tang, F., Barbacioru, C., Wang, Y., Nordman, E., Lee, C., Xu, N., Wang, X., Bodeau, J., Tuch, B. B., Siddiqui, A., Lao, K., & Surani, M. A. (2009). mRNA-Seq whole-transcriptome analysis of a single cell. *Nat Methods*, 6(5), 377-382.

Thorvaldsdóttir, H., Robinson, J. T., & Mesirov, J. P. (2012). Integrative Genomics Viewer (IGV): high-performance genomics data visualization and exploration. *Briefings in Bioinformatics*, 14(2), 178-192.

- Toubeau, G., Poilve, A., Baras, E., Nonclercq, D., De Moor, S., Beckers, J. F., Dessy-Doize, C., & Heuson-Stiennon, J. A. (1991). Immunocytochemical study of cell type distribution in the pituitary of *Barbus barbus* (Teleostei, Cyprinidae). *General and Comparative Endocrinology*, 83(1), 35-47.
- Traverso, V., Christian, H. C., Morris, J. F., & Buckingham, J. C. (1999). Lipocortin 1 (Annexin 1): A Candidate Paracrine Agent Localized in Pituitary Folliculo-Stellate Cells1. *Endocrinology*, 140(9), 4311-4319.
- Trudeau, V. L., Spanswick, D., Fraser, E. J., Larivière, K., Crump, D., Chiu, S., MacMillan, M., & Schulz, R. W. (2000). The role of amino acid neurotransmitters in the regulation of pituitary gonadotropin release in fish. *Biochemistry and Cell Biology*, 78(3), 241-259.
- Tsutsui, K. (2009). A new key neurohormone controlling reproduction, gonadotropin-inhibitory hormone (GnIH): Biosynthesis, mode of action and functional significance. *Progress in Neurobiology*, 88(1), 76-88.
- Tung, P.-Y., Blischak, J. D., Hsiao, C. J., Knowles, D. A., Burnett, J. E., Pritchard, J. K., & Gilad, Y. (2017). Batch effects and the effective design of single-cell gene expression studies. *Scientific Reports*, 7(1), 39921.
- Van den Berge, K., Perraudeau, F., Soneson, C., Love, M. I., Risso, D., Vert, J.-P., Robinson, M. D., Dudoit, S., & Clement, L. (2018). Observation weights unlock bulk RNA-seq tools for zero inflation and single-cell applications. *Genome Biology*, 19(1), 24.
- Van den Berge, K., Roux de Bézieux, H., Street, K., Saelens, W., Cannoodt, R., Saeys, Y., Dudoit, S., & Clement, L. (2020). Trajectory-based differential expression analysis for single-cell sequencing data. *Nature Communications*, 11(1), 1201.
- van der Maaten, L. H., G., (2008). Visualizing data using t-SNE. *The Journal of Machine Learning Research*, 9(2579-2605), 85.
- Vandesompele, J., De Preter, K., Pattyn, F., Poppe, B., Van Roy, N., De Paepe, A., & Speleman, F. (2002). Accurate normalization of real-time quantitative RT-PCR data by geometric averaging of multiple internal control genes. *Genome Biology*, 3(7), research0034.0031.
- Velculescu Victor, E., Zhang, L., Vogelstein, B., & Kinzler Kenneth, W. (1995). Serial Analysis of Gene Expression. *Science*, 270(5235), 484-487.
- Voss, J., & Rosenfeld, M. (1992). Anterior pituitary development: Short tales from dwarf mice. *Cell*, 70, 527-530.
- Wagner, G. F., & McKeown, B. A. (1983). The immunocytochemical localization of pituitary somatotrops in the genus *Oncorhynchus* using an antiserum to growth hormone of chum salmon (*Oncorhynchus keta*). *Cell and Tissue Research*, 231(3), 693-697.
- Wang, F., Flanagan, J., Su, N., Wang, L.-C., Bui, S., Nielson, A., Wu, X., Vo, H.-T., Ma, X.-J., & Luo, Y. (2012). RNAscope: a novel in situ RNA analysis platform for formalin-fixed, paraffin-embedded tissues. *The Journal of molecular diagnostics : JMD*, 14(1), 22-29.

- Weltzien, F.-A., Norberg, B., Helvik, J. V., Andersen, Ø., Swanson, P., & Andersson, E. (2003). Identification and localization of eight distinct hormone-producing cell types in the pituitary of male Atlantic halibut (*Hippoglossus hippoglossus* L.). *Comparative Biochemistry and Physiology Part A: Molecular & Integrative Physiology*, 134(2), 315-327.
- Weltzien, F. A., Andersson, E., Andersen, O., Shalchian-Tabrizi, K., & Norberg, B. (2004). The brain-pituitary-gonad axis in male teleosts, with special emphasis on flatfish (Pleuronectiformes). *Comp Biochem Physiol A Mol Integr Physiol*, 137(3), 447-477.
- Weltzien, F. A., Hildahl, J., Hodne, K., Okubo, K., & Haug, T. M. (2014). Embryonic development of gonadotrope cells and gonadotropic hormones--lessons from model fish. *Mol Cell Endocrinol*, 385(1-2), 18-27.
- Weltzien, F. A., Norberg, B., Helvik, J. V., Andersen, O., Swanson, P., & Andersson, E. (2003). Identification and localization of eight distinct hormone-producing cell types in the pituitary of male Atlantic halibut (*Hippoglossus hippoglossus* L.). *Comp Biochem Physiol A Mol Integr Physiol*, 134(2), 315-327.
- Wills, Q. F., Livak, K. J., Tipping, A. J., Enver, T., Goldson, A. J., Sexton, D. W., & Holmes, C. (2013). Single-cell gene expression analysis reveals genetic associations masked in whole-tissue experiments. *Nat Biotechnol*, 31(8), 748-752.
- Wingstrand, K. G. (1966). *Comparative anatomy and evolution of thehypophysis. In: The Pituitary Gland: Anterior Pituitary* (Vol. 1). California: University of California press.
- Wootton, R. J. (1990). *Ecology of teleost fishes*. . Chapman and Hall.
- Yang, A., Zhang, W., Wang, J., Yang, K., Han, Y., & Zhang, L. (2020). Review on the Application of Machine Learning Algorithms in the Sequence Data Mining of DNA. *Frontiers in bioengineering and biotechnology*, 8, 1032-1032.
- Yaron, Z., Gur, G., Melamed, P., Rosenfeld, H., Elizur, A., & Levavi-Sivan, B. (2003). Regulation of fish gonadotropins. *Int Rev Cytol*, 225, 131-185.
- Zhang, X., Li, T., Liu, F., Chen, Y., Yao, J., Li, Z., Huang, Y., & Wang, J. (2019). Comparative Analysis of Droplet-Based Ultra-High-Throughput Single-Cell RNA-Seq Systems. *Molecular Cell*, 73(1), 130-142.e135.
- Zheng, G. X. Y., Terry, J. M., Belgrader, P., Ryvkin, P., Bent, Z. W., Wilson, R., Ziraldo, S. B., Wheeler, T. D., McDermott, G. P., Zhu, J., Gregory, M. T., Shuga, J., Montesclaros, L., Underwood, J. G., Masquelier, D. A., Nishimura, S. Y., Schnell-Levin, M., Wyatt, P. W., Hindson, C. M., Bharadwaj, R., Wong, A., Ness, K. D., Beppu, L. W., Deeg, H. J., McFarland, C., Loeb, K. R., Valente, W. J., Ericson, N. G., Stevens, E. A., Radich, J. P., Mikkelsen, T. S., Hindson, B. J., & Bielas, J. H. (2017). Massively parallel digital transcriptional profiling of single cells. *Nature Communications*, 8(1), 14049.
- Ziegenhain, C., Vieth, B., Parekh, S., Reinius, B., Guillaumet-Adkins, A., Smets, M., Leonhardt, H., Heyn, H., Hellmann, I., & Enard, W. (2017). Comparative Analysis of Single-Cell RNA Sequencing Methods. *Mol Cell*, 65(4), 631-643 e634.

Zilionis, R., Nainys, J., Veres, A., Savova, V., Zemmour, D., Klein, A. M., & Mazutis, L. (2017). Single-cell barcoding and sequencing using droplet microfluidics. *Nature Protocols*, *12*(1), 44-73.

Zohar, Y., Munoz-Cueto, J. A., Elizur, A., & Kah, O. (2010). Neuroendocrinology of reproduction in teleost fish. *Gen Comp Endocrinol*, *165*(3), 438-455.

Appendix: Papers I-III

8





I



OPEN

Characterization of hormone-producing cell types in the teleost pituitary gland using single-cell RNA-seq

DATA DESCRIPTOR

Khadeeja Siddique, Eirill Ager-Wick, Romain Fontaine , Finn-Arne Weltzien  & Christiaan V. Henkel 

The pituitary is the vertebrate endocrine gland responsible for the production and secretion of several essential peptide hormones. These, in turn, control many aspects of an animal's physiology and development, including growth, reproduction, homeostasis, metabolism, and stress responses. In teleost fish, each hormone is presumably produced by a specific cell type. However, key details on the regulation of, and communication between these cell types remain to be resolved. We have therefore used single-cell sequencing to generate gene expression profiles for 2592 and 3804 individual cells from the pituitaries of female and male adult medaka (*Oryzias latipes*), respectively. Based on expression profile clustering, we define 15 and 16 distinct cell types in the female and male pituitary, respectively, of which ten are involved in the production of a single peptide hormone. Collectively, our data provide a high-quality reference for studies on pituitary biology and the regulation of hormone production, both in fish and in vertebrates in general.

Background & Summary

The pituitary is a master endocrine gland in vertebrates, which is involved in the control of a variety of essential physiological functions including growth, metabolism, homeostasis, reproduction, and response to stress^{1–3}. These functions are modulated by the secretion of several peptide hormones, produced by different endocrine cell types of the adenohypophysis².

While in mammals the endocrine cells are distributed throughout the adenohypophysis^{2,4}, the pituitary of teleost fish is highly compartmentalized, with specialized hormone-producing cell types located in specific regions². As the teleost pituitary produces at least eight peptide hormones in distinct cell types², the physiology of the pituitary gland is relatively complex⁵. The *rostral pars distalis* contains lactotropes and corticotropes, which produce prolactin (Prl) and adrenocorticotropic hormone (Acth), respectively. Somatotropes (producing growth hormone, Gh), gonadotropes (luteinizing hormone, Lh and follicle-stimulating hormone, Fsh) and thyrotropes (thyroid-stimulating hormone, Tsh) are located in the *proximal pars distalis*, and somatolactotropes (somatolactin, Sl) and melanotropes (α -melanocyte stimulating hormone, α -Msh) in the *pars intermedia*⁴. In addition, in tetrapods, the gonadotropins Lh and Fsh can be produced in the same cell, while fish gonadotropes are generally thought to secrete either Fsh or Lh, but not both^{2,6–8}.

In recent years, transcriptome sequencing (RNA-seq) has emerged as a powerful technology to study the expression and regulation of pituitary genes. For example, RNA-seq has been used to study gene expression in the zebrafish pituitary during maturation⁹, in prepubertal female silver European eel pituitary glands¹⁰, and in FACS-selected Lh cells from the Japanese medaka pituitary¹¹. Although these studies provide a valuable perspective on the regulation of hormone production, RNA-seq is a bulk technology, which averages gene expression over the entire tissue sample. As a result, it does not provide information on which hormones are produced in which cells. Knowledge on the physiology and development of the individual pituitary cell types, as well as on the regulatory mechanisms involved in hormone production, therefore remains limited.

Physiology Unit, Faculty of Veterinary Medicine, Norwegian University of Life Sciences, Ås, Norway. ✉e-mail: finn-arne.weltzien@nmbu.no; christiaan.henkel@nmbu.no

In this study, we employed single-cell RNA-seq (scRNA-seq) technology, which allows the study of biological questions in which cell-specific changes in the transcriptome are important, e.g. cell type identification, variability in gene expression, and heterogeneity within populations of genetically identical cells^{12,13}. scRNA-seq has recently been used to describe the heterogeneity within the pituitary cell populations in mammals^{14,15} and zebrafish¹⁶. Unlike bulk RNA-seq, scRNA-seq promises to disentangle the processes at work in pituitary hormone production.

We used medaka (*Oryzias latipes*)^{17,18} to construct a transcriptomic snapshot of the cell types in the adult pituitary gland. Medaka is an emerging model species, which has a small genome (800 Mbp) and is a representative of the largest radiation within the teleosts (euteleosts, Cohort¹⁹ Euteleostomorpha). As such, it is a complementary model to zebrafish¹⁶, which belongs to another major teleost clade (Cohort Otomorpha)¹⁹.

We used the 10x Genomics scRNA-seq platform to analyze female and male pituitaries separately and obtained 2592 and 3804 high-quality cellular transcriptome profiles, respectively. This dataset provides a comprehensive transcriptomic reference on the teleost pituitary, as well as on its constituent cell types. After bioinformatics analysis, we found these profiles to belong to 15 and 16 distinct cell populations in the female and male pituitary, respectively, of which ten are involved in the production of a single peptide hormone. This suggests the teleost pituitary is subject to a higher degree of division of labour than its mammalian counterpart, in which many cells express multiple hormone-encoding genes¹⁴.

Methods

Fish strain and animal husbandry. For this study, we used a transgenic line of Japanese medaka derived from the d-rR genetic background, in which the Lh β gene (*lhb*) promoter drives the expression of the green fluorescent protein (*hr-gfpII*) gene^{20,21}. Fish were kept in a re-circulating system (up to 10–12 fish per 3-liter tank) at 28 °C on a 14/10 h light/darkness cycle and were fed three times a day with a mix of dry food and *Artemia*. The animal experiments performed in this study were approved by the Norwegian University of Life Sciences, following guidelines for the care and welfare of research animals.

Pituitary sampling and cell dissociation. Pituitaries were collected from 24 female and 23 male adult medaka of approximately 8 months old (eggs fertilized 20 October 2017, sampling 6 June 2018). At this age, medaka are fully mature and sexually dimorphic. Fish were sacrificed between 07.30–09.00 h in the morning (around the time of spawning induced by the start of the artificial light period) by hypothermic shock (immersion in ice water) to minimize distress²². The pituitary was dissected immediately after severing the spinal cord. In order to reduce the influence of sampling time on the results, fish were processed in alternating batches of ten individuals of each sex at a time.

After sampling, pituitaries were pooled per sex and cells were dissociated as described²³. Briefly, fresh pituitaries were put in an Eppendorf tube with modified PBS (phosphate buffered saline, pH 7.75, 290 mOsm/kg, 0.05% bovine serum albumin) and kept on ice until processing. Pituitaries were treated with 0.1% w/v trypsin type II S for 30 minutes at 26 °C, then with 0.1% w/v trypsin inhibitor type I S supplemented with 2 μ g/mL DNase I for 20 minutes at 26 °C, and subsequently gently mechanically dissociated by repeated aspiration with a strained glass pipette. The cell solution was filtered through a 35 μ m cell strainer (BD Pharmingen) to remove potentially remaining clumps of cells. Dissociated pituitary cells were resuspended in 90 μ l modified PBS, counted and visually inspected for good cell dissociation and quality. Samples were kept on ice for approximately 30 minutes until scRNA-seq library preparation, which commenced at 12.00 h on the same day.

10x Genomics library preparation. We prepared scRNA-seq libraries on the 10x Genomics Chromium Controller at the Genomics Core Facility of the Radium Hospital (part of Oslo University Hospital). For the initial step of the library preparation (GEM generation and barcoding) 35 μ l of the cell suspension prepared in the previous step was used, containing approximately 10,000 (female) and 11,000 (male) cells. The 10x Genomics Single Cell 3' Reagents Kits v2 were used according to the manufacturer's guidelines (<https://support.10xgenomics.com/single-cell-gene-expression/library-prep/doc/user-guide-chromium-single-cell-3-reagent-kits-user-guide-v31-chemistry>) to prepare cDNA libraries for a target of 4,000 cells.

Sequencing. Per sample, four redundant sequencing libraries (without additional sequencing controls) were analyzed on an Illumina NextSeq 500 at the Genomics Core Facility. Read 1 was sequenced for 28 cycles (covering the 26 nt cellular barcode and UMI), read 2 for 96 cycles (covering the cDNA insert). For downstream analyses, the resulting FASTQ files were collated per sample.

Reference genome and annotation. We used the chromosome-scale Hd-rR medaka reference genome (Ensembl release 94) for alignments. In preliminary analyses, we noticed that many reads for expected pituitary-specific transcripts were mapped near, but outside the 3' boundary of gene annotations. Therefore, in order to improve transcript quantification accuracy, we manually inspected the read alignment to these and other highly expressed genes (using Samtools²⁴ v 1.10 and the Integrative Genomics Viewer²⁵ v 2.3), and adjusted 3' UTR annotations where necessary (Table 1). The resulting custom gene transfer file (GTF) was then supplied using the 10x Genomics Cell Ranger v 3.0.2 (<https://support.10xgenomics.com/single-cell-gene-expression/software/pipelines/latest/what-is-cell-ranger>) *mkref* command.

Initial data processing. We used the standard 10x Genomics Cell Ranger (v 3.0.2) pipeline with default parameters for preliminary analyses. It includes quality control of the FASTQ files, alignment of FASTQ files to the customized medaka reference using STAR²⁶ (v 2.5.1b), demultiplexing of cellular barcodes, and quantification of gene expression. Table 2 summarizes the Cell Ranger quality control and output.

Gene	Ensembl ID	Feature	Original	Updated
<i>pomca</i>	ENSORLG00000025908	3' exon	2:10971088–10975672 (–)	2:10971088–10971837 (–)
<i>prl</i>	ENSORLG00000016928	3' exon	8:23591803–23592288 (+)	8:23591803–23592634 (+)
<i>smtla</i>	ENSORLG00000013460	3' exon	13:26485894–26486532 (+)	13:26485894–26486136 (+)
<i>gh</i>	ENSORLG00000019556	3' exon	8:75404–76751 (+)	8:75404–75568 (+)
<i>tshba</i>	ENSORLG00000029251	3' exon	5:13105690–13108242 (–)	5:13107640–13108242 (–)
<i>fshb</i>	ENSORLG00000029237	3' exon	3:9888850–9890682 (–)	3:9890408–9890682 (–)
<i>lhb</i>	ENSORLG00000003553	3' exon	15:14339670–14339965 (+)	15:14339670–14340309 (+)
<i>nr5a1</i>	ENSORLG00000013196	3' exon	12:24979868–24980234 (–)	12:24979864–24980234 (–)
<i>Cga</i>	ENSORLG00000022598	3' exon	22:10122990–10126745 (–)	22:10126430–10126745 (–)
		alt. transcript	22:10124168–10144948 (–)	removed
<i>mdkb</i>	ENSORLG00000014169	3' exon	6:26806299–26806315 (–)	6:26805916–26806315 (–)
<i>eef1a</i>	ENSORLG00000007614	3' exon	11:17258988–17259109 (–)	11:17258988–17258678 (–)
<i>fh1a</i>	ENSORLG00000005872	3' exon	3:17888694–17888835 (–)	3:17888418–17888835 (–)
		3' exon	3:17888677–17888835 (–)	3:1788841817888835 (–)
		exon	3:17888057–17888070 (–)	removed
<i>mcee</i>	ENSORLG00000022009	3' exon	3:17885682–17890772 (+)	3:17885682–17886310 (+)

Table 1. Genome annotation adjustments.

	Female	Male
Number of reads	165818560	142738097
Q30 bases in barcodes	97.5%	97.4%
Q30 bases in RNA reads	79.7%	80.3%
Q30 bases in UMI reads	83.4%	81.5%
Reads mapped to genome	84.1%	85.4%
Reads mapped confidently to exonic regions	59.9%	62.5%
Reads mapped uniquely to genome	82.4%	83.8%
Estimated number of cells	2890	4321
Fraction of reads in cells	83.4%	81.5%
Mean reads per cell	57376	33033
Median genes detected per cell	1182	1063
Total genes detected	17321	17775

Table 2. Sequencing and Cell Ranger statistics.

	Female	Male
Unfiltered cells	74338	77520
Filtered cells	4945	7334
Filtered genes detected	18786	19043
Genes with exons	17284	17882
Genes with introns	15036	15598
Cells pre-doublet detection	2644	3921
Cells post-doublet detection	2592	3804

Table 3. Final cell quantification statistics.

Cell Ranger also performs automated cell clustering based on the similarity of gene expression profiles. We used the Loupe Cell Browser v 3.1.1 (<https://support.10xgenomics.com/single-cell-gene-expression/software/visualization/latest/what-is-loupe-cell-browser>) to visualize these results. Unsupervised graph-based clustering suggested nine and eleven cell populations in the female and male medaka pituitary, respectively (see Code Availability).

For a more detailed analysis, we used the Seurat²⁷ R toolkit (v 3.1.5) and dropEst²⁸ (v 0.8.5) for accurate estimation of molecular counts per cell (Table 3). We used the *.bam* files produced by Cell Ranger as the input for dropEst.

Quality control (QC). dropEst by default reports any barcode with more than 100 UMIs as cellular (filtered cells in Table 3). Presumably, this relaxed threshold still includes many non-cellular and debris barcodes. Therefore, we explored these data using Seurat, and derived additional selection criteria for cellular barcodes based on the UMIs counts, mitochondrial fraction and globin expression. After imposing these thresholds, 2644 and 3921 cells remained for the female and male pituitary, respectively.

Cell types	Hormone	Female cells	%	Male cells	%	Marker gene	References
1. Melanotropes	α -Msh	54	2.1	53	1.4	<i>pomca, oacyl</i>	2,15
2. Corticotropes	Ath	25	1.0	55	1.5	<i>pomca</i>	15
3. Lactotropes	Prl	123	4.7	175	4.6	<i>prl</i>	14,15
4. Lactotropes	Prl	69	2.7	222	5.8	<i>prl</i>	14,15
5. Somatolactotropes	Sl	15	0.6	38	0.9	<i>smtla</i>	16,30
6. Somatotropes	Gh	52	2.0	127	3.3	<i>gh</i>	14,15
7. Thyrotropes	Tsh	69	2.7	46	1.2	<i>tshba</i>	14,15
8. Fsh- gonadotropes	Fsh	72	2.8	198	5.2	<i>fshb</i>	15,31
9. Lh- gonadotropes	Lh	535	20.6	895	23.5	<i>lhb</i>	2,15,21,30
10. Gonadotrope-like		597	23.0	444	11.7	<i>ega, nr5a1b</i>	31,32
11. Red blood cells		371	14.3	559	14.7	<i>gb</i>	
12. Macrophages		15	0.6	15	0.4	<i>clqa, clqb, clqc</i>	14,15
13. Uncharacterized		277	10.7	410	10.8		
14. Uncharacterized		198	7.6	386	10.2		
15. <i>ega</i> -expressing cells		120	4.6	160	4.2	<i>ega</i>	30
16. Uncharacterized				21	0.6		

Table 4. Cells per cluster in scRNA-seq data.

Since single-cell capture is sensitive to the formation of doublets, we used the R package DoubletFinder²⁹ (v 2.0.3) to detect hybrid expression profiles in our data. The number of expected real doublets depends on the number of cells captured. We selected a 2% doublet rate for the female sample and a 3% doublet rate for the male sample, based on the 10x Genomics specifications (<https://support.10xgenomics.com/single-cell-gene-expression/index/doc/user-guide-chromium-single-cell-3-reagent-kits-user-guide-v2-chemistry>). We removed 52 and 117 putative doublets from the female and male pituitary data, respectively.

Clustering. After QC, we normalized the data with the *LogNormalize* method in Seurat and identified highly variable genes by using the *vst* method. Subsequently, we used these variable genes ($n = 2000$) to identify significant principal components (PCs) based on the *jackStraw* function. We used ten informative PC dimensions in both samples as the input for uniform manifold approximation and projection (UMAP). After the dimensionality reduction, we clustered the cells using the *FindClusters* function with a resolution of 0.5 and 0.9 for the female and male data sets, respectively, and initially characterized 11 different clusters in both the female and male pituitary.

Cell type assignment. We used differentially expressed genes per cluster (*FindAllMarkers* with *min.pct = 0.25*) to help assign tentative cell type identities to these clusters. Marker genes (Table 4) reported in previous studies^{2,14–16,21,30–32} were used for cell type assignment.

Cluster refinement. During initial data exploration, we observed several clusters sharing many common markers. Therefore, we further inspected their heterogeneity iterating the clustering function on selected subsets of the data. Subclusters were detected across multiple clustering resolutions (0.2 and 0.5) of the *FindClusters* function in Seurat. We subsequently used the *FindAllMarkers* function to find differentially expressed genes between each of these subclusters to highlight the differences and finally decided on the cell type boundaries for these ‘zoomed-in’ sub-clusters.

Data integration. We combined the female and male datasets using the Seurat *FindIntegrationAnchors* and *IntegrateData* functions, using default settings. For subsequent visualization, we randomly downsampled the male data to 2592 cells.

Bulk RNA-seq analyses. We quantified the Cell Ranger *.bam* files without cellular barcode demultiplexing using htseq-count³³ (v 0.11.2) with the *intersection-nonempty* setting. In addition, we quantified gene expression from comparable (adult) samples of a separate bulk RNA-seq study^{34,35} on the medaka pituitary gland. Sequencing libraries for these samples (females 122–124, 249–277 days post-fertilization; and males 137–139, 96–129 days post-fertilization) were previously prepared using the Smart-SEQ HT kit (Takara Bio), sequenced at 2×151 nt on an Illumina NovaSeq 6000, and aligned to the modified medaka reference genome using STAR. For both studies, 23635 annotated protein-coding genes were quantified in counts per million reads (CPM).

Data Records

We present a characterization of the cell types of the medaka pituitary gland, as a basis for more in-depths analyses of the regulation of and inter-communication between different hormones and cell types.

Our data set on the medaka pituitary consists of gene expression values for 2592 and 3804 adult female and male cells, respectively. These can be assigned to 15 or 16 distinct cell populations, respectively, one of which appears to be unique to male pituitaries. We assigned biological identities to 12 populations based on the expression of known hormone-encoding genes. Figure 1 and Table 4 provide an overview of the cell types of the medaka pituitary.

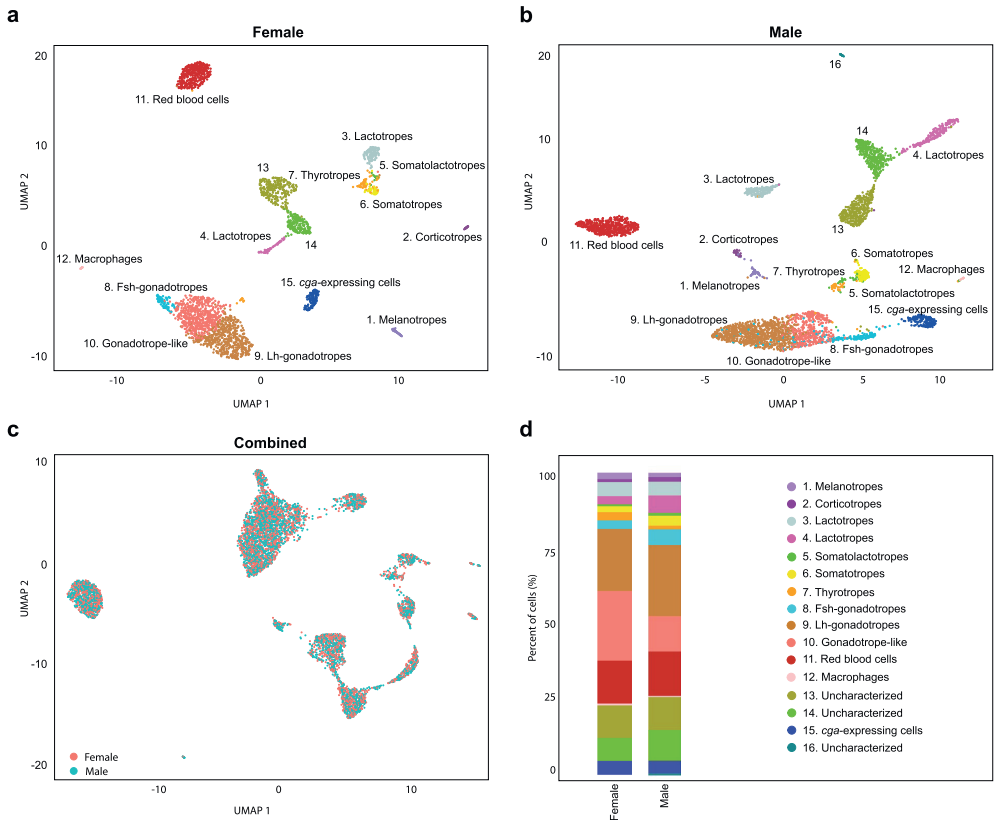


Fig. 1 Clustering of scRNA-seq data reveals the cell populations of the female and male medaka pituitary. **(a)** Uniform manifold approximation and projection (UMAP) plot showing the classification of distinct cell types of the female pituitary **(b)** UMAP plot showing the classification of distinct cell types of the male pituitary. UMAP offers a projection of individual cellular expression profiles (which are high-dimensional data points) into two dimensions. Cells are represented by dots; close proximity of cells in the UMAP projection indicates their expression profiles are similar. Therefore, cells of a distinct type appear as clusters. See Table 4 for details on cluster identity assignment. **(c)** UMAP visualization of unsupervised Seurat integration of the female and male datasets shows the cell types for both samples are comparable. **(d)** Barplots showing the percentage of cells per cluster in both samples (see Table 4).

Availability. The main data record³⁶ consists of *barcodes.tsv*, *features.tsv* and *matrix.mtx* files, listing raw UMI counts for each gene (feature) in each cell (barcode) in a sparse matrix format. In addition, we provide a table of cell type assignments and UMAP projections for each individual cell (barcode), as well as a summary of the top differentially expressed genes per cell type. Raw sequencing data are available in FASTQ format³⁷. Finally, the data record contains matrix files on exonic and intronic expression, which can be used for Velocyto gene expression dynamics analyses³⁸. These data can be accessed through the project accession number GSE162787 at the NCBI Gene Expression Omnibus³⁶.

The bulk RNA-seq data used for validation can be accessed through GSE179598 at the NCBI Gene Expression Omnibus³⁵, and will be described in more detail in a separate publication³⁴.

Technical Validation

In order to validate the quality of our data, we investigated their reproducibility, the influence of technical variables, and the biological perspective.

Reproducibility. At the level of cell type clustering (Fig. 1a–b), both datasets appear superficially similar. We further investigated whether the cells in the female and male medaka pituitary are comparable by integrating both datasets in a single analysis. The resulting UMAP visualization (Fig. 1c) suggests this is indeed the case, with all major cell clusters remaining intact in this projection. In general, the numbers of cells per cluster are

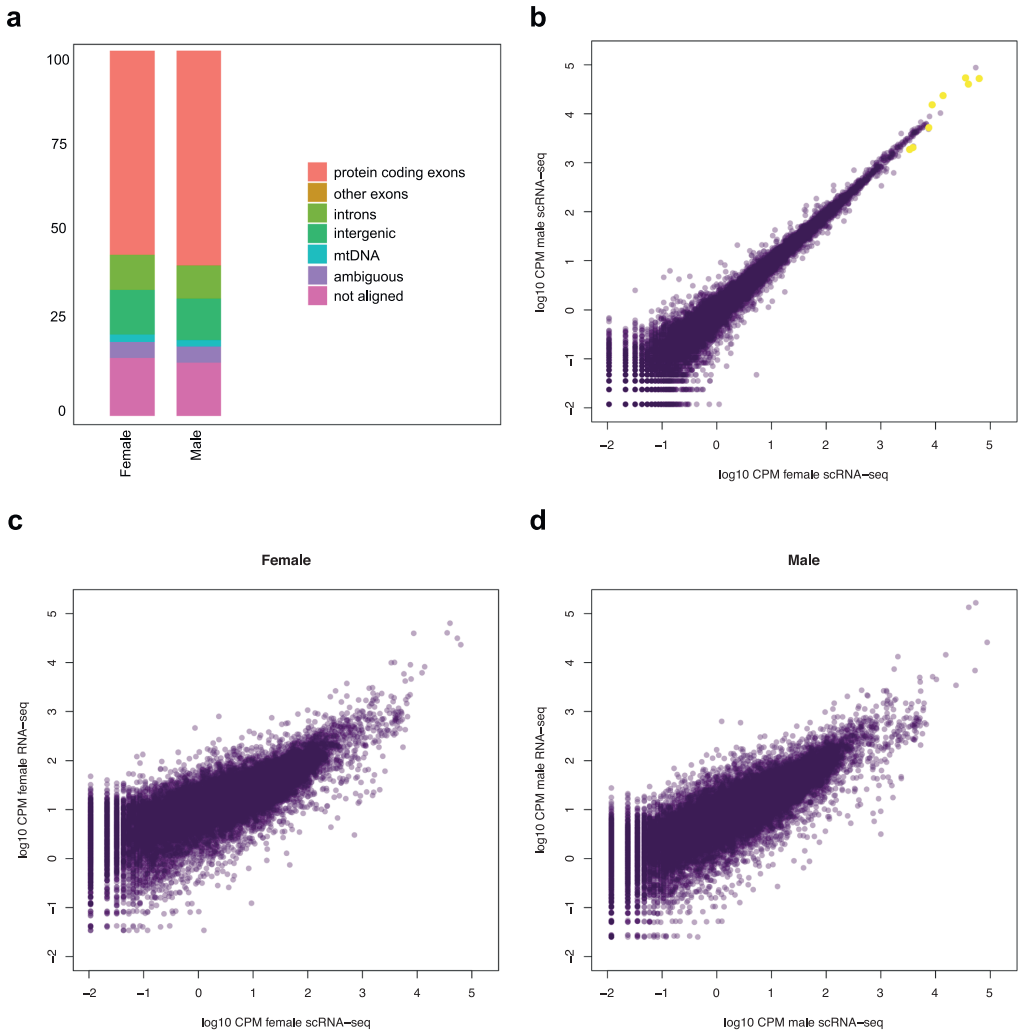


Fig. 2 Sequencing reproducibility. **(a)** Stacked barplots of read mapping to genomic fractions for both samples. **(b)** Scatterplot of gene expression in both scRNA-seq samples processed as bulk samples, showing good correspondence between females and males. Yellow dots indicate the major protein hormone-encoding genes. CPM: counts per million. **(c)** Scatterplot of compound gene expression (CPM) in female scRNA-seq compared to bulk RNA-seq (CPM) on comparable samples (mean of three samples). **(d)** Idem for male scRNA-seq and three comparable male RNA-seq samples.

similar between the two samples (Fig. 1d), with minor differences that are consistent with previously established sex-specific patterns³⁹.

This analysis also suggests both datasets are highly reproducible. We further established this by comparing the compound expression of protein-coding genes in the data (Fig. 2a), i.e. without deconvolution into constituent cells. At the level of read counts per million (CPM), female and male data are again highly similar (Fig. 2b, Spearman rank correlation 0.98).

As one of our intended uses for this scRNA-seq dataset is to interpret patterns in additional RNA-seq studies, we also compared these counts to CPM derived from bulk RNA-seq on biologically similar samples (Fig. 2c,d). Here, the overall gene expression patterns remain qualitatively similar (Spearman rank correlation 0.80–0.87), although expression level quantification is presumably affected by differences in library preparation protocols (3'-specific 10x Genomics versus full transcript Smart-SEQ).

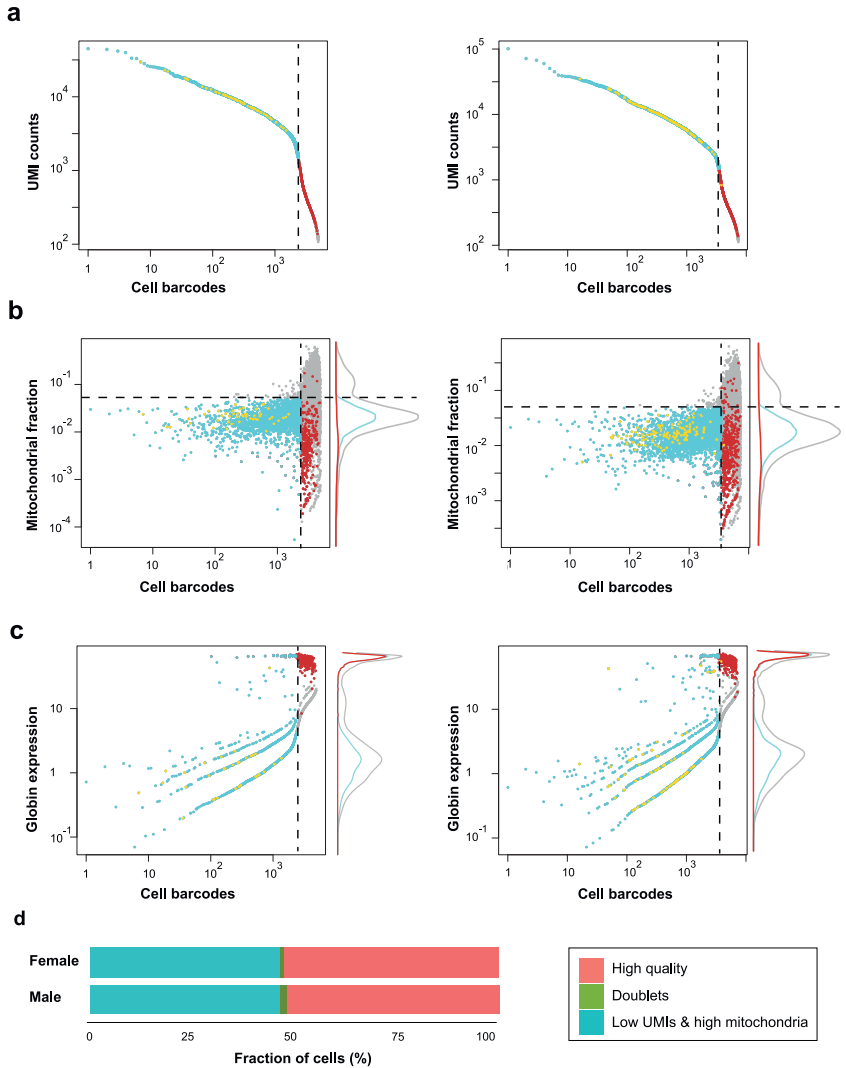


Fig. 3 Selection of cellular barcodes in pituitary single-cell data. Left panels: female sample, right panels: male sample. **(a)** Threshold 1: QC based on the UMIs counts. The cyan dots illustrate the final selected barcodes, grey dots represent barcodes not meeting selection criteria, orange dots indicate potential doublets, and red dots represent globin-expressing cells. The dotted line represents the UMI cutoff value. **(b)** Threshold 2: QC based on the mitochondrial fraction. The horizontal dotted line indicates the 5% threshold. Marginal plots indicate the densities of barcode sets at different values (grey line: all cells). **(c)** Threshold 3: QC based on globin (*gb*)-expressing cells (red dots), which do not meet the UMI count criterion (panel and dotted line) but are included in our final dataset. Note that the axes are on logarithmic scales, and that the horizontal axis is identical for all the panels of a sample. **(d)** Breakdown of cellular QC for the 4945 (female) and 7334 (male) barcodes reported by dropEst.

Technical quality control. Interpretation of single-cell transcriptomics data is highly sensitive to technical artifacts. For example, expression profiles can derive from low quality cells, cellular debris, or ambient RNA. We therefore determined empirical thresholds distinguishing genuine cellular expression profiles from noise (Fig. 3). We defined selection criteria for cellular barcodes based on UMI counts (Fig. 3a), expression of mitochondrial genes (Fig. 3b, cyan dots), expression of genes specific to red blood cells (Fig. 3c, red dots), and a probability score for cellular doublets (Fig. 3a–c, orange dots). Based on the distribution of UMI counts per barcode, we defined

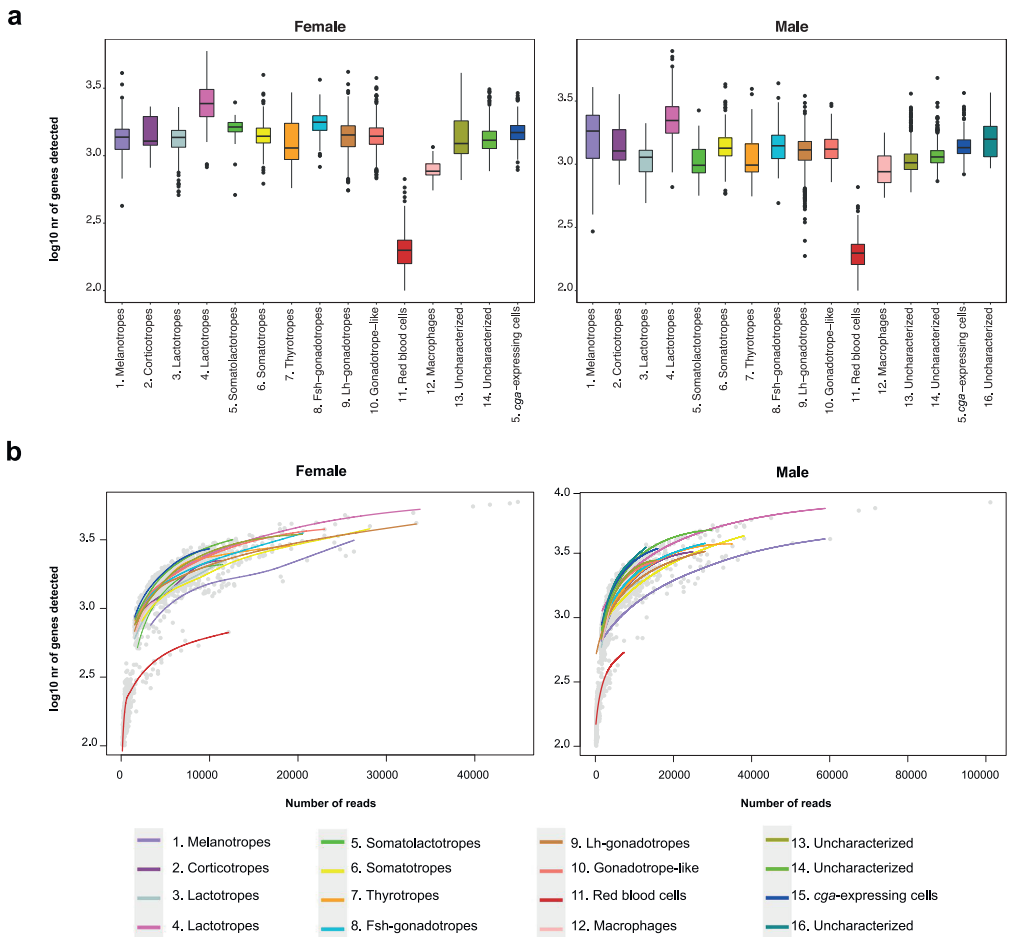


Fig. 4 Cell type quality. **(a)** Boxplots showing the number of genes detected per cell type for both samples. Boxes correspond to the interquartile range (IQR), whiskers indicate $1.5 \times$ the IQR. **(b)** Sequencing saturation curves. Grey dots represent individual cellular gene expression profiles, coloured lines are loess local regression curves for each cell type.

as cellular barcodes those with ≥ 1500 UMIs in both female and male samples. High levels of expression of mitochondrial genes have been interpreted as an indication of damaged cells^{40,41}. We therefore excluded barcodes in which mitochondrial gene expression contributes more than 5% of the total (for both females and males, Fig. 3b).

In initial clustering analyses, we noticed that these criteria exclude both technical artifacts (data not shown) and a single cluster of cells with low overall UMI counts, but a very clearly defined expression profile. Based on their expression profile we interpret these barcodes to represent red blood cells. Although they are developmentally only very distantly related to the other cells in the pituitary, our data show that they are an intrinsic (if transient) component. Therefore, including them in our dataset will allow for more precise interpretation of patterns in bulk RNA-seq studies (e.g. Figure 2c–d).

With the exception of these red blood cells, all other defined cell types show a high and consistent number of genes expressed per individual cell (Fig. 4a). In addition, a saturation analysis (Fig. 4b), contrasting the number of genes expressed per cell and the sequencing depth per cell, suggests the latter is sufficient to capture most of the transcriptomic complexity for each cell type.

Biological quality control. In order to validate the biological relevance of the cell type identities shown in Fig. 1, we have compared their gene expression patterns with known expression profiles from both teleosts and mammals. Initially, we identified eleven different populations based on optimized Seurat clustering. However, there were several clusters that shared high expression of known, specific marker genes. We therefore

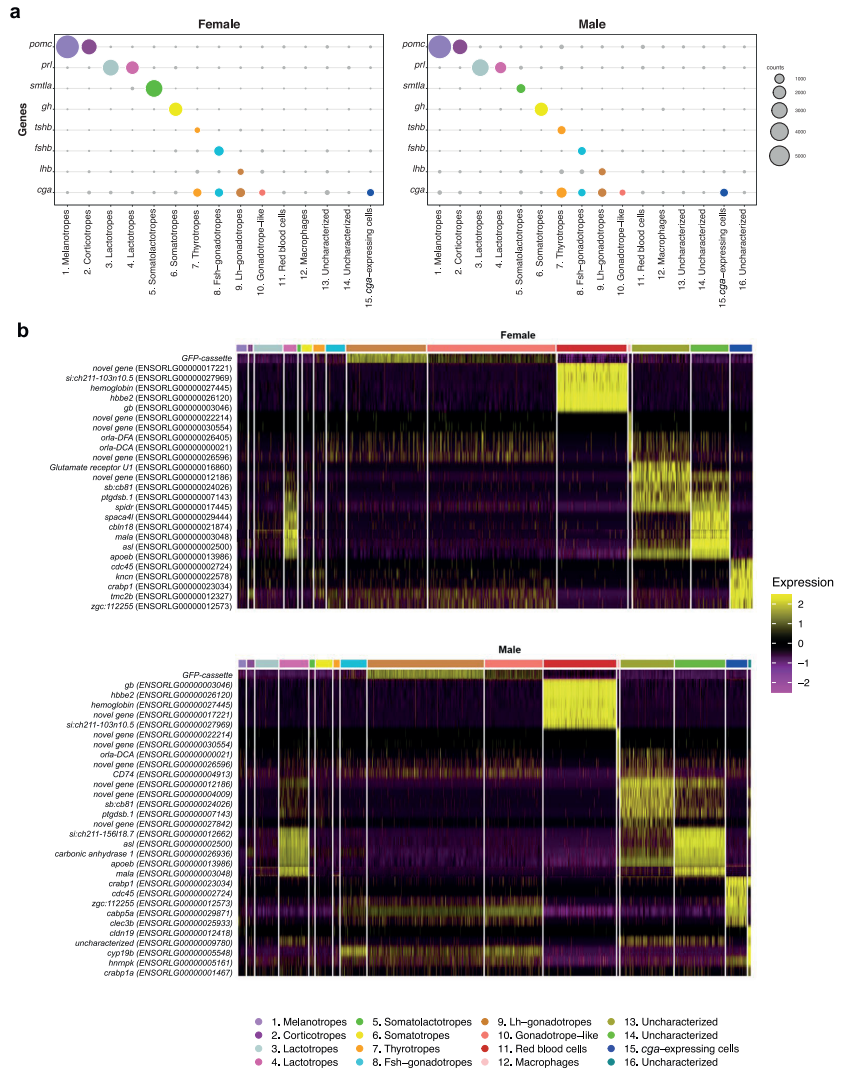


Fig. 5 Cell type functions. **(a)** The expression of hormone-encoding genes in female and male pituitary, respectively. Values are the mean of normalized expression over all cells in a cluster. The grey dots indicate low expression of genes. **(b)** Expression pattern heatmaps for uncharacterized cell types in both female and male data.

evaluated expression heterogeneity within each cluster and manually defined final clusters (see Methods). We defined two subclusters for the initial cluster expressing *pomca* (ENSORLG00000025908), which encodes pro-opiomelanocortin, the protein precursor for α -Msh and Acth. The first subcluster has high expression of *pomca*, *oacyl* (ENSORLG00000005993), *crhbp* (ENSORLG00000002228), *pck2* (ENSORLG00000006472) and *pax7* (ENSORLG00000004269), which are markers for the α -Msh-secreting melanotropes; the second subcluster was identified as Acth-secreting corticotropes due to lower expression of *pax7* and *pomca*¹⁵.

Next, a large compound cluster on the right side of Fig. 1 (both females and males) shares three important hormone-encoding genes: *tshb*, *gh* and *smtla*. We therefore divided it into three subclusters using Seurat, gene expression patterns and differentially expressed (DE) genes (see available code for details). The first subcluster has strong expression of *tshba* (ENSORLG00000029251, encoding the β subunit of Tsh), which is a robust marker for thyrotropes (orange color in Fig. 1). The second subcluster expresses *gh* (ENSORLG00000019556), which demarcates the somatotropes (yellow). The last subcluster (light green) has expression of *smtla* (ENSORLG00000013460,

which encodes Sl, a hormone produced by the teleost, but not the mammalian, pituitary gland)^{16,21,30,42}. In contrast to in the zebrafish pituitary¹⁶, we did not observe the expression of *pou1f1* (ENSORLGG00000015870) in somatolactotropes.

Finally, Seurat initially divided the big cluster of gonadotrope cells (expressing the gonadotropin α -subunit *cga*, ENSORLGG00000022598) at the bottom of Fig. 1 into two subclusters for the males, but not for the females. However, based on the heterogeneity of the expression pattern in the female cluster, and its apparent homology to the two male clusters, we defined two subclusters: one is enriched for *lhb* (ENSORLGG00000003553, encoding the β subunit of Lh) and *gnhr2* (ENSORLGG00000012659, also known as *gnhr2a*⁴³) expression, both of which are exclusively associated with Lh production in teleosts^{43,44}; the other expresses *nr5a1b* (ENSORLGG00000013196), encoding a nuclear receptor involved in gonadotropin regulation in the mammalian pituitary and teleosts^{16,32}.

Three remaining cell clusters we directly assigned to specific hormone-producing cell types, based on the very high expression of hormone-encoding genes: two distinct populations of lactotropes expressing *prl* (ENSORLGG00000016928) and *fshb*-expressing gonadotropes (ENSORLGG00000029237, encoding the β subunit of Fsh).

After final clustering, we define 15 and 16 distinct expression patterns in female and male data, respectively, which we interpret as distinct cell types (see Fig. 1 and Table 4). Based on their expression patterns, we could assign unambiguous cell type identities to twelve of these (Fig. 5). Ten clusters show high expression of genes encoding protein hormones (Fig. 5a and Table 4). In addition, one cluster expresses *cga*, but no gene encoding a β subunit. Two clusters appear to be red blood cells and macrophages (Fig. 5b and Table 4). Based on detailed expression patterns (Fig. 5b) we could not unequivocally define the elusive folliculostellate cell population of the pituitary. In the mammalian pituitary, these cells (of partly unknown function) are characterized by marker genes¹⁴ that show significant, but specific expression in two of our uncharacterized cell populations (clusters 13 and 14, Fig. 1).

Traditionally, a marker for these cells is the *s100* gene^{45,46}, however, this gene has at least eight homologs in the medaka genome, most of which do not show an unambiguous expression pattern in the pituitary.

Overall, our assignments of biological function largely confirm a 'one cell type, one hormone' (Fig. 5a) division of labour, in which major hormones are produced by a single, dedicated cell type. This is in apparent contrast to the mammalian pituitary, in which cells are often responsible for producing and releasing multiple hormones¹⁴.

Code availability

The R code used in the analysis of the scRNA-seq data is available on GitHub (<https://github.com/sikh09/Medaka-pituitary-scRNA-seq>).

Received: 5 January 2021; Accepted: 9 September 2021;

Published online: 28 October 2021

References

- Kelberman, D., Rizzoti, K., Lovell-Badge, R., Robinson, I. C. & Dattani, M. T. Genetic regulation of pituitary gland development in human and mouse. *Endocr. Rev.* **30**, 790–829 (2009).
- Weltzien, F. A., Andersson, E., Andersen, O., Shalchian-Tabrizi, K. & Norberg, B. The brain-pituitary-gonad axis in male teleosts, with special emphasis on flatfish (Pleuronectiformes). *Comp. Biochem. Physiol. A Mol. Integr. Physiol.* **137**, 447–477 (2004).
- Ooi, G. T., Tawadros, N. & Escalona, R. M. Pituitary cell lines and their endocrine applications. *Mol. Cell. Endocrinol.* **228**, 1–21 (2004).
- Pogoda, H. M. & Hammerschmidt, M. Molecular genetics of pituitary development in zebrafish. *Semin. Cell. Dev. Biol.* **18**, 543–558 (2007).
- Perez-Castro, C., Renner, U., Haedo, M. R., Stalla, G. K. & Arzt, E. Cellular and molecular specificity of pituitary gland physiology. *Physiol. Rev.* **92**, 1–38 (2012).
- Golan, M., Martin, A. O., Mollard, P. & Levavi-Sivan, B. Anatomical and functional gonadotrope networks in the teleost pituitary. *Sci. Rep.* **6**, 23777 (2016).
- Yaron, Z. *et al.* Regulation of fish gonadotropins. *Int. Rev. Cytol.* **225**, 131–185 (2003).
- Fontaine, R. *et al.* Gonadotrope plasticity at cellular, population and structural levels: A comparison between fishes and mammals. *Gen. Comp. Endocrinol.* **287**, 113344 (2020).
- He, W., Dai, X., Chen, X., He, J. & Yin, Z. Zebrafish pituitary gene expression before and after sexual maturation. *J. Endocrinol.* **221**, 429–440 (2014).
- Ager-Wick, E. *et al.* The pituitary gland of the European eel reveals massive expression of genes involved in the melanocortin system. *PLoS One* **8**, e77396 (2013).
- Ager-Wick, E., Henkel, C. V., Haug, T. M. & Weltzien, F. A. Using normalization to resolve RNA-Seq biases caused by amplification from minimal input. *Physiol. Genomics* **46**, 808–820 (2014).
- Kolodziejczyk, A. A., Kim, J. K., Svensson, V., Marioni, J. C. & Teichmann, S. A. The technology and biology of single-cell RNA sequencing. *Mol. Cell* **58**, 610–620 (2015).
- Rostom, R., Svensson, V., Teichmann, S. A. & Kar, G. Computational approaches for interpreting scRNA-seq data. *FEBS Lett.* **591**, 2213–2225 (2017).
- Ho, Y. *et al.* Single-cell transcriptomic analysis of adult mouse pituitary reveals sexual dimorphism and physiologic demand-induced cellular plasticity. *Protein Cell* **11**, 565–583 (2020).
- Cheung, L. Y. M. *et al.* Single-cell RNA sequencing reveals novel markers of male pituitary stem cells and hormone-producing cell types. *Endocrinology* **159**, 3910–3924 (2018).
- Fabian, P. *et al.* Lineage analysis reveals an endodermal contribution to the vertebrate pituitary. *Science* **370**, 463–467 (2020).
- Wittbrodt, J., Shima, A. & Scharl, M. Medaka – a model organism from the far East. *Nat. Rev. Genet.* **3**, 53–64 (2002).
- Ishikawa, Y. Medaka fish as a model system for vertebrate developmental genetics. *Bioessays* **22**, 487–495 (2000).
- Betancur, R. R. *et al.* Phylogenetic classification of bony fishes. *BMC Evol. Biol.* **17**, 162 (2017).
- Hildahl, J. *et al.* Developmental tracing of luteinizing hormone beta-subunit gene expression using green fluorescent protein transgenic medaka (*Oryzias latipes*) reveals a putative novel developmental function. *Dev. Dyn.* **241**, 1665–1677 (2012).
- Fontaine, R., Ager-Wick, E., Hodne, K. & Weltzien, F. A. Plasticity of Lh cells caused by cell proliferation and recruitment of existing cells. *J. Endocrinol.* **240**, 361–377 (2019).
- Köhler, A. *et al.* Report of Workshop on Euthanasia for Zebrafish – a matter of welfare and science. *Zebrafish* **14**, 547–551 (2017).
- Ager-Wick, E. *et al.* Preparation of a high-quality primary cell culture from fish pituitaries. *J. Vis. Exp.* **138**, e58159 (2018).
- Li, H. *et al.* The Sequence Alignment/Map format and SAMtools. *Bioinformatics* **25**, 2078–2079 (2009).

25. Thorvaldsdóttir, H., Robinson, J. T. & Mesirov, J. P. Integrative Genomics Viewer (IGV): high-performance genomics data visualization and exploration. *Brief. Bioinform.* **14**, 178–192 (2013).
26. Dobin, A. *et al.* STAR: ultrafast universal RNA-seq aligner. *Bioinformatics* **29**, 15–21 (2013).
27. Satija, R., Farrell, J. A., Gennert, D., Schier, A. F. & Regev, A. Spatial reconstruction of single-cell gene expression data. *Nat. Biotechnol.* **33**, 495–502 (2015).
28. Petukhov, V. *et al.* dropEst: pipeline for accurate estimation of molecular counts in droplet-based single-cell RNA-seq experiments. *Genome Biol.* **19**, 78 (2018).
29. McGinnis, C. S., Murrow, L. M. & Gartner, Z. J. DoubletFinder: Doublet detection in single-cell RNA sequencing data using artificial nearest neighbors. *Cell Syst.* **8**, 329–337 (2019).
30. Weltzien, F. A., Hildahl, J., Hodne, K., Okubo, K. & Haug, T. M. Embryonic development of gonadotrope cells and gonadotropic hormones—lessons from model fish. *Mol. Cell. Endocrinol.* **385**, 18–27 (2014).
31. Kazeto, Y. *et al.* Japanese eel follicle-stimulating hormone (Fsh) and luteinizing hormone (Lh): production of biologically active recombinant Fsh and Lh by *Drosophila* S2 cells and their differential actions on the reproductive biology. *Biol. Reprod.* **79**, 938–946 (2008).
32. Fletcher, P. A. *et al.* Cell type- and sex-dependent transcriptome profiles of rat anterior pituitary cells. *Front. Endocrinol.* **10**, 623 (2019).
33. Anders, S., Pyl, P. T. & Huber, W. HTSeq – a Python framework to work with high-throughput sequencing data. *Bioinformatics* **31**, 166–169 (2015).
34. Ager-Wick, E. *et al.* Ectopic expression of lipid homeostasis genes in rare cells of the teleost pituitary gland. Preprint at BioRxiv, <https://doi.org/10.1101/2021.06.11.448009> (2021).
35. *Gene Expression Omnibus* <https://identifiers.org/geo:GSE179598> (2021).
36. *Gene Expression Omnibus* <https://identifiers.org/geo:GSE162787> (2020).
37. *NCBI Sequence Read Archive* <https://identifiers.org/insdc.sra:SRP296792> (2020).
38. La Manno, G. *et al.* RNA velocity of single cells. *Nature* **560**, 494–498 (2018).
39. Royan, M. R. *et al.* 3D atlas of the pituitary gland of the model fish medaka (*Oryzias latipes*). *Front. Endocrinol.* **12**, 719843 (2021).
40. Ilicic, T. *et al.* Classification of low quality cells from single-cell RNA-seq data. *Genome Biol.* **17**, 29 (2016).
41. Luecken, M. D. & Theis, F. J. Current best practices in single-cell RNA-seq analysis: a tutorial. *Mol. Syst. Biol.* **15**, e8746 (2019).
42. Herkenhoff, M. E. *et al.* Expression profiles of growth-related genes in two Nile tilapia strains and their crossbred provide insights into introgressive breeding effects. *Anim. Genet.* **51**, 611–616 (2020).
43. Ciani, E. *et al.* GnRH receptor gnhr2bbalpha is expressed exclusively in lhb-expressing cells in Atlantic salmon male parr. *Gen. Comp. Endocrinol.* **285**, 113293 (2020).
44. Hodne, K., Fontaine, R., Ager-Wick, E. & Weltzien, F. A. GnRH1-induced responses are indirect in female medaka Fsh cells, generated through cellular networks. *Endocrinology* **160**, 3018–3032 (2019).
45. Lloyd, R. V. & Mailloux, J. Analysis of S-100 protein positive folliculo-stellate cells in rat pituitary tissues. *Am. J. Pathol.* **133**, 338–346.
46. Itakura, E. *et al.* Generation of transgenic rats expressing green fluorescent protein in S-100beta-producing pituitary folliculo-stellate cells and brain astrocytes. *Endocrinology* **148**, 1518–1523 (2007).

Acknowledgements

We are thankful to Susanne Lorenz for sequencing and Lourdes Carreon G Tan for fish facility maintenance. This work was supported by NMBU and the Norwegian Research Council grants no. 251307, 255601, and 248828.

Author contributions

Eirill Ager-Wick, Finn-Arne Weltzien and Christiaan Henkel conceived and designed the project. Eirill Ager-Wick isolated the cells. Khadeeja Siddique, Romain Fontaine and Christiaan Henkel analyzed the data and wrote the paper with input from all other authors.

Competing interests

The authors declare no competing interests.

Additional information

Correspondence and requests for materials should be addressed to F.-A.W. or C.V.H.

Reprints and permissions information is available at www.nature.com/reprints.

Publisher's note Springer Nature remains neutral with regard to jurisdictional claims in published maps and institutional affiliations.



Open Access This article is licensed under a Creative Commons Attribution 4.0 International License, which permits use, sharing, adaptation, distribution and reproduction in any medium or format, as long as you give appropriate credit to the original author(s) and the source, provide a link to the Creative Commons license, and indicate if changes were made. The images or other third party material in this article are included in the article's Creative Commons license, unless indicated otherwise in a credit line to the material. If material is not included in the article's Creative Commons license and your intended use is not permitted by statutory regulation or exceeds the permitted use, you will need to obtain permission directly from the copyright holder. To view a copy of this license, visit <http://creativecommons.org/licenses/by/4.0/>.

The Creative Commons Public Domain Dedication waiver <http://creativecommons.org/publicdomain/zero/1.0/> applies to the metadata files associated with this article.

© The Author(s) 2021

II



3D Atlas of the Pituitary Gland of the Model Fish Medaka (*Oryzias latipes*)

Muhammad Rahmad Royan¹, Khadeeja Siddique¹, Gergely Csucs², Maja A. Puchades², Rasoul Nourizadeh-Lillabadi¹, Jan G. Bjaalie², Christiaan V. Henkel¹, Finn-Arne Weltzien¹ and Romain Fontaine^{1*}

¹ Physiology Unit, Faculty of Veterinary Medicine, Norwegian University of Life Sciences, Ås, Norway, ² Institute of Basic Medical Sciences, University of Oslo, Oslo, Norway

OPEN ACCESS

Edited by:

Ishwar Parhar,
Monash University Malaysia, Malaysia

Reviewed by:

Matan Golan,
Agricultural Research Organization
(ARO), Israel
Gustavo M. Somoza,
Instituto Tecnológico de Chascomús
(INTECH) (CONICET), Argentina

*Correspondence:

Romain Fontaine
romain.fontaine@nmbu.no

Specialty section:

This article was submitted to
Neuroendocrine Science,
a section of the journal
Frontiers in Endocrinology

Received: 03 June 2021

Accepted: 12 July 2021

Published: 23 August 2021

Citation:

Royan MR, Siddique K, Csucs G,
Puchades MA, Nourizadeh-Lillabadi R,
Bjaalie JG, Henkel CV, Weltzien F-A
and Fontaine R (2021) 3D Atlas of the
Pituitary Gland of the Model Fish
Medaka (*Oryzias latipes*).
Front. Endocrinol. 12:719843.
doi: 10.3389/fendo.2021.719843

In vertebrates, the anterior pituitary plays a crucial role in regulating several essential physiological processes via the secretion of at least seven peptide hormones by different endocrine cell types. Comparative and comprehensive knowledge of the spatial distribution of those endocrine cell types is required to better understand their physiological functions. Using medaka as a model and several combinations of multi-color fluorescence *in situ* hybridization, we present the first 3D atlas revealing the gland-wide distribution of seven endocrine cell populations: lactotropes, thyrotropes, Lh and Fsh gonadotropes, somatotropes, and *pomca*-expressing cells (corticotropes and melanotropes) in the anterior pituitary of a teleost fish. By combining *in situ* hybridization and immunofluorescence techniques, we deciphered the location of corticotropes and melanotropes within the *pomca*-expressing cell population. The 3D localization approach reveals sexual dimorphism of *tshba*-, *pomca*-, and *lhb*-expressing cells in the adult medaka pituitary. Finally, we show the existence of bi-hormonal cells co-expressing *lhb-fshb*, *fshb-tshba* and *lhb-sl* using single-cell transcriptomics analysis and *in situ* hybridization. This study offers a solid basis for future comparative studies of the teleost pituitary and its functional plasticity.

Keywords: pituitary, atlas, teleost, hormone, multihormonal cells, medaka, single-cell transcriptomics

HIGHLIGHTS

- We offer the first 3D atlas of a teleost pituitary, which presents a valuable resource to the endocrinology and model fish community.
- The atlas reveals the 3D spatial distribution of the seven endocrine cell types and blood vessels in the juvenile/adult male and female pituitary.
- Gene expression for *tshba*, *pomca*, and *lhb*, as well as the volume of the cell population expressing these genes, displays obvious sexual dimorphism in the adult medaka pituitary.
- Multi-color *in situ* hybridization and single cell RNA-seq reveal the existence of bi-hormonal cells, co-expressing *lhb-fshb*, *fshb-tshba*, *lhb-sl*, and a few multi-hormonal cells.
- An online version of the atlas is available at <https://www.nmbu.no/go/mpg-atlas>.

INTRODUCTION

In vertebrates, the pituitary is considered the *chef d'orchestre* of the endocrine system, regulating several essential biological and physiological functions throughout the life cycle. Located beneath the hypothalamus, it is divided into the anterior part (adenohypophysis) and posterior part (neurohypophysis). The former comprises several endocrine cell types which produce and release specific peptide hormones, controlling many important aspects of life, including growth, stress, metabolism, homeostasis, and reproduction (1, 2).

During embryogenesis, different cellular developmental trajectories specify several endocrine cell types in the adenohypophysis, characterized by the hormones they produce (3). In general, the vertebrate adenohypophysis consists of lactotropes (producing prolactin; Prl), corticotropes (adrenocorticotropic hormone; Acth), thyrotropes (thyrotropin; Tsh), gonadotropes (follicle-stimulating and luteinizing hormone; Fsh and Lh), somatotropes (growth hormone; Gh), and melanotropes (melanocyte-stimulating hormone; α -Msh), which have specific roles in regulating certain physiological functions (2, 4). Teleosts, in addition, have an endocrine cell type that is unique to these animals, i.e. somatolactotropes (somatolactin; Sl) (5). In contrast to mammals and birds, Fsh and Lh are mostly secreted by distinct endocrine cell types in teleosts (6), although both transcripts or hormones have sometimes been observed in the same cells in some species (7–10). Unlike mammals, teleost endocrine cells are arranged in discrete zones. Lactotropes and corticotropes are commonly located in the *rostral pars distalis* (RPD), thyrotropes, gonadotropes, and somatotropes in the *proximal pars distalis* (PPD), and melanotropes and somatolactotropes in the *pars intermedia* (PI) (5, 11).

Over the past five decades, endocrine cell type organization in the teleost pituitary has been documented in various species. Despite having approximately similar patterns, the pituitary endocrine cell maps exhibit differences in terms of variety of cell types that are reported. For instance, the localization of endocrine cell populations in dorado fish shows only four distinct types of endocrine cells across the adenohypophysis (12). By contrast, studies of other species described five [Japanese medaka (13)], six [fourspine sculpin (14); cardinal and bloodfin tetra (15)], seven [greater weever (16); white seabream (17); dimerus cichlid (18)], and eight [Atlantic halibut (19); Nile tilapia (20); saddle wrasse (21)] cell types.

Even though these previous studies have provided interesting information on the spatial organization of endocrine cell populations, they lack information due to the techniques available and used at the time. First, the use of mid- and parasagittal sections of the pituitary to reconstruct organizational patterns of endocrine cells overlooks information on the lateral sides. Second, the single-labeling method and non-species specific antibodies typically used do not provide sufficient detail on arrangements among different endocrine cell populations, or on the possible existence of multi-hormonal cells as described in mammals (22–25). These features will be important to better understand their roles in fish physiology and

endocrinology. Moreover, the distribution of the blood vessels within the pituitary, which play an essential role by transporting the released hormones, is poorly known. A better knowledge will help understand how endocrine cells arranged within a vascularized system that is thought to facilitate signaling within the pituitary (26). Also, since it has been shown that the pituitary is a plastic organ with changes occurring at cellular and population levels (27), it is essential to describe the cell composition, spatial organization, and vascularization of the pituitary in detail.

The Japanese medaka (*Oryzias latipes*) is a teleost model commonly used to investigate vertebrate and teleost physiology, genetics, and development, due to easy access to a wide range of genetic and molecular techniques (28, 29). We have recently used single-cell RNA sequencing to describe seven distinct endocrine cell types (expressing *prl*, *pomca*, *fshb*, *lhb*, *tshba*, *gh*, and *sl*) in the medaka pituitary (30). Here, we extend this study by describing differences in the spatial distribution of the seven endocrine cell populations, in juvenile and adult fish from both sexes. Using multi-color *in situ* hybridization techniques together with single-cell transcriptomics analysis, this study offers the first 3D atlas of teleost pituitary endocrine cell populations, allowing the characterization of differences in spatial distribution between sexes and stages, as well as demonstrating the existence of multi-hormonal cells.

MATERIALS AND METHODS

Experimental Animals

Juvenile (2 months old) and adult (6 months old) wild type medaka (WT, d-rR strain) were reared at 28°C in a re-circulating water system (pH 7.5; 800 μ S) with 14 hours light and 10 hours dark. Fish were fed with artemia and dry food three times daily. Sex determination was based on secondary sexual characteristics (31). Experiments were conducted in accordance with recommendations on experimental animal welfare at the Norwegian University of Life Sciences.

Quantitative Polymerase Chain Reaction

RNA extraction from pituitaries ($n = 7$) was performed as previously described in (32). Fish were euthanized by immersion in ice water and pituitaries were collected and stored at -80°C in 300 μ l of TRIzol (Invitrogen, Carlsbad, USA) with 6 zirconium oxide beads (Bertin Technologies, Versailles, France; diameter 1.4 μ m). Later, tissues were homogenized and mixed with 120 μ l chloroform. After centrifugation, the supernatant was mixed with isopropanol, and the RNA pellet was rinsed with 75% cold ethanol before resuspended with 14 μ l of nuclease free water. Due to the size of the tissue, 3 juvenile pituitaries were pooled per replicate. A total of 33 ng of RNA was used to synthesize cDNA using SuperScript III Reverse Transcriptase (Invitrogen, Carlsbad, CA, USA) and random hexamer primers (ThermoFisher scientific). 5 \times diluted cDNA samples were analyzed in duplicate, using 3 μ l of the cDNA and 5 μ M each of forward and reverse primer in a total

volume of 10 µl (Table 1). PCR cycle parameters were: 10 min pre-incubation at 95°C, followed by 42 cycles of 95°C for 10 s, 60°C for 10 s and 72°C for 6 s, followed by melting curve analysis to assess PCR specificity. The mRNA level was normalized using *rpl7* as the reference gene as no significant difference of expression was found between groups.

Multi-Color Fluorescence *In Situ* Hybridization

Tissue Preparation

Fish were euthanized by immersion in ice water. Each brain and pituitary complex was fixed overnight at 4°C in 4% paraformaldehyde (PFA, Electron Microscopy Sciences, Hatfield, Pennsylvania) diluted with phosphate buffered saline with Tween (PBST: PBS, 0.1%; Tween-20), approximately 50× the tissue volume. Tissue was then dehydrated in a series of increasing ethanol concentrations (25%, 50%, 75%, 96%), followed by storage in 100% methanol at -20°C until use.

Cloning and RNA Probe Synthesis

DNA sequences for the probes were obtained from NCBI as listed in Table 2. Sequences were selected according to the high

expression in the pituitary for those having more than one paralog in the medaka genome (*tshb* and *pomc*). PCR primers for the amplification of the probe genes were designed from transcribed sequences (mRNA) for each gene using Primer3 (<https://primer3.ut.ee/>). Following RNA extraction and cDNA synthesis as described above, cDNA was used to amplify the sequence of interest by PCR using Taq DNA polymerase (Thermo Fisher Scientific) with a 3-min denaturation step at 94°C, followed by 35 cycles at 94°C for 15s, 50°C for 15s, and 72°C for 60s, and finally 1 cycle of 72°C for 5 mins. The amplified PCR products were isolated using a gel extraction kit (Qiagen) and cloned into the pGEM-T Easy vector (Promega) following manufacturer instructions and verified by sequencing. PCR products from the verified plasmids were used as template to synthesize sense and anti-sense complementary RNA probes using *in vitro* transcription with T7 or SP6 RNA polymerase (Promega, Madison, Wisconsin). RNA probes were tagged with dinitrophenol-11-UTP (DNP, Perkin Elmer, Waltham, Massachusetts), fluorescein-12-UTP (FITC, Roche Diagnostics), or digoxigenin-11-UTP (DIG, Roche Diagnostics). Finally, the probes were purified using the Nucleospin RNA clean-up kit (Macherey-Nagel, Hoerd, France)

TABLE 1 | Primer sequences used for the mRNA level analysis in the medaka pituitary.

Gene Name	Sequence (5' - 3')	Ensembl Gene Name	Accession Number (NCBI/Ensembl)	Amplicon size (bp)	Efficiency	Reference
<i>rpl7</i>	F: TGCTTTGGTGGAGAAAGCTC R: TGGCAGGCTTGAAGTTCTTT	<i>rpl7</i>	NM_001104870 ENSORLG00000007967	98	2.03	(32)
<i>prl</i>	F: TCAGATGGGAACCAAGAGGAC R: GATGTCCACGGCTTTACACA	<i>prl1</i>	XM_004071867.4 ENSORLG00000016928	85	1.987	This study
<i>tshba</i>	F: ATGTGGAGAAGCCAGAATGC R: CTCATGTTGCTGTCCCTTGA	<i>tshba</i>	XM_004068796.4 ENSORLG00000029251	88	2	This study
<i>lhb</i>	F: CCACTGCCTTACCAAGGACC R: AGGAAGCTCAAATGTCTTGATG	<i>lhb</i>	NM_001137653.2 ENSORLG00000003553	100	2	(33)
<i>fshb</i>	F: GACGGTGCTACCATGAGGAT R: TCCCCACTGCAGATCTTTTC	<i>fshb</i>	NM_001309017.1 ENSORLG00000029237	73	2.03	(32)
<i>gh</i>	F: TCGCTCTTTGTCTGGGAGTT R: ACATTCTGATTGCCCCTGAT	<i>gh1</i>	XM_004084500.3 ENSORLG00000019556	102	1.94	This study
<i>pomca</i>	F: GTGGTGGTGTCCGGTGGG R: GTGAGGTCAGAGCCGCGCAG	<i>pomca</i>	XM_004066456.3 ENSORLG00000025908	122	1.956	This study
<i>sl</i>	F: CACCAAAGCATTACCCATCC R: ACCAGCATCAGCACAGAATG	<i>smtla</i>	NM_001104790.1 ENSORLG00000013460	87	1.965	This study

TABLE 2 | Primer sequences used to make the *in situ* hybridization (ISH) probes of seven endocrine cell types in the medaka pituitary.

Gene	Sequence (5' - 3')	Ensembl gene name	Accession Number (NCBI/Ensembl)	PCR product size (bp)	Reference
<i>lhb</i>	F: CACAGCCTGCAGATACATGAG R: AGGAAGCTCAAATGTCTTGATG	<i>lhb</i>	NM_001137653.2 ENSORLG00000003553	318	(33)
<i>fshb</i>	F: GAGGAAGCAACACTTTTCAGC R: GCACAGTTCTTTATTTCAAGTGC	<i>fshb</i>	NM_001309017.1 ENSORLG00000029237	500	(34)
<i>pomca</i>	F: ATGTATACCGTTTGGTTGCT R: AAATGCTTCATCTTGTAGGAG	<i>pomca</i>	XM_004066456.3 ENSORLG00000025908	515	This study
<i>sl</i>	F: CCACTCTTTTCACTGTAAAGT R: ATACTGGAAGGCACCTTGT	<i>smtla</i>	NM_001104790.1 ENSORLG00000013460	506	This study
<i>prl</i>	F: GAAAAGCCGAGGAGGAACTG R: TTGCAGAGTTGGACAGGACC	<i>prl1</i>	XM_004071867.4 ENSORLG00000016928	381	This study
<i>gh</i>	F: TCTCTGCAGACTGAGGAACA R: AGCCACAGTCAGGTAGGTCT	<i>gh1</i>	XM_004084500.3 ENSORLG00000019556	501	This study
<i>tshba</i>	F: ACAGGCTAAACTCAAGTTAA R: AGGATCATATAGGTGCTCTG	<i>tshba</i>	XM_004068796.4 ENSORLG00000029251	473	This study

and the concentration was measured using the Epoch Spectrophotometer System (BioTek, Winooski, VT, USA).

Hybridization

Multi-color FISH was performed as previously described in (35) with minor modifications. Tissues were serially rehydrated, and the pituitary was detached from the brain. Afterwards, whole pituitaries were hybridized with the probes (0.11 – 3.17 ng/μl) for 18 hours at 55°C, and incubated with different combinations of anti-DNP- (Perkin Elmer), anti-FITC-, and anti-DIG-conjugated antibodies (Roche Diagnostics), followed by TAMRA- (ThermoFisher), Cy5- (Perkin Elmer) and FITC-conjugated tyramides (Sigma). The nuclei were stained with DAPI (1:1000, 4', 6-diamidino-2-phenylindole dihydrochloride; Sigma). The absence of labeling when using sense probes was used to confirm the specificity of the anti-sense probes. Whole pituitaries were mounted using Vectashield H-1000 Mounting Medium (Vector, Eurobio/Abcys) between microscope slides and cover slips (Menzel Glässer, VWR) with spacers (Reinforcement rings, Herma) in between for the juveniles, and between two cover slips with spacers for adults.

Combined FISH and Immunofluorescence

To distinguish the localization of adrenocorticotrophic-releasing hormone (Acth) and alpha-melanocyte stimulating hormone (α -Msh) cells within *pomca*-expressing cells separately, IF was performed using the antibodies shown in Table 3. After FISH for *pomca* labelled with FITC-conjugated tyramide, the pituitaries were embedded in 3% agarose (H₂O) and para-sagittally sectioned with 60 μm thickness using a vibratome (Leica). From a single pituitary, odd and even ordered slices were processed to detect Acth and α -Msh IF, respectively. Tissue slices were incubated for 10 minutes at room temperature (RT) in permeabilizing buffer (0.3% Triton in PBST) with agitation, before incubation for 1 hour at RT in blocking solution (Acth: 3% normal goat serum (NGS); 0.3% Triton; 1% dimethylsulfoxide (DMSO) in PBST; α -Msh: 3% NGS; 5% Triton; 7% DMSO in PBST). Sections were then incubated at 4°C overnight with primary antibodies or without (control) in blocking solution, followed by 4 hours at RT with secondary antibodies in blocking solution with extensive PBST washes in between. Nuclei were stained with DAPI (1/1000). Antibody dilution factors are provided in Table 3.

Blood Vessel Staining

Blood vessels were stained by cardiac perfusion as previously described (38). The fish were anesthetized with 0.04% Tricaine (pH 7), and the anterior abdomen was cut to allow access to the

heart. Afterwards, 0.05% of DiI (1,1'-Dioctadecyl-3,3,3',3'-Tetramethylindocarbocyanine Perchlorate; Invitrogen) solution diluted in 4% PFA (in PBS) was administered to the *bulbus arteriosus* through the ventricle using a glass needle. The pituitary was dissected and fixed in 4% PFA (in PBS) for 2 hours in the dark, then washed 2 times with PBS and mounted as described above.

Image Processing and Analysis

Fluorescent images were obtained using an LSM710 Confocal Microscope (Zeiss) with 25× (for adult pituitary) and 40× (for juvenile pituitary) objectives. Lasers with wavelength of 405 (DAPI), 555 (TAMRA; Alexa-555), 633 (Cy5) and 488 (FITC; Alexa-488) nm were used. Channels were acquired sequentially to prevent cross-signaling of fluorophores. Due to the size of the adult pituitaries, the image acquisition was done from the dorsal and ventral sides of the pituitary with some overlaps in the middle. In conjunction with the microscope, ZEN software (v2009, Zeiss) was used to process the images, and ImageJ (1.52p; <http://rsbweb.nih.gov/ij/>) was used for processing z-projections from confocal image stacks. The dorsal and ventral stacks of adult pituitaries were aligned using HWada (<https://signaling.riken.jp/en/en-tools/imagej/635/>) and StackReg plugins (<http://bigwww.epfl.ch/thevenaz/stackreg/>), before presenting them in orthogonal views.

3D Volume Measurement of Cell Populations

Cell volumes from the pituitary image stacks (n = 4-8 per group) were measured using ImageJ. Briefly, the channels of the image stack were split, and the threshold was adjusted to select only the objects of interest and to exclude background. The Otsu threshold method was used to separate foreground objects from background. To calculate the object volume, the area of the slice was multiplied by the depth of the slice. The absolute volume of each population was calculated by summing the population volume of each slice. Then, the relative volume of each population as a percent of the total pituitary volume (determined by DAPI staining) was calculated.

3D Atlasing

While juvenile pituitaries were imaged as one block, adult pituitaries were imaged from the ventral and dorsal side with confocal imaging as described above. The two sides of the adult pituitaries were then merged using landmarks visible with the DAPI staining. Finally, eight pituitaries labeled for different markers were aligned to the same coordinate system also using manually selected landmarks. These data were used for the

TABLE 3 | Primary and secondary antibodies used for immunofluorescence (IF) to distinguish Acth and α -Msh cells within *pomca*-expressing cells in the medaka pituitary.

Antibody	Dilution	Source	Reference
Rabbit anti-human ACTH antibody	1:1000	abcam (ab74976)	(36)
Rabbit anti-human α -MSH antibody	1:3000	abcam (ab123811)	(37)
Goat anti-rabbit antibody (Alexa-555)	1:500	Invitrogen (A21429)	(34)

creation of four 3D atlases of the pituitary gland, using the principle approaches previously outlined (39).

The creation of the 3D atlases involved several steps. Merging and alignment was done using LandmarkReg (<https://github.com/Tevemadar/LandmarkReg>, with accompanying utilities <https://github.com/Tevemadar/LandmarkReg-utils>). Image stacks were saved in NIfTI format (<https://imagej.nih.gov/ij/plugins/nifti.html>) and converted with the “NIfTI2TopCubes” utility before the matching anatomical positions (“landmarks”) were manually identified in volume-pairs. Both the signal from endocrine cells and the DAPI background were inspected, and four or more landmarks were recorded for each volume-pair. In case of ventral-dorsal half images (adult samples), a custom utility “PituBuild” was used for merging the two halves, based on partial overlap. Finally, each set of complete pituitary volumes was aligned to a common anatomical space using the “Match” utility. The resulting NIfTI volumes were then converted to TIFF stacks for viewing and analysis.

To enable 3D viewing of the pituitary atlases, data were prepared for the MeshView tool (RRID: SCR_017222, <https://www.nitrc.org/projects/meshview/>) developed for 3D brain atlas viewing (40). Volumes were first binarized using the “BinX” utility with a threshold value of 50. MeshGen (<https://www.nitrc.org/projects/meshgen/>) was then used to generate surface meshes in standard STL format (<http://paulbourke.net/dataformats/stl/>) before conversion using PackSTL (<https://github.com/Tevemadar/MeshView-PackSTL>) to allow viewing in MeshView.

Single-Cell Transcriptomics Analysis (scRNA-Seq)

We used processed scRNA-seq dataset from 23 male and 24 female adult medaka pituitaries where doublet cells were removed (30). Briefly, 2644 and 3921 cells remained after quality control for the female and male pituitary, respectively. Then, each cell was awarded a doublet likelihood score in the doublet removal analysis. We removed 2-3% of the cells with the highest doublet score from the original dataset according to 10x Genomics stochastic loading data, ending with 2592 female and 3804 male cells. We then filtered out red blood cells to avoid noise, and we applied a cut-off to differentiate between cells with high and low expression for specific genes to distinguish expression from background (Supplementary Figure 1). This dataset was further used to generate the pair-wise scatterplots using the R package ggplot2 (version 2.3.3.2), to investigate cells expressing more than one hormone-encoding gene. We identified 191 and 229 multiple hormone-producing cells in female and male pituitaries, respectively. To identify whether these cells express more than two hormone-encoding genes, we generated clustered heatmaps using pheatmap (version 1.0.12) to visualize the expression levels of all hormone-producing genes in each cell.

Statistical Analysis

Levene’s test was performed to analyze the homogeneity of variance while the normality was tested using the Shapiro-Wilk

Normality test. Differences in mRNA levels and in absolute and relative cell population volumes were evaluated using One-way ANOVA followed by Tukey *post hoc* test. The data are shown as mean + SEM (Standard Error of Mean) unless otherwise stated in the figure legend. $p < 0.05$ was used as a threshold for statistical significance.

Data Availability

All image files are available in a data repository (<https://doi.org/10.18710/NOGJQ2>). The 3D atlases (Figure 1) can be found on a webpage containing explanatory videos and other types of data completing the online pituitary atlas (<https://www.nmbu.no/go/mpg-atlas>), allowing easy access and navigation through the data.

RESULTS

3D Atlases of the Medaka Pituitary

Using several combinations of multi-color FISH, we combined the labeling to form four 3D pituitary atlases now available online <http://arken.nmbu.no/medaka-pituitary-atlas/JF/>; <http://arken.nmbu.no/medaka-pituitary-atlas/JM/>; <http://arken.nmbu.no/medaka-pituitary-atlas/AF/>; <http://arken.nmbu.no/medaka-pituitary-atlas/AM/>), allowing us to precisely localize the seven endocrine cell types (*prl*, *pomca*, *tshba*, *fshb*, *lhb*, *gh* and *sl*) and blood vessels in the adenohypophysis of medaka.

prl-Expressing Cells (Lactotropes)

In both adults and juveniles (Supplementary Figure 2), *prl*-expressing cells make up almost the entirety of the RPD from the dorsal to the ventral side of the pituitary, without any obvious difference in distribution between males and females. They border on and intermingle with a *pomca*-expressing cell population (Supplementary Figure 9). In some fish, a few *prl*-expressing cells are also localized peripherally in the dorsal area of PPD (data not shown).

pomca-Expressing Cells (Corticotropes and Melanotropes)

pomca-expressing cells are observed in two distinct regions. One population is localized in the dorsal part of RPD, where it is mostly clustered centrally if observed from the transverse perspective, and the second is detected in the PI area (Supplementary Figure 3). While the first one is adjacent to and mixing with *prl*-expressing cells, in close proximity to *tshba*-expressing cells (Supplementary Figure 9), the second population intermingles with *sl*-expressing cells (Supplementary Figure 10).

tshba-Expressing Cells (Thyrotropes)

tshba-expressing cells are localized in the dorsal side of anterior PPD towards the *pars nervosa* (PN; analogous to neurohypophysis in the anterior part of the pituitary), next to the *prl*- and *pomca*-expressing cells (Supplementary Figure 4 and Supplementary Figure 9). From the transverse perspective, *tshba*-expressing cells are mostly concentrated centrally in the

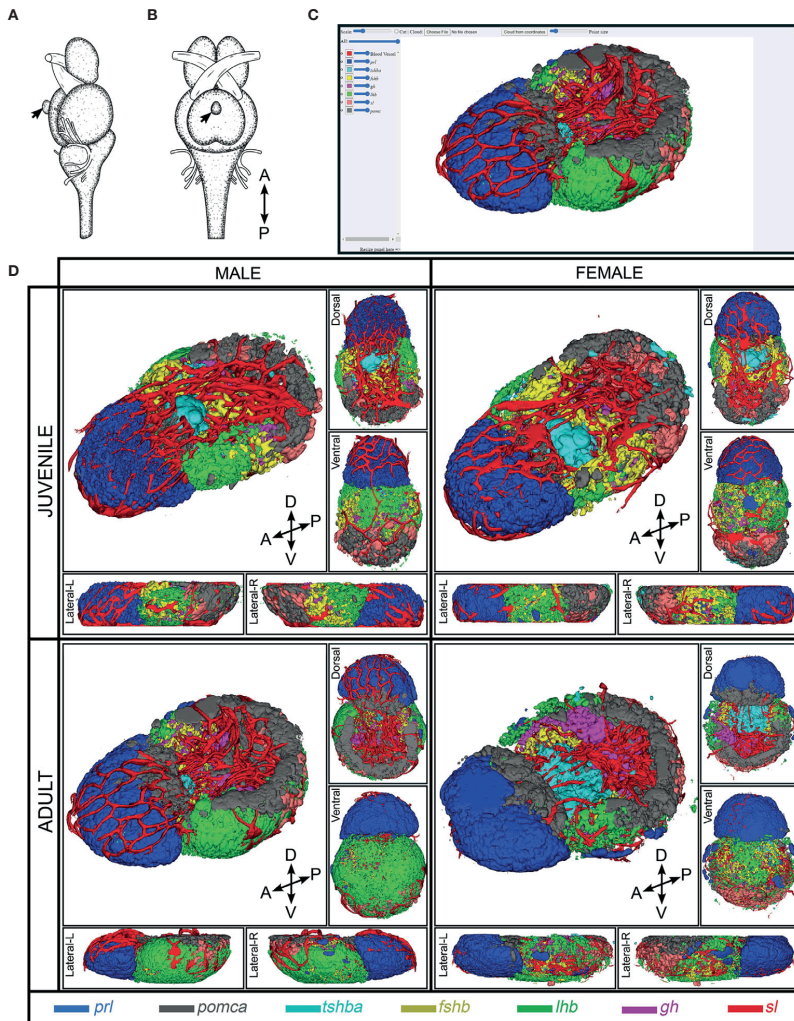


FIGURE 1 | 3D reconstruction of medaka anterior pituitary containing seven endocrine cell populations and blood vessel. Illustration of brain and pituitary (marked by black arrow) of medaka from lateral view **(A)** and ventral view **(B)** [Figure is adopted and modified with permission from (41)]. The navigation platform of 3D spatial distribution of endocrine cell populations that are now available online **(C)**. Snapshots of 3D reconstruction of endocrine cell populations from juvenile and adult medaka male and female **(D)**. Snapshots of 3D representations of the pituitary atlas captured from different perspectives: lateral (L, left; R, right), dorsal, and ventral. Four direction arrows display the direction of the pituitary (A, anterior; P, posterior; D, dorsal; V, ventral). The legend shows the color code for each cell type.

PPD (**Supplementary Figure 4**) where they border and mix with *fshb*-expressing cells (**Supplementary Figure 11**).

***fshb*-Expressing Cells (Gonadotropes)**

fshb-expressing cells are detected from the anterior to middle part of the PPD, distributed in both lateral sides of the pituitary from the

transverse perspective (**Supplementary Figure 5**). These cells cover the PN from a frontal perspective (**Supplementary Figure 5**). They border and mix with *tshba*-expressing cells in the dorsal (**Supplementary Figure 11**), *lhb*-expressing cells in the ventral (**Supplementary Figure 12**) and *gh*-expressing cells in the posterior part of the PPD (**Supplementary Figure 13**).

lhb-Expressing Cells (Gonadotropes)

In both juveniles and adults, *lhb*-expressing cells are commonly distributed in the peripheral area of the PPD, covering almost the entire ventral side of the pituitary (Supplementary Figure 6). In adults, *lhb*-expressing cells are also localized in the proximity of peripheral area of the PI (Supplementary Figure 6). These cells border and mix with *fshb*-expressing cells in the PPD (Supplementary Figure 12), and with *pomca*- and *sl*-expressing cells in the PI of adult pituitary (Supplementary Figure 10).

gh-Expressing Cells (Somatotropes)

gh-expressing cells are localized on the dorsal side of the PPD towards the PN area (Supplementary Figure 7). They are distributed in both lateral sides of the pituitary, mixing with *fshb*-expressing cells (Supplementary Figure 13), but extend posteriorly, encompassing and bordering with the PN (Supplementary Figure 7).

sl-Expressing Cells (Somatolactotropes)

sl-expressing cells are intermingled within *pomca*-expressing cells located in the PI (Supplementary Figure 8 and Supplementary Figure 10). In the adult pituitary, these cells border and mix with *lhb*-expressing cells in the PI (Supplementary Figure 10).

Distinction of Acth and α -Msh Cell Populations

The combination of FISH for *pomca* with IF for Acth or α -Msh shows that Acth cells overlap the entire *pomca* signal, while melanotropes overlap *pomca* signals in the PI, both in adults (Figure 2) and in juvenile pituitaries (Supplementary Figure 14).

Blood Vessels

3D reconstruction shows that blood vessels encompass the entire adenohypophysis, without any obvious differences between sexes and stages (Figure 3).

Sex and Stage Differences

For each pituitary endocrine cell population, we analyzed the mRNA levels for the hormone-encoding genes, as well as the absolute and relative volumes of each population (Figure 4).

Although no stage difference is observed in *prl* and *gh* mRNA levels, the *prl*-expressing cell volume is significantly larger in adults than in juveniles, and the absolute *gh*-expressing cell volume is significantly larger in adult females than juveniles or adult males. However, the relative volume of these populations remains stable. In contrast, *sl* mRNA levels are significantly higher in juveniles compared to adult males ($p < 0.05$), while the absolute cell volume tends to be larger (but not significantly) in adults than in juveniles.

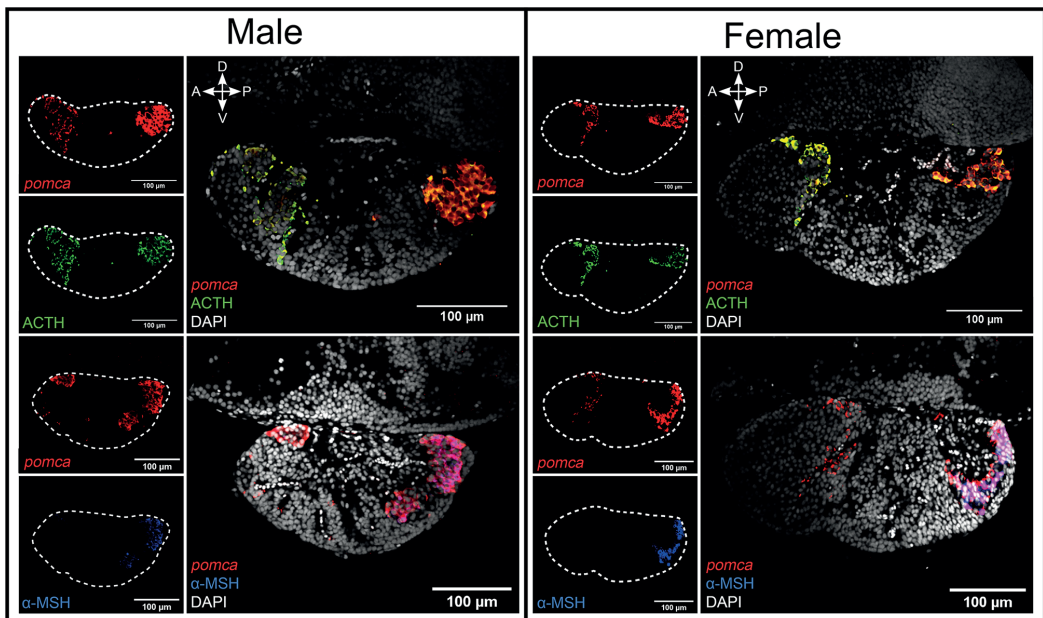


FIGURE 2 | The combination of FISH for *pomca* and IF for Acth or α -Msh allows the distinction of two clear *pomca* expressing cell populations. The distinction of Acth (green) and α -Msh (blue) producing cells from *pomca*-labelled (red) in the pituitary from adult male and female medaka. The dashed lines represent the pituitaries shown in the right panel. Four direction arrows display the direction of the pituitary (A, anterior; P, posterior; D, dorsal; V, ventral).

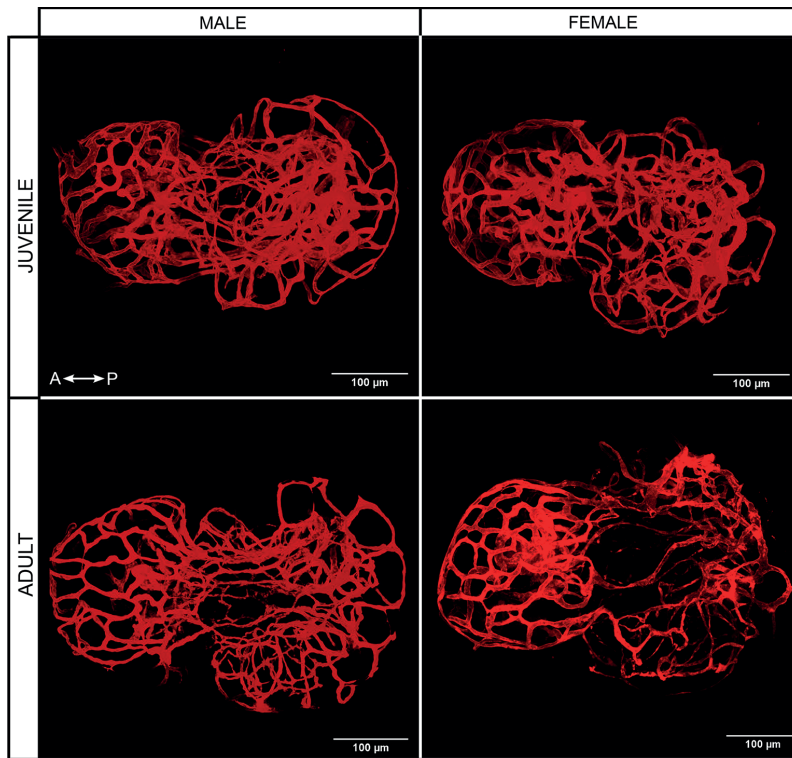


FIGURE 3 | 3D projection of blood vessels from juvenile and adult male and female medaka pituitaries from the dorsal side. Left right arrow symbol shows the direction of the pituitary (A, anterior; P, posterior).

However, the relative volume of the *sl*-expressing cell population remains stable across sexes and stages.

Adult females have significantly higher mRNA levels of both *fshb* ($p < 0.01$) and *lhb* ($p < 0.0001$) compared to the other groups, which is consistent with the tendency of larger cell volume for both cell types. However, the relative volumes of these populations also remain stable. *tshba* mRNA levels are significantly higher in adult female ($p < 0.0001$), consistent with the significantly larger *tshba*-expressing cell absolute and relative volumes in the adult female pituitary. In contrast, *pomca* mRNA levels are significantly higher in adult male ($p < 0.0001$), in agreement with the increased absolute volume of the *pomca*-expressing cell population in adults compared to juveniles, which tends to be larger in adult males than in adult females. Furthermore, the relative volume of *pomca*-expressing cells is significantly larger in adult males than adult females.

Despite obvious differences in mRNA transcript levels and cell volume observed respectively with qPCR and FISH, we could not detect any differences in the proportions of each cell type between adult males and females by scRNA-seq.

Cells Producing Multiple Hormones

Using scRNA-seq, we identified 191 and 229 bi-hormonal cells in the adult female and male medaka pituitaries, respectively (**Figure 5A** and **Supplementary Table 1**). Both sexes show a number of cells co-expressing *lhb*- and *fshb*-, *lhb*- and *tshba*- and *fshb* and *tshba*. Meanwhile, some cells co-expressing *lhb* and *sl*, *fshb* and *sl*, *fshb* and *prl*, *fshb* and *pomca*, *tshba* and *prl*, *tshba* and *pomca*, *prl* and *gh*, and *prl* and *pomca* were unique to adult males, whereas cells co-expressing *fshb* and *gh* were only found in adult females. The existence of cells co-expressing *lhb*-*fshb* and *fshb*-*tshba* in both sexes and *lhb*-*sl* in adult male was confirmed using multi-color FISH (**Figure 6**). While the co-localization of *lhb*-*fshb* and *fshb*-*tshba* was observed in several individuals, the *lhb*-*sl* expressing cells were observed only in 1 of 13 adult male pituitaries analyzed. However, we could not detect colocalization between *tshba* and *lhb* by FISH.

We then investigated whether some of these bi-hormonal cells were expressing more than two hormone-encoding genes (**Figure 5B** and **Supplementary Figure 15**). We found a few cells co-expressing three hormone-encoding genes, although these are

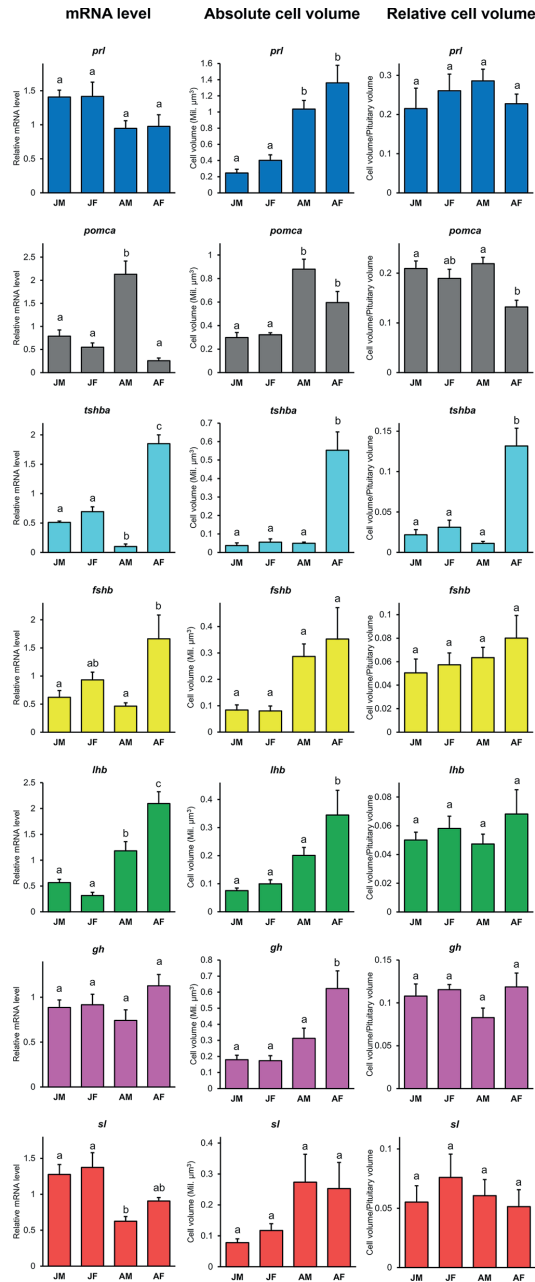


FIGURE 4 | Relative mRNA levels for seven hormone-encoding genes (*prl*, *pomca*, *tshba*, *fshb*, *lhb*, *gh*, and *sl*), absolute cell population volumes and relative cell volumes in juvenile and adult medaka males and females (juvenile male, JM; juvenile female, JF; adult male, AM; adult female, AF). Graphs are provided as mean + SEM (n = 4 - 8). Different letters display statistical differences ($p < 0.05$) between groups as evaluated by One-way ANOVA followed by Tukey *post hoc* test.

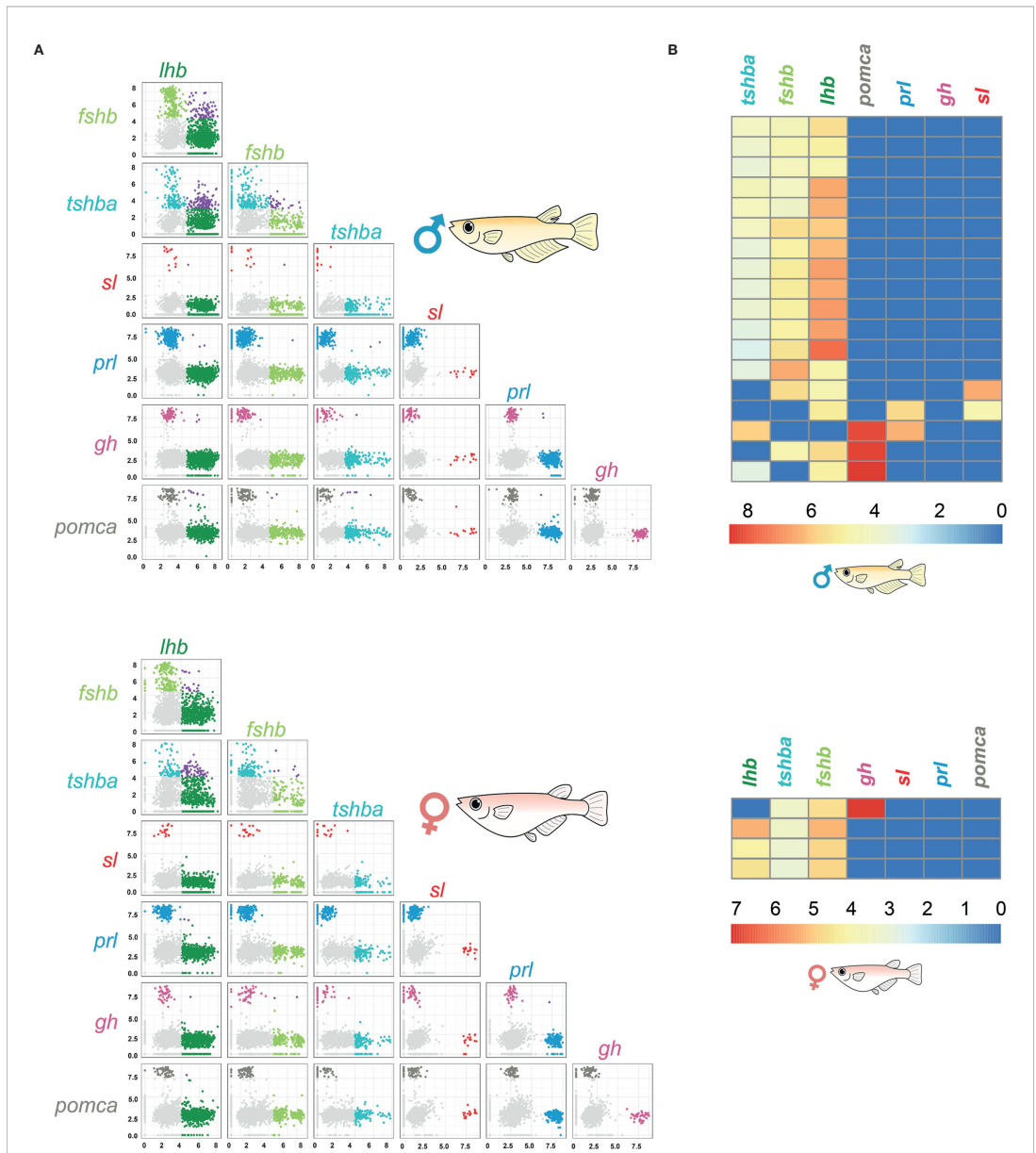


FIGURE 5 | scRNA-seq data reveal the presence of bi-hormonal and multi-hormonal cells in the medaka pituitary. Pair wise plots of 2228 cells in female and 3245 cells in male pituitary (A). Colored by filtered cells (light gray), *lhb* expressing cells (light green), *fshb* expressing cells (dark green), *tshba* expressing cells (cyan), *sl* expressing cells (red), *prl* expressing cells (blue), *gh* expressing cells (magenta), *pomca* expressing cells (dark grey) and cells expressing more than one endocrine gene (purple). Light grey cells represent the cells where gene expression for the investigated hormone is considered as part of the background. Axes are log normalized. Zoom in from the heatmap of seven hormone-encoding genes of the male and female pituitary shown in **Supplementary Figure 15**, displaying the cells expressing more than two hormone-encoding genes (B). Each row represents one cell, and low expressions are shown in blue and high expressions are shown in red. For all hormone-encoding genes, expression levels below the threshold established in **Supplementary Figure 1** were replaced by zero and thus appear in blue.

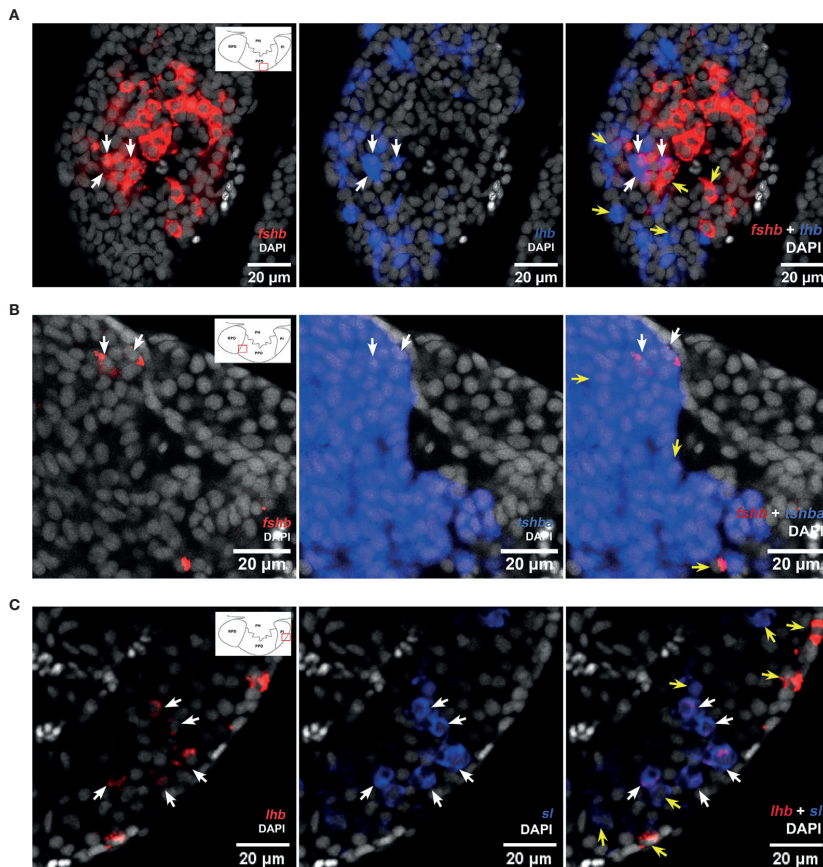


FIGURE 6 | Multi-color FISH reveals some cells co-expressing more than one hormone-encoding genes in the medaka pituitary. Single confocal planes (pinhole aperture 1 Airy Unit (0.8–1.1 μm section)) confirming colocalization of *lhb* and *fshb* (A), and *fshb* and *tshb* (B) in both male and female, and *lhb* and *sl* in the adult male medaka pituitary (C). White arrows show cells with co-expressed mRNAs, while yellow arrows show cells without (can be used as control of probe's specificity). The location of the bi-hormonal cells is in the proximity of the red rectangles as illustrated in the schematic drawings of the pituitaries in left panels.

rare, representing only 0.15% and 0.47% of all pituitary cells in females and males, respectively. We did not detect any cell co-expressing more than three hormone-encoding genes. These multi-hormonal cells could not be detected using multi-color FISH.

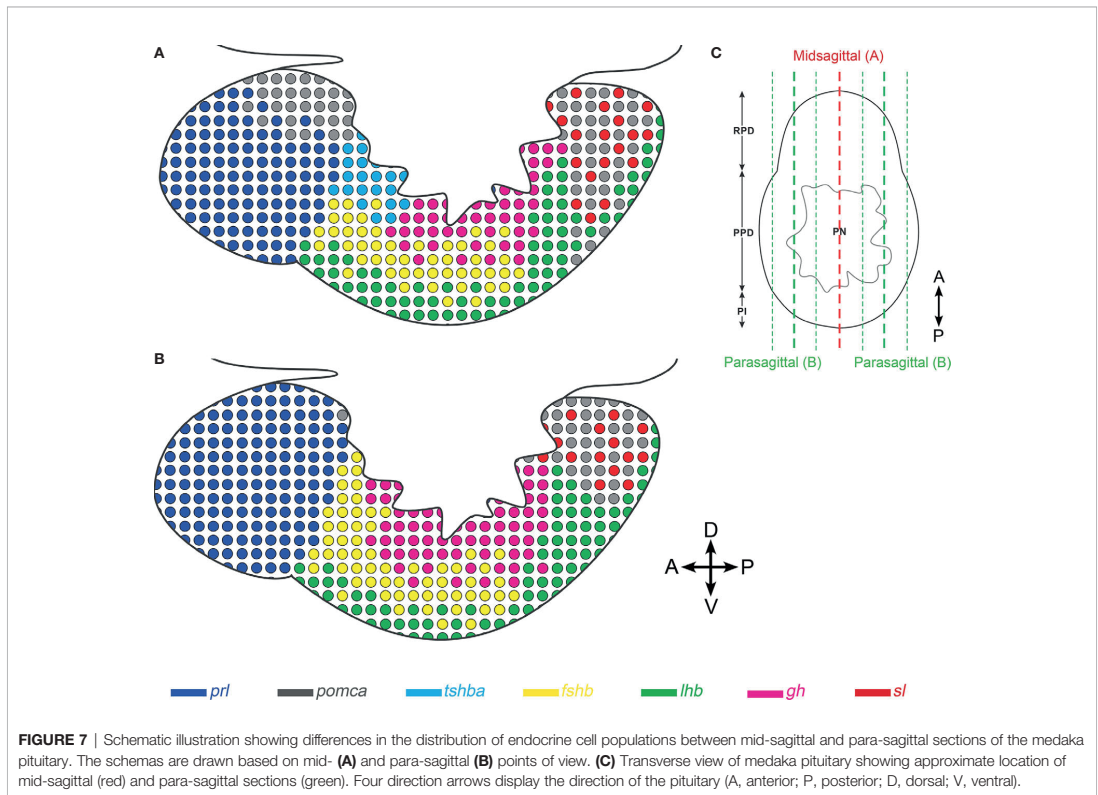
DISCUSSION

3D Spatial Distribution of Endocrine Cell Populations and Blood Vessels

We have recently used scRNA-seq to identify and characterize seven endocrine cell types in the teleost model organism medaka (30). Although a 3D atlas of the pituitary gland development has

been previously described in zebrafish (42), the present atlas is the first 3D atlas of all pituitary endocrine cell populations in a teleost fish. It provides more precise and detailed information on the distribution and organization of the different cell types, and clearly demonstrates that endocrine cells are distributed differently in mid-sagittal versus para-sagittal sections (Figure 7).

As reported in coho (43) and chum salmon (44, 45), seabass (46), gilt-head seabream (47), common barbel (48) and striped bass (49), we observed some lactotropes in the ventro-peripheral area of the PPD. However, these cells were found only in some fish and not always at the same location, making them difficult to map. We found Lh gonadotropes in the PI, in addition to in the PPD, but only in adults, and we did not observe Lh cells in RPD as reported by some studies (15, 16, 50–52). The extra-PPD



localization of Lh gonadotropes might be due to extension of the PPD into the PI (19) or to Lh cell migration to other zones during the ontogeny of the adenohypophysis (53). Meanwhile, several studies reported somatotropes in the RPD (49, 54) and PI (55, 56), and somatolactotropes and melanotropes in the teleost PPD (12, 15–17, 55). However, we did not observe this in medaka. The wide localization of Gh, Sl, and α -Msh cells in these immunohistochemical studies might also be explained by antigenic similarities as previously suggested (12, 15, 57).

The vasculature is ubiquitously spread throughout nearly the entire adenohypophysis in medaka, without obvious differences between sexes and stages. This agrees with previous studies in zebrafish (58, 59) showing a highly vascularized pituitary. Such complex vasculature is, of course, central to the endocrinological function of the pituitary, as it allows for the efficient transport of secreted hormones to peripheral organs. In addition, it may facilitate intra-pituitary signaling (26).

Sexual Dimorphism of *tshba*-, *pomca*-, and *lhb*-Expressing Cell Populations

While studies using only para-sagittal pituitary sections were unable to resolve differences of endocrine cell population between sexes and stages, whole pituitary labeling methods allow us to detect such differences. For instance, we show for

the first time that *tshba*-expressing cell volumes are the largest in adult females, and *pomca*-expressing cell volumes are the largest in adult males. Our qPCR data on *tshba* and *pomca* levels agree with a previous study in medaka (60) and further support the sexual dimorphism. In that study, androgens were shown to stimulate transcription of *tph1*, which encodes an enzyme required for serotonin synthesis, in *pomc*-expressing cells. The authors hypothesized that in males, higher androgen levels lead to higher serotonin levels, which repress the expression of some hormone-encoding genes including *tshb*. We also found significantly lower *tshba* levels in adult compared to juvenile males where the androgen levels are generally lower [for review, see (61, 62)], supporting the inhibitory role of androgens on *tshba* levels. It will be interesting to test this hypothesis in future research using orchidectomy which drastically reduce androgen levels (63). However, although higher *tshb* levels are also observed in female half-barred wrasse (64), and *tshb* levels are higher in juvenile than in adult male Atlantic salmon (65), zebrafish show no sexual dimorphism of *tshb* and *pomc* (66), suggesting species differences.

We also observed sexual dimorphism of *fshb* and *lhb* mRNA levels in adults, in agreement with a previous medaka study (60). Although *lhb*-expressing cell volume also shows sexual dimorphism, we do not observe this for *fshb*-expressing cells.

This suggests a difference in gonadotrope cell activity, as supported by the absence of significant differences in Fsh cell numbers in a previous study (8). In contrast, we observed an increase of *lhb* mRNA levels from juvenile to adult stages, which might be due to increased cell numbers as previously reported (41). Surprisingly, we did not observe a significant difference in *fshb* mRNA levels between juveniles and adults, despite a previous report of an increase in Fsh cell numbers during sexual maturation (8). While neither sexual dimorphism nor stage differences were observed for *prl* or *gh* levels, we found a stage effect on the absolute volume of *prl*-expressing cells, and sexual dimorphism of the absolute volume of *gh*-expressing cells in adults. The latter finding is consistent with a previous study that showed sexual dimorphism of *gh* levels in adult medaka (60), while previous studies in blue gourami (67) and gilthead seabream (68) contrast with our findings on *prl* levels, suggesting species differences. Meanwhile, although *sl*-expressing cell volumes tend to be larger in adults than juveniles, we found the opposite for the mRNA levels, with higher levels in juveniles than in adults, suggesting higher cell activity in juveniles. Indeed, somatolactin has been associated with sexual maturation in some teleosts, such as coho salmon (69), Nile tilapia (70) and flathead grey mullet (71). The upregulation of *sl* levels in teleosts is thought to be related to gonadal growth, as it is highly expressed at the onset of gonadal growth and lowly expressed post-ovulation (72, 73). This implies that in the current study, the adult fish used may have been in a post-ovulation phase while the juveniles may have been initiating gonadal development.

scRNA-seq and Multi-Color FISH Reveal the Presence of Multi-Hormonal Cells in the Adult Medaka Pituitary

The presence of cells expressing more than one hormone in the anterior pituitary has been shown in many studies, both in teleosts and in mammals [for review see (27, 74–76)]. Using scRNA-seq technology, multi-hormonal cells have been described in the mouse pituitary (77), but never before in a teleost. While scRNA-seq has previously been used to analyze the zebrafish pituitary, the existence of multi-hormonal cells was not investigated (78). Using similar approaches, we previously could not identify any clusters of multi-hormonal cells in the medaka pituitary (30). Thus, in the present study, we more deeply analyzed our scRNA-seq data and found a relatively small number of bi-hormonal and very few multi-hormonal cells. Such low numbers of multi-hormonal cells could explain the lack of detection of cell clusters in the previous medaka study (30).

In the current study, we show the presence of gonadotrope cells co-expressing *lhb* and *fshb* which has previously been reported in medaka (8) and in other teleost species (7, 9, 10). We also found cells co-expressing *fshb-tshba* and *sl-lhb*. Although previous immunohistochemistry studies on the pituitary of several teleost species showed cross-reaction between Tsh and Lh/Fsh (47, 57) and between Lh and Sl antibodies (15, 57, 79, 80), we show discrete labeling of *tshba*, *fshb*, *lhb*, and *sl* cells in the current study confirming the

specificity of the probes. Therefore, the observation of colocalization of *fshb-tshba* and *sl-lhb* supports that these bi-hormonal cells exist in the medaka pituitary. Meanwhile, several studies have shown co-staining between Prl, Gh and Sl (12, 19, 21, 44, 55). However, our analysis of scRNA-seq data revealed only a few cells co-expressing *prl* and *gh*. While antigenic similarities could explain co-staining between these cell types in previous studies (12, 15, 57), their low occurrence in the medaka pituitary might prevent their identification with FISH. We also show that very few cells in the adult medaka pituitary express more than two hormone-encoding genes. The current study is the first to show the presence of such multi-hormonal cells in the teleost pituitary. However, it differs noticeably from mammals, where multi-hormonal cells are numerous and thus form a cluster in the scRNA-seq data (77), which is not the case in medaka (30). Although we could not confirm their existence using FISH, most likely because of their low incidence, the evidence of their existence using scRNA-seq raises questions about their origin and roles in the teleost pituitary.

In mammals, the presence of multi-hormonal cells has been described and associated with pituitary plasticity where the cell number is changing to fulfill physiological demands [for review, see (75)]. Hypothetical origins of these cells have been previously discussed (27, 74, 75, 81–85). They may originate from differentiating progenitor cells where a non-fully differentiated transient state could allow the expression of several hormone-encoding genes. This hypothesis is supported in mammals by the identification of a cluster of multi-hormonal cells expressing PROP1, a progenitor cell marker (77). However, there is no such evidence yet found in teleosts, as we could not find such a cluster in the medaka pituitary in the previous (30) and current studies. Indeed, we found only very few cells expressing more than two hormone-encoding genes, with a maximum of three hormone-encoding genes expressed. A previous study in medaka also demonstrated that gonadotropes do not appear as bi-hormonal cells but as either Lh or Fsh during early development (8), suggesting that progenitor cells might not be multi-hormonal in the teleost pituitary. In addition, multi-hormonal cells may also appear during trans-differentiation (when one cell changes phenotype). Indeed, a study in medaka showed that *fshb*-expressing cells could start to express *lhb in vitro*, becoming at least temporarily bi-hormonal (8). Interestingly, most of the multi-hormonal cells in our scRNA-seq data express *lhb/fshb*, *lhb/tshba* or *fshb/tshba*. In mammals, differentiation of progenitor cells to both gonadotropes and thyrotropes requires the transcription factor *Gata2* (86, 87), but co-expression with *Sfi* leads to gonadotropes whereas co-expression with *Pit1* leads to thyrotropes (88–91). In contrast, relatively little is known regarding pituitary cell lineage in teleosts. Nevertheless, it is plausible that trans-differentiation occurs between the gonadotrope and thyrotrope cell types in teleosts, as previously described in mammals (92).

Within the *pomca*-expressing cell population, we observed Acth staining alone at the border of the RPD/PPD and staining of both Acth and α -Msh in the PI. Co-staining between Acth and α -Msh is not uncommon as Acth-immunoreactive cells have

been found in RPD and PI areas in other teleost species (7, 17, 19–21, 46, 47, 93). However, it must be noted that the target antigen of anti-Acth used in this study and most previous studies contains the target antigen for anti- α -Msh (https://www.uniprot.org/uniprot/P01189#PRO_0000024970). This might explain why we found both Acth and α -Msh cells in the PI. A previous study pre-incubating anti-Acth with α -Msh antigen demonstrated that Acth cells are localized in the RPD while α -Msh cells are found in the PI (20). This might also be the case in medaka.

Finally, the 3D atlas platform that is provided online will help research community to take a close look on the spatial distribution of endocrine cells and the vascularization of blood vessels in the pituitary.

DATA AVAILABILITY STATEMENT

The datasets presented in this study can be found in online repositories. The single-cell transcriptomics data can be accessed through the project accession number GSE162787 at the NCBI Gene Expression Omnibus (GEO: <https://ncbi.nlm.nih.gov/geo/>). The imaging data can be found at the NMBU open research data (<https://doi.org/10.18710/NOGJQ2>).

ETHICS STATEMENT

The animal study was reviewed and approved by Norwegian University of Life Sciences.

AUTHOR CONTRIBUTIONS

RF and F-AW conceptualized and planned the work. RF, MP, JB, and F-AW obtained funding. NR did all cloning. MR and RF performed the experiments and acquired the imaging data. MR and GC processed the imaging data and developed the online 3D model, supervised by MP and JB. CH and KS analyzed the single cell transcriptome data. MR, CH, and RF wrote the paper with the inputs from all authors. All authors contributed to the article and approved the submitted version.

FUNDING

This study was funded by the Norwegian University of Life Sciences (to RF) and the Norwegian Research Council grants No. 251307, 255601, and 248828 (to F-AW). The tools development received support from the European Union's Horizon 2020 Framework Programme for Research and Innovation under the

Specific Grant Agreement No. 945539 (Human Brain Project SGA3) (to JB) and the Research Council of Norway under Grant Agreement No. 269774 (INCF Norwegian Node) (to JB).

ACKNOWLEDGMENTS

The authors thank Ms Lourdes Carreon G. Tan for her assistance in the fish husbandry and Prof Dianne M. Baker for reviewing and editing the text.

SUPPLEMENTARY MATERIAL

The Supplementary Material for this article can be found online at: <https://www.frontiersin.org/articles/10.3389/fendo.2021.719843/full#supplementary-material>

Supplementary Figure 1 | Density plots of seven hormone-encoding genes in the pituitary of adult male (A) and female (B) medaka. Red line represents a cut-off to differentiate between the cells with high gene expression (considered as endocrine cells) and low gene expression (considered as background and non-endocrine cells). X-axis represents the expression level on a logarithmic scale.

Supplementary Figure 2–8 | Orthogonal views of each endocrine cell types in juvenile and adult male and female medaka. (2, *prl*; 3, *pomca*; 4, *tshba*; 5, *fshb*; 6, *lhb*; 7, *gh*; 8, *sl*). The pictures were captured from different perspectives: transverse (i), frontal (ii) and para-sagittal (iii). Up down arrow symbol shows the direction of the pituitary (A, anterior; P, posterior; D, dorsal; V, ventral).

Supplementary Figure 9–13 | Transverse views of multi-color FISH of endocrine cells in juvenile and adult male and female medaka. (9, *prl-tshba-pomca*; 10, *sl-lhb-pomca*; 11, *fshb-tshba*; 12, *fshb-lhb*; 13, *fshb-gh*) (A, anterior; P, posterior; D, dorsal; V, ventral).

Supplementary Figure 14 | The combination of FISH for *pomca* and IF for Acth or α -Msh allows the distinction of two clear *pomca*-expressing cell populations in the juvenile medaka pituitary. The distinction of Acth (green) and α -Msh (blue) producing cells from *pomca*-labelled cells (red) in the pituitary from juvenile male and female medaka. Dashed lines represent the pituitaries shown in the right panel. Four direction arrows display the direction of the pituitary (A, anterior; P, posterior; D, dorsal; V, ventral).

Supplementary Figure 15 | Heatmap of seven hormone-encoding genes from the 229 and 191 bi-hormonal cells found in the adult male and female medaka pituitaries, respectively. Each row represents one cell. Low expressions are shown in blue and high expressions are shown in red. All expression levels below the threshold established in **Supplementary Figure 1** were replaced by zero values.

Supplementary Table 1 | Percentage of cells expressing two hormone-encoding genes in male and female pituitary scRNA-seq data. For instance, when looking at *lhb*- and *fshb*-expressing cells in males, we can observe that 72.6% of the cells express *lhb* but not *fshb*, 23.4% express *fshb* but not *lhb* while 4% express both *fshb* and *lhb*. The bi-hormonal *lhb/fshb* cells represent 1.79% of all pituitary cells. Empty spaces mean that no bi-hormonal cells were found.

REFERENCES

- Yeung C-M, Chan C-B, Leung P-S, Cheng CHK. Cells of the Anterior Pituitary. *Int J Biochem Cell Biol* (2006) 38(9):1441–9. doi: 10.1016/j.biocel.2006.02.012
- Ooi GT, Tawadros N, Escalona RM. Pituitary Cell Lines and Their Endocrine Applications. *Mol Cell Endocrinol* (2004) 228(1):1–21. doi: 10.1016/j.mce.2004.07.018
- Brinkmeier ML, Davis SW, Carninci P, MacDonald JW, Kawai J, Ghosh D, et al. Discovery of Transcriptional Regulators and Signaling Pathways in the

- Developing Pituitary Gland by Bioinformatic and Genomic Approaches. *Genomics* (2009) 93(5):449–60. doi: 10.1016/j.ygeno.2008.11.010
4. Le Tissier PR, Hodson DJ, Lafont C, Fontanaud P, Schaeffer M, Mollard P. Anterior Pituitary Cell Networks. *Front Neuroendocrinol* (2012) 33(3):252–66. doi: 10.1016/j.yfrne.2012.08.002
 5. Kaneko T. Cell Biology of Somatolactin. In: KW Jeon, editor. *International Review of Cytology*, vol. 169. Academic Press (1996). p. 1–24.
 6. Weltzien F-A, Hildahl J, Hodne K, Okubo K, Haug TM. Embryonic Development of Gonadotrope Cells and Gonadotropic Hormones – Lessons From Model Fish. *Mol Cell Endocrinol* (2014) 385(1):18–27. doi: 10.1016/j.mce.2013.10.016
 7. Hernández MPGA, García Ayala A, Zandbergen MA, Agulleiro B. Investigation Into the Duality of Gonadotropic Cells of Mediterranean Yellowtail (*Seriola Dumerilii*, Risso 1810): Immunocytochemical and Ultrastructural Studies. *Gen Comp Endocrinol* (2002) 128(1):25–35. doi: 10.1016/S0016-6480(02)00052-7
 8. Fontaine R, Ager-Wick E, Hodne K, Weltzien F-A. Plasticity in Medaka Gonadotropes via Cell Proliferation and Phenotypic Conversion. *J Endocrinol* (2020) 245(1):21. doi: 10.1530/JOE-19-0405
 9. Candelma M, Fontaine R, Colella S, Santojanni A, Weltzien F-A, Carnevali O. Gonadotropin Characterization, Localization and Expression in the European Hake (*Merluccius Merluccius*). *Reproduction* (2017) 153(2):123. doi: 10.1530/REP-16-0377
 10. Golan M, Biran J, Levavi-Sivan B. A Novel Model for Development, Organization, and Function of Gonadotropes in Fish Pituitary. *Front Endocrinol* (2014) 5(182). doi: 10.3389/fendo.2014.00182
 11. Schreiberman MP, Leatherland JF, McKeown BA. Functional Morphology of the Teleost Pituitary Gland. *Am Zoologist* (2015) 13(3):719–42. doi: 10.1093/icb/13.3.719
 12. Honji RM, Nóbrega RH, Pandolfi M, Shimizu A, Borella MI, Moreira RG. Immunohistochemical Study of Pituitary Cells in Wild and Captive *Salminus hilarii* (Characiformes: Characidae) Females During the Annual Reproductive Cycle. *SpringerPlus* (2013) 2(1):460. doi: 10.1186/2193-1801-2-460
 13. Aoki K, Umeura H. Cell Types in the Pituitary of the Medaka (*Oryzias latipes*). *Endocrinologia Japonica* (1970) 17(1):45–55. doi: 10.1507/endocrj1954.17.45
 14. Mukai T, Oota Y. Histological Changes in the Pituitary, Thyroid Gland and Gonads of the Fourspine Sculpin (*Cottus kazika*) During Downstream Migration. *Zool Sci* (1995) 12(1):91–7. doi: 10.2108/zsj.12.91
 15. Camacho LR, Pozzi AG, de Freitas EG, Shimizu A, Pandolfi M. Morphological and Immunohistochemical Comparison of the Pituitary Gland Between a Tropical Paracheirodon Axelrodi and a Subtropical Aphyocharax Anistisi Characids (Characiformes: Characidae). *J Neotropical Ichthyol* (2020) 18(1). doi: 10.1590/1982-0224-2019-0092
 16. Sánchez Cala F, Portillo A, Martín del Río MP, Mancera JM. Immunocytochemical Characterization of Adenohypophyseal Cells in the Greater Weever Fish (*Trachinus draco*). *Tissue Cell* (2003) 35(3):169–78. doi: 10.1016/S0040-8166(03)00018-1
 17. Segura-Noguera MM, Laiz-Carrión R, Martín del Río MP, Mancera JM. An Immunocytochemical Study of the Pituitary Gland of the White Seabream (*Diplodus sargus*). *Histochemical J* (2000) 32(12):733–42. doi: 10.1023/A:1004101127461
 18. Pandolfi M, Cánepa MM, Meijide FJ, Alonso F, Vázquez GR, Maggese MC, et al. Studies on the Reproductive and Developmental Biology of *Cichlasoma dimerus* (Perciformes, Cichlidae). *Biocell* (2009) 33(1):1–18. doi: 10.32604/biocell.2009.33.001
 19. Weltzien F-A, Norberg B, Helvik JV, Andersen Ø, Swanson P, Andersson E. Identification and Localization of Eight Distinct Hormone-Producing Cell Types in the Pituitary of Male Atlantic Halibut (*Hippoglossus hippoglossus* L.). Comparative Biochemistry and Physiology Part A. *Mol Integr Physiol* (2003) 134(2):315–27. doi: 10.1016/S1095-6433(02)00266-0
 20. Kasper RS, Shved N, Takahashi A, Reinecke M, Eppler E. A Systematic Immunohistochemical Survey of the Distribution Patterns of GH, Prolactin, Somatolactin, β -TSH, β -FSH, β -LH, ACTH, and α -MSH in the Adenohypophysis of Oreochromis niloticus, the Nile Tilapia. *Cell Tissue Res* (2006) 325(2):303–13. doi: 10.1007/s00441-005-0119-7
 21. Parhar IS, Nagahama Y, Grau EG, Ross RM. Immunocytochemical and Ultrastructural Identification of Pituitary Cell Types in the Protogynous (*Thalassoma duperrey*) During Adult Sexual Ontogeny. *Zool Sci* (1998) 15(2):263–76. doi: 10.2108/zsj.15.263
 22. Childs GV. Development of Gonadotropes may Involve Cyclic Transdifferentiation of Growth Hormone Cells. *Arch Physiol Biochem* (2002) 110(1-2):42–9. doi: 10.1076/apab.110.1.42.906
 23. Childs GV. Multipotential Pituitary Cells That Contain Adrenocorticotropin (ACTH) and Other Pituitary Hormones. *Trends Endocrinol Metab* (1991) 2(3):112–7. doi: 10.1016/S1043-2760(05)80007-4
 24. Frawley LS, Boockfor FR. Mammosomatotropes: Presence and Functions in Normal and Neoplastic Pituitary Tissue. *Endocrine Rev* (1991) 12(4):337–55. doi: 10.1210/edrv-12-4-337
 25. Fukami K, Tasaka K, Mizuki J, Kasahara K, Masumoto N, Miyake A, et al. Bihormonal Cells Secreting Both Prolactin and Gonadotropins in Normal Rat Pituitary Cells. *Endocrine J* (1997) 44(6):819–26. doi: 10.1507/endocrj.44.819
 26. Ben-Shlomo A, Melmed S. Chapter 2 - Hypothalamic Regulation of Anterior Pituitary Function. In: S Melmed, editor. *The Pituitary (Third Edition)*, vol. p. San Diego: Academic Press (2011). p. 21–45.
 27. Fontaine R, Ciani E, Haug TM, Hodne K, Ager-Wick E, Baker DM, et al. Gonadotrope Plasticity at Cellular, Population and Structural Levels: A Comparison Between Fishes and Mammals. *Gen Comp Endocrinol* (2020) 287:113344. doi: 10.1016/j.ygcen.2019.113344
 28. Wittbrodt J, Shima A, Scharl M. Medaka — a Model Organism From the Far East. *Nat Rev Genet* (2002) 3(1):53–64. doi: 10.1038/nrg704
 29. Hori H. A Glance at the Past of Medaka Fish Biology. In: K Naruse, M Tanaka, H Takeda, editors. *Medaka: A Model for Organogenesis, Human Disease, and Evolution*, vol. p. Tokyo: Springer Japan (2011). p. 1–16.
 30. Siddique K, Ager-Wick E, Fontaine R, Weltzien F-A, Henkel CV. Characterization of Hormone-Producing Cell Types in the Medaka Pituitary Gland Using Single-Cell RNA-Seq. *bioRxiv* (2020). doi: 10.1101/2020.12.14.422690
 31. Murata K, Kinoshita M, Naruse K, Tanaka M, Kamei Y. Looking at Adult Medaka. In: K Murata, M Kinoshita, K Naruse, M Tanaka, Y Kamei, editors. *Medaka: Biology, Management, and Experimental Protocols*. John Wiley & Sons (2019). p. 49–95. 2.
 32. Burrow S, Fontaine R, von Krogh K, Mayer I, Nourizadeh-Lillabadi R, Hollander-Cohen L, et al. Medaka Follicle-Stimulating Hormone (Fsh) and Luteinizing Hormone (Lh): Developmental Profiles of Pituitary Function and Gene Expression Levels. *Gen Comp Endocrinol* (2019) 272:93–108. doi: 10.1016/j.ygcen.2018.12.006
 33. Hildahl J, Sandvik GK, Lifjeld R, Hodne K, Nagahama Y, Haug TM, et al. Developmental Tracing of Luteinizing Hormone β -Subunit Gene Expression Using Green Fluorescent Protein Transgenic Medaka (*Oryzias latipes*) Reveals a Putative Novel Developmental Function. *Dev Dyn* (2012) 241(11):1665–77. doi: 10.1002/dvdy.23860
 34. Hodne K, Fontaine R, Ager-Wick E, Weltzien F-A. GnRH-1-Induced Responses Are Indirect in Female Medaka Fsh Cells, Generated Through Cellular Networks. *Endocrinology* (2019) 160(12):3018–32. doi: 10.1210/en.2019-00595
 35. Fontaine R, Afaticati P, Yamamoto K, Jolly C, Bureau C, Baloch S, et al. Dopamine Inhibits Reproduction in Female Zebrafish (*Danio rerio*) via Three Pituitary D2 Receptor Subtypes. *Endocrinology* (2013) 154(2):807–18. doi: 10.1210/en.2012-1759
 36. Romanò N, McClafferty H, Walker JJ, Le Tissier P, Shipston MJ. Heterogeneity of Calcium Responses to Secretagogues in Corticotrophs From Male Rats. *Endocrinology* (2017) 158(6):1849–58. doi: 10.1210/en.2017-00107
 37. Pravdiviy I, Ballanyi K, Colmers WF, Wevrick R. Progressive Postnatal Decline in Leptin Sensitivity of Arcuate Hypothalamic Neurons in the Magel2-Null Mouse Model of Prader-Willi Syndrome. *Hum Mol Genet* (2015) 24(15):4276–83. doi: 10.1093/hmg/ddv159
 38. Fontaine R, Weltzien F-A. Labeling of Blood Vessels in the Teleost Brain and Pituitary Using Cardiac Perfusion With a Dil-Fixative. *J Visualized Experiments* (2019) 148:e59768. doi: 10.3791/59768
 39. Bjerke IE, Øvsthus M, Papp EA, Yates SC, Silvestri L, Fiorilli J, et al. Data Integration Through Brain Atlasing: Human Brain Project Tools and Strategies. *Eur Psychiatry* (2018) 50:70–6. doi: 10.1016/j.eurpsy.2018.02.004
 40. Yates SC, Groenboom NE, Coello C, Lichtenthaler SF, Kuhn P-H, Demuth H-U, et al. QUINT: Workflow for Quantification and Spatial Analysis of

- Features in Histological Images From Rodent Brain. *Front Neuroinformatics* (2019) 13(75). doi: 10.3389/fninf.2019.00075
41. Fontaine R, Ager-Wick E, Hodne K, Weltzien F-A. Plasticity of Lh Cells Caused by Cell Proliferation and Recruitment of Existing Cells. *J Endocrinol* (2019) 240(2):361. doi: 10.1530/JOE-18-0412
 42. Chapman SC, Sawitzke AL, Campbell DS, Schoenwolf GC. A Three-Dimensional Atlas of Pituitary Gland Development in the Zebrafish. *J Comp Neurol* (2005) 487(4):428–40. doi: 10.1002/cne.20568
 43. Farbridge KJ, McDonald-Jones G, McLean CL, Lowry PJ, Etches RJ, Leatherland JF. The Development of Monoclonal Antibodies Against Salmon (Oncorhynchus Kisutch and O. Keta) Pituitary Hormones and Their Immunohistochemical Identification. *Gen Comp Endocrinol* (1990) 79(3):361–74. doi: 10.1016/0016-6480(90)90066-U
 44. Naito N, Takahashi A, Nakai Y, Kawauchi H, Hirano T. Immunocytochemical Identification of the Prolactin-Secreting Cells in the Teleost Pituitary With an Antiserum to Chum Salmon Prolactin. *Gen Comp Endocrinol* (1983) 50(2):282–91. doi: 10.1016/0016-6480(83)90229-0
 45. Wagner GF, McKeown BA. The Immunocytochemical Localization of Pituitary Somatotrops in the Genus *Oncorhynchus* Using an Antiserum to Growth Hormone of Chum Salmon (*Oncorhynchus Keta*). *Cell Tissue Res* (1983) 231(3):693–7. doi: 10.1007/BF00218126
 46. Cambré ML, Verdonck W, Ollevier F, Vandesande F, Batten TFC, Kühn ER. Immunocytochemical Identification and Localization of the Different Cell Types in the Pituitary of the Seabass (*Dicentrarchus Labrax*). *Gen Comp Endocrinol* (1986) 61(3):368–75. doi: 10.1016/0016-6480(86)90222-4
 47. Quesada J, Lozano MT, Ortega A, Agulleiro B. Immunocytochemical and Ultrastructural Characterization of the Cell Types in the Adenohypophysis of Sparus Aurata L. (Teleost). *Gen Comp Endocrinol* (1988) 72(2):209–25. doi: 10.1016/0016-6480(88)90204-3
 48. Toubeau G, Poilve A, Baras E, Nonclercq D, De Moor S, Beckers JF, et al. Immunocytochemical Study of Cell Type Distribution in the Pituitary of Barbus Barbus (Teleostei, Cyprinidae). *Gen Comp Endocrinol* (1991) 83(1):35–47. doi: 10.1016/0016-6480(91)90103-D
 49. Huang L, Specker JL. Growth Hormone- and Prolactin-Producing Cells in the Pituitary Gland of Striped Bass (*Morone Saxatilis*): Immunocytochemical Characterization at Different Life Stages. *Gen Comp Endocrinol* (1994) 94(2):225–36. doi: 10.1006/gcen.1994.1079
 50. Borella MI, Venturieri R, Mancera JM. Immunocytochemical Identification of Adenohypophysal Cells in the Pirarucu (*Arapaima Gigas*), an Amazonian Basal Teleost. *Fish Physiol Biochem* (2009) 35(1):3–16. doi: 10.1007/s10695-008-9254-x
 51. Oliveuru M, Nagahama Y. Immunocytochemistry of Gonadotropic Cells in the Pituitary of Some Teleost Species. *Gen Comp Endocrinol* (1983) 50(2):252–60. doi: 10.1016/0016-6480(83)90225-3
 52. Dubourg P, Burzawa-Gerard E, Chamolle P, Kah O. Light and Electron Microscopic Identification of Gonadotrophic Cells in the Pituitary Gland of the Goldfish by Means of Immunocytochemistry. *Gen Comp Endocrinol* (1985) 59(3):472–81. doi: 10.1016/0016-6480(85)90407-1
 53. Nozaki M, Naito N, Swanson P, Miyata K, Nakai Y, Oota Y, et al. Salmonid Pituitary Gonadotrophs I. Distinct Cellular Distributions of Two Gonadotrophs, GTH I and GTH II. *Gen Comp Endocrinol* (1990) 77(3):348–57. doi: 10.1016/0016-6480(90)90224-A
 54. Grandi G, Colombo G, Chicca M. Immunocytochemical Studies on the Pituitary Gland of *Anguilla Anguilla L.*, in Relation to Early Growth Stages and Diet-Induced Sex Differentiation. *Gen Comp Endocrinol* (2003) 131(1):66–76. doi: 10.1016/S0016-6480(02)00646-9
 55. García-Hernández MP, García-Ayala A, Elbal MT, Agulleiro B. The Adenohypophysis of Mediterranean Yellowtail, *Seriola Dumerilii* (Risso, 1810): An Immunocytochemical Study. *Tissue Cell* (1996) 28(5):577–85. doi: 10.1016/S0040-8166(96)80060-7
 56. Grandi G, Chicca M. Early Development of the Pituitary Gland in *Acipenser Naccarii* (Chondrostei, Acipenseriformes): An Immunocytochemical Study. *Anat Embryol* (2004) 208(4):311–21. doi: 10.1007/s00429-004-0402-5
 57. Batten TFC. Immunocytochemical Demonstration of Pituitary Cell Types in the Teleost *Poecilia Latipinna*, by Light and Electron Microscopy. *Gen Comp Endocrinol* (1986) 63(1):139–54. doi: 10.1016/0016-6480(86)90192-9
 58. Gutnick A, Blechman J, Kaslin J, Herwig L, Belting H-G, Affolter M, et al. The Hypothalamic Neuropeptide Oxytocin Is Required for Formation of the Neurovascular Interface of the Pituitary. *Dev Cell* (2011) 21(4):642–54. doi: 10.1016/j.devcel.2011.09.004
 59. Golan M, Zelinger E, Zohar Y, Levavi-Sivan B. Architecture of GnRH-Gonadotrope-Vasculature Reveals a Dual Mode of Gonadotropin Regulation in Fish. *Endocrinology* (2015) 156(11):4163–73. doi: 10.1210/en.2015-1150
 60. Kawabata-Sakata Y, Nishiike Y, Fleming T, Kikuchi Y, Okubo K. Androgen-Dependent Sexual Dimorphism in Pituitary Tryptophan Hydroxylase Expression: Relevance to Sex Differences in Pituitary Hormones. *Proc R Soc B: Biol Sci* (2020) 287(1928):20200713. doi: 10.1098/rspb.2020.0713
 61. Taranger GL, Carrillo M, Schulz RW, Fontaine P, Zanuy S, Felip A, et al. Control of Puberty in Farmed Fish. *Gen Comp Endocrinol* (2010) 165(3):483–515. doi: 10.1016/j.ygcen.2009.05.004
 62. Borg B. Androgens in Teleost Fishes. Comparative Biochemistry and Physiology Part C: Pharmacology. *Toxicol Endocrinol* (1994) 109(3):219–45. doi: 10.1016/0742-8413(94)00063-G
 63. Royan MR, Kanda S, Kayo D, Song W, Ge W, Weltzien F-A, et al. Gonadectomy and Blood Sampling Procedures in the Small Size Teleost Model Japanese Medaka (*Oryzias Latipes*). *JoVE* (2020) 166:e62006. doi: 10.3791/62006
 64. Ohta K, Mine T, Yamaguchi A, Matsuyama M. Sexually Dimorphic Expression of Pituitary Glycoprotein Hormones in a Sex-Changing Fish (*Pseudolabrus Sieboldi*). *J Exp Zool Part A: Ecol Genet Physiol* (2008) 309A(9):534–41. doi: 10.1002/jez.485
 65. Martin SAM, Wallner W, Youngson AF, Smith T. Differential Expression of Atlantic Salmon Thyrotropin β Subunit mRNA and Its cDNA Sequence. *J Fish Biol* (1999) 54(4):757–66. doi: 10.1111/j.1095-8649.1999.tb02031.x
 66. He W, Dai X, Chen X, He J, Yin Z. Zebrafish Pituitary Gene Expression Before and After Sexual Maturation. *J Endocrinol* (2014) 221(3):429. doi: 10.1530/JOE-13-0488
 67. Degani G, Yom-Din S, Goldberg D, Jackson K. cDNA Cloning of Blue Gourami (*Trichogaster Trichopterus*) Prolactin and Its Expression During the Gonadal Cycles of Males and Females. *J Endocrinological Invest* (2010) 33(1):7–12. doi: 10.1007/BF03346543
 68. Cavaco JEB, Santos CLRA, Ingleton PM, Canario AVM, Power DM. Quantification of Prolactin (PRL) and PRL Receptor Messenger RNA in Gilthead Seabream (*Sparus Aurata*) After Treatment With Estradiol-17 β . *Biol Reprod* (2003) 68(2):588–94. doi: 10.1095/biolreprod.102.009209
 69. Rand-Weaver M, Swanson P, Kawauchi H, Dickhoff WW. Somatotactin, a Novel Pituitary Protein: Purification and Plasma Levels During Reproductive Maturation of Coho Salmon. *J Endocrinol* (1992) 133(3):393. doi: 10.1677/joe.0.1330393
 70. Mousa MA, Mousa SA. Immunocytochemical Study on the Localization and Distribution of the Somatotactin Cells in the Pituitary Gland and the Brain of Oreochromis Niloticus (Teleostei, Cichlidae). *Gen Comp Endocrinol* (1999) 113(2):197–211. doi: 10.1006/gcen.1998.7200
 71. Mousa MA, Mousa SA. Implication of Somatotactin in the Regulation of Sexual Maturation and Spawning of Mugil Cephalus. *J Exp Zool* (2000) 287(1):62–73. doi: 10.1002/1097-010X(20000615)287:1<62::AID-JEZ8>3.0.CO;2-0
 72. Benedet S, Björnsson BT, Taranger GL, Andersson E. Cloning of Somatotactin Alpha, Beta Forms and the Somatotactin Receptor in Atlantic Salmon: Seasonal Expression Profile in Pituitary and Ovary of Maturing Female Broodstock. *Reprod Biol Endocrinol* (2008) 6:42–. doi: 10.1186/1477-7827-6-42
 73. Onuma T, Kitahashi T, Taniyama S, Saito D, Ando H, Urano A. Changes in Expression of Genes Encoding Gonadotropin Subunits and Growth Hormone/Prolactin/Somatolactin Family Hormones During Final Maturation and Freshwater Adaptation in Prespawning Chum Salmon. *Endocrine* (2003) 20(1):23–33. doi: 10.1385/ENDO:20:1-2:23
 74. Fontaine R, Royan MR, von Krogh K, Weltzien F-A, Baker DM. Direct and Indirect Effects of Sex Steroids on Gonadotrope Cell Plasticity in the Teleost Fish Pituitary. *Front Endocrinol* (2020) 11(858). doi: 10.3389/fendo.2020.605068
 75. Childs GV, MacNicol AM, MacNicol MC. Molecular Mechanisms of Pituitary Cell Plasticity. *Front Endocrinol* (2020) 11(656). doi: 10.3389/fendo.2020.00656
 76. Rizzotti K. Adult Pituitary Progenitors/Stem Cells: From *In Vitro* Characterization to *In Vivo* Function. *Eur J Neurosci* (2010) 32(12):2053–62. doi: 10.1111/j.1460-9568.2010.07524.x

77. Ho Y, Hu P, Peel MT, Chen S, Camara PG, Epstein DJ, et al. Single-Cell Transcriptomic Analysis of Adult Mouse Pituitary Reveals Sexual Dimorphism and Physiologic Demand-Induced Cellular Plasticity. *Protein Cell* (2020) 11(8):565–83. doi: 10.1007/s13238-020-00705-x
78. Fabian P, Tseng KC, Smeeton J, Lancman JJ, Dong PDS, Cerny R, et al. Lineage Analysis Reveals an Endodermal Contribution to the Vertebrate Pituitary. *Science* (2020) 370(6515):463–7. doi: 10.1126/science.aba4767
79. Batten T, Ball JN, Benjamin M. Ultrastructure of the Adenohypophysis in the Teleost *Poecilia Latipinna*. *Cell Tissue Res* (1975) 161(2):239–61. doi: 10.1007/BF00220372
80. Margolis-Kazan H, Peute J, Schreiberman MP, Halpern LR. Ultrastructural Localization of Gonadotropin and Luteinizing Hormone Releasing Hormone in the Pituitary Gland of a Teleost Fish (the Platyfish). *J Exp Zool* (1981) 215(1):99–102. doi: 10.1002/jez.1402150112
81. Andoniadou CL. Pituitary Stem Cells During Normal Physiology and Disease. In: D Pfaff, Y Christen, editors. *Stem Cells in Neuroendocrinology*. Cham: Springer International Publishing (2016). p. 103–11.
82. Horvath E, Kovacs K. Folliculo-Stellate Cells of the Human Pituitary: A Type of Adult Stem Cell? *Ultrastructural Pathol* (2002) 26(4):219–28. doi: 10.1080/01913120290104476
83. Horvath E, Kovacs K, Killinger DW, Smyth HS, Weiss MH, Ezrin C. Mammosomatotroph Cell Adenoma of the Human Pituitary: A Morphologic Entity. *Virchows Archiv A* (1983) 398(3):277–89. doi: 10.1007/BF00583585
84. Vidal S, Horvath E, Kovacs K, Lloyd RV, Smyth HS. Reversible Transdifferentiation: Interconversion of Somatotrophs and Lactotrophs in Pituitary Hyperplasia. *Modern Pathol: an Off J United States Can Acad Pathol Inc* (2001) 14(1):20–8. doi: 10.1038/modpathol.3880252
85. Vidal S, Horvath E, Kovacs K, Cohen SM, Lloyd RV, Scheithauer BW. Transdifferentiation of Somatotrophs to Thyrotrophs in the Pituitary of Patients With Protracted Primary Hypothyroidism. *Virchows Archiv* (2000) 436(1):43–51. doi: 10.1007/PL00008197
86. Charles MA, Saunders TL, Wood WM, Owens K, Parlow AF, Camper SA, et al. Pituitary-Specific *Gata2* Knockout: Effects on Gonadotrope and Thyrotrope Function. *Mol Endocrinol* (2006) 20(6):1366–77. doi: 10.1210/me.2005-0378
87. Dasen JS, O'Connell SM, Flynn SE, Treier M, Gleiberman AS, Szeto DP, et al. Reciprocal Interactions of *Pit1* and *GATA2* Mediate Signaling Gradient-Induced Determination of Pituitary Cell Types. *Cell* (1999) 97(5):587–98. doi: 10.1016/S0092-8674(00)80770-9
88. Pulichino A-M, Vallette-Kasic S, Tsai JP-Y, Couture C, Gauthier Y, Drouin J. *Tpit* Determines Alternate Fates During Pituitary Cell Differentiation. *Genes Dev* (2003) 17(6):738–47. doi: 10.1101/gad.1065703
89. Kelberman D, Rizzotti K, Lovell-Badge R, Robinson ICAF, Dattani MT. Genetic Regulation of Pituitary Gland Development in Human and Mouse. *Endocrine Rev* (2009) 30(7):790–829. doi: 10.1210/er.2009-0008
90. Sanno N, Tahara S, Kurotani R, Matsumo A, Teramoto A, Yoshiyuki Osamura R. Cytochemical and Molecular Biological Aspects of the Pituitary and Pituitary Adenomas — Cell Differentiation and Transcription Factors. *Prog Histochem Cytochem* (2001) 36(4):263–99. doi: 10.1016/S0079-6336(00)80003-0
91. Tahara S, Kurotani R, Sanno N, Takumi I, Yoshimura S, Osamura RY, et al. Expression of Pituitary Homeo Box 1 (*Ptx1*) in Human Non-Neoplastic Pituitaries and Pituitary Adenomas. *Modern Pathol* (2000) 13(10):1097–108. doi: 10.1038/modpathol.3880204
92. Mitrofanova LB, Kononov PV, Krylova JS, Polyakova VO, Kvetnoy IM. Plurihormonal Cells of Normal Anterior Pituitary: Facts and Conclusions. *Oncotarget* (2017) 8(17):29282–99. doi: 10.18632/oncotarget.16502
93. Yan HY, Thomas P. Histochemical and Immunocytochemical Identification of the Pituitary Cell Types in Three Sciaenid Fishes: Atlantic Croaker (*Micropogonias Undulatus*), Spotted Seatrout (*Cynoscion Nebulosus*), and Red Drum (*Sciaenops Ocellatus*). *Gen Comp Endocrinol* (1991) 84(3):389–400. doi: 10.1016/0016-6480(91)90086-L

Conflict of Interest: The authors declare that the research was conducted in the absence of any commercial or financial relationships that could be construed as a potential conflict of interest.

Publisher's Note: All claims expressed in this article are solely those of the authors and do not necessarily represent those of their affiliated organizations, or those of the publisher, the editors and the reviewers. Any product that may be evaluated in this article, or claim that may be made by its manufacturer, is not guaranteed or endorsed by the publisher.

Copyright © 2021 Royan, Siddique, Csucs, Puchades, Nourizadeh-Lillabadi, Bjaalie, Henkel, Weltzien and Fontaine. This is an open-access article distributed under the terms of the Creative Commons Attribution License (CC BY). The use, distribution or reproduction in other forums is permitted, provided the original author(s) and the copyright owner(s) are credited and that the original publication in this journal is cited, in accordance with accepted academic practice. No use, distribution or reproduction is permitted which does not comply with these terms.

III

1 Heterogeneity of pituitary lactotrope populations in the teleost model

2 medaka (*Oryzias latipes*)

3 Khadeeja Siddique, Muhammad Rahmad Royan, Finn-Arne Weltzien, Romain Fontaine, Christiaan

4 Henkel

5 Physiology unit, Faculty of Veterinary Medicine, Norwegian University of Life Sciences, Ås, Norway

7 Abstract

8 In fish, the prolactin cell population, located in the anterior part of the pituitary, plays an essential role
9 in osmoregulation. In Japanese medaka, a euryhaline fish, we recently described two *prl*-expressing cell
10 populations (lactotropes) with single cell RNA-seq (scRNA-seq). In several other species, smaller
11 satellite populations of prolactin cells have been described in other parts of the pituitary. The functional
12 and developmental backgrounds of these extra populations are not known. In this study, we explore the
13 hypothesis that the two transcriptomically distinct lactotrope populations in our medaka scRNA-seq
14 data represent the two spatially distinct cell populations found in other species. We investigate this
15 assumption using both scRNA-seq data and an *in situ* hybridization approach. Initially, we identified
16 two distinct types of *prl*-expressing cells using scRNA-seq data (termed primary and secondary
17 lactotropes). Primary lactotropes have an expression profile comparable to that of cells expressing
18 growth hormone or somatotactin. By contrast, secondary lactotropes exhibit an expression profile
19 similar to that of stem-cell-like populations and show some of the hallmarks of a technical artifact.
20 Using *in situ* hybridization, we confirm that the secondary lactotropes do form a distinct biological
21 subpopulation. In addition, we show that, like other teleosts, the medaka pituitary often develops
22 multiple lactotrope cell clusters later in life. Somewhat surprisingly, there does not appear to be a clear
23 correspondence between the stem cell-like secondary lactotropes and these newly emerging secondary
24 populations. However, our data support the hypothesis that the transcriptomic secondary lactotropes are
25 an intrinsic developmental stage in the development of every spatially distinct lactotrope cluster.

26
27 Keywords: prolactin, pituitary, development, osmoregulation, plasticity

29 Introduction

30 The pituitary is a key endocrine gland in vertebrates, which regulates essential physiological functions,
31 including growth, stress, homeostasis, and reproduction. Under the control of the brain, which integrates
32 internal and environmental stimuli, the pituitary centralizes the command of many peripheral organs
33 through the production and release of several hormones into the blood circulation. Located below the
34 hypothalamic region of the brain, the pituitary is divided in two main parts: the neurohypophysis
35 (posterior pituitary) and adenohypophysis (anterior pituitary), of which the latter is in teleosts further
36 subdivided into two distinct parts: the *pars distalis* (PD) and the *pars intermedia* (PI) ¹.

37
38 The teleost adenohypophysis contains up to eight endocrine cell types which produce and release
39 specific peptide hormones. Among them are the lactotropes (also called mammotropes in mammals),
40 which produce prolactin (Prl). First discovered as a stimulating factor of milk production in mammals,
41 over 300 different functions have been associated to Prl in vertebrates, such as water and electrolyte
42 balance, growth and development, among others. ². The importance of Prl in fish osmoregulation was
43 first demonstrated in the 1950s by studies on the killifish (*Fundulus heteroclitus*), a euryhaline teleost

44 ³. In fish, Prl plays an important role in freshwater osmoregulation by preventing both the loss of ions
45 and the uptake of water ⁴.

46

47 The Japanese medaka (*Oryzias latipes*) is a freshwater teleost that is frequently used as a model in the
48 research ^{5,6}. Additionally, it is also an euryhaline species (salinity tolerant) and thus has been used as
49 model to study osmoregulation and physiological adaptation to hyperosmotic environments ⁷⁻¹¹.
50 Interestingly, medaka belongs to the order Belontiiformes, in which most of the species are seawater fish
51 (e.g., flying fish, saury and halfbeak). For this reason, medaka is thought of as a freshwater fish that
52 evolved from a seawater-inhabiting ancestor ^{12,13}. Indeed, some *Oryzias* species inhabit and reproduce
53 in brackish water and seawater ⁷.

54

55 In mammals, several Prl isoforms exist; some occur from alternate splicing of *prl* mRNA, while the
56 majority are the product of post-translational modification. Although there is little evidence to support
57 this, it has been claimed that Prl molecular heterogeneity in mammals contributes to functional variety
58 ^{14,15}. There are no reports of distinct Prl isoforms originating from alternative splicing or protein
59 processing in fish, although this may simply reflect a lack of studies. Different *prl* isoforms encoding
60 177 and 188 amino acids have been identified in Nile tilapia ¹⁶. Duplicate genes are almost certainly
61 present in other species, such as Mozambique tilapia ^{17,18} and chum salmon ^{19,20}. The presence of
62 "additional" genes in fish relative to other vertebrates is easily explained by the evolutionary concept
63 of genome duplication ²¹⁻²³. Medaka also possesses two genes encoding Prl in its genome, *prla/prl*
64 (ENSORLG00000016928) and *prlb* (ENSORLG00000012617) ^{24,25}. We recently used scRNA-seq to
65 characterize the major endocrine cell populations in the medaka pituitary and identified two different
66 *prl*-expressing cell populations (lactotropes) ²⁶. In these cells, only the *prl* paralogue is expressed; *prlb*
67 is not expressed in the pituitary.

68

69 Pituitary lactotropes have been reported to be mainly clustered in the *rostral pars distalis* (RPD) ^{1,4}, the
70 most anterior part of the pituitary. However, in several teleost species, a few *prl*-expressing cells have
71 also been described in the ventral and lateral surface of the PI or the *proximal pars distalis* (PPD),
72 sometimes forming small clusters. This is the case for instance in striped bass ²⁵, Mediterranean
73 yellowtail ²⁷, ayu ²⁸, greater weever fish ²⁹, chum salmon and rainbow trout ³⁰. However, the origin and
74 role of these patches, and whether the prolactin cells forming them are developmentally and functionally
75 distinct from those in the major anterior cluster, remain unknown.

76

77 In different species, and through different experimental lenses, the teleost pituitary therefore appears to
78 harbor multiple populations of lactotropes. In this study, we explore the hypothesis that the two
79 transcriptomically distinct lactotrope populations in our medaka scRNA-seq data represent the two
80 spatially distinct cell populations found in other species.

81

82 **Results**

83 **Two prolactin populations with different *prl* expression**

84 Our scRNA-seq data on the medaka pituitary show *prl* expression in two distinct cell clusters, in both
85 female and male fish (Fig. 1A and B left panel). Expression of *prl* within these two clusters revealed
86 that the gene is more highly expressed in one of them (Fig. 1A and B right panel) in both sexes, further
87 implying that the lactotrope populations in adult medaka are functionally or developmentally distinct
88 (Fig. 1A and B). By examining the top ten differentially expressed genes between these two lactotrope
89 populations (Fig. 1C right panel), we discovered that many of the same genes are differentially
90 expressed in male and female datasets. As the data do not indicate sex differences, we opted to combine

91 male and female data for the rest of the study. After integrating the datasets of the two sexes, as
92 expected, two distinct lactotrope populations remained. These findings imply that the male and female
93 lactotrope populations are indeed identical, and hence may be examined concurrently, which provides
94 a higher resolution by increasing the number of cells (Fig. 1C left panel). We refer to the population
95 with overall higher and lower *prl* expression as the primary and secondary lactotropes, respectively.
96

97 **Stem cell populations**

98 Based on the UMAP visualization, we found that the secondary lactotrope population appears similar
99 in expression profile to two uncharacterized cell clusters (Fig. 1A, B and C left panel). To investigate
100 the relation, we identified 207 genes (48 upregulated and 159 downregulated) that are differentially
101 expressed between primary lactotropes (group 1) vs. secondary lactotropes and uncharacterized
102 populations (group 2). Fig. 2A shows the expression levels of the top ten up- and twenty down-regulated
103 genes across the four clusters. Among the differentially expressed genes, several markers for proliferating
104 stem cells were identified, including *sox2* (SRY-box transcription factor 2) and *mala* (encoding MAL,
105 the myelin and lymphocyte T-cell differentiation protein) in uncharacterized clusters which we named
106 “stem cell populations”. We detected *sox2* and *mala* expression in both stem cell populations and in the
107 secondary lactotropes (which appear closely related by UMAP dimensions), but not in the other primary
108 population (Fig. 2A and B).
109

110 **Two prolactin populations with different transcriptome profiles**

111 Next, we investigated the differences among both lactotrope populations (Fig. 1C right panel). Apart
112 from *prl* gene expression levels (Fig 1), the secondary lactotropes expressed more genes and had in
113 general a higher read count per cell than the primary lactotropes (Fig. 3). As the secondary lactotropes
114 combine gene expression characteristics of both the stem cells and primary lactotropes, this suggests
115 that these profiles could be technical artifacts, in which single cells of these populations combine to
116 form a hybrid ‘cell’ with elevated expression.
117

118 **Spatial distribution of *prl* expression in the pituitary**

119 Using RNAscope to label for *prl* RNA, we then investigated whether the lactotropes in medaka are
120 spatially restricted to a single location in the pituitary. As in other fish species, a number of medaka
121 from both sexes had additional prolactin cells in a different location than the expected RPD. The latter,
122 however, always remains the major prolactin cell cluster in all individuals. We could distinguish two
123 types of patterns for the *prl* cells located outside the RPD, with these either forming a big cluster on one
124 side of the pituitary or forming multiple small clusters (patches) distributed on the ventral and lateral
125 surfaces of the PPD (Fig. 4A).
126

127 By investigating the size of the prolactin population within the non-RPD of fish at different stages of
128 development (Fig. 4B), we observed that in both males and females, the percentage of fish showing one
129 or several developing non-RPD prolactin cluster(s) increases with age. We also observed that the size
130 of these non-RPD clusters increases with fish age in both sexes.
131

132 **Identification and localization of the two Prl-populations**

133 In order to investigate whether the two distinct *prl*-expressing populations (primary and secondary)
134 found in the scRNA-seq data correspond to the two types of *prl*-expressing populations discovered by
135 FISH, we performed *in situ* hybridization with a marker specific to one of the scRNA-seq populations.

136 *mala* is specifically and highly expressed in the secondary lactotropes and the related stem cell
137 populations (Fig. 2B), but not in the primary lactotropes. We investigated the location of the expression
138 of *mala* using RNAscope. If the RPD and non-RPD populations correspond to primary and secondary
139 lactotropes, respectively, *mala* should be expressed in the non-RPD Prl-populations only. However, we
140 found *mala* is expressed in both RPD and non-RPD Prl-populations (Fig. 4C). Interestingly, we
141 observed *mala* expression in the middle of all populations, where the *prl* expression levels also appeared
142 lower in *in situ* images (Fig. 4C and D). Indeed, the borders of the RPD Prl-populations always show
143 higher *prl* expression than the centers. This pattern agrees with the scRNA-seq data where *prl*
144 expression is found to be higher in the primary lactotropes (Fig. 1A and B), which also do not express
145 *mala* (Fig. 2B). These results demonstrate that the Prl-population is heterogeneous, but that the
146 heterogeneity does not seem to depend on the location in the pituitary (RPD or non-RPD), but rather on
147 the location *within* the clusters (border or internal).

148
149 Finally, we then investigated the spatial expression of *sox2*, which the scRNA-seq data predict to be
150 expressed in all *mala*-expressing cells, and in an additional cluster of stem cell-like cells (Fig. 2B).
151 However, *sox2* was found in high quantities in the brain, but only in a few cells in the pituitary (Fig.
152 4D). We observed *sox2* expression in non-RPD regions of the pituitary, but never in the *prl*-expressing
153 cells. In addition, we also investigated *mala* and *sox2* co-expression (Fig. 4E) and could never observe
154 colocalization of the two signals.
155

156 Discussion

157 Prolactin has been identified as the "freshwater-adapting hormone" in teleost fishes, regulating ion
158 conservation and water secretion mechanisms via the gill, kidney, gut, and urinary bladder^{31,32}.
159 Prolactin is a member of a family of structurally related proteins, including growth hormone and the
160 teleost-specific somatolactin²⁴. Although *prl* gene expression was originally found in the RPD area of
161 the pituitary, numerous fish species have patches of *prl*-expressing cells in non-RPD areas. In this study,
162 we describe a similar phenomenon in medaka.
163

164 In addition, we discovered two types of *prl*-expressing cells by scRNA-seq data, which we named
165 primary and secondary lactotropes. Based on the UMAP visualization, the primary lactotropes are
166 similar in expression profile to cells expressing either growth hormone or somatolactin. In contrast, the
167 secondary lactotropes are similar in expression profile to stem-cell-like populations. As the smaller,
168 non-RPD patches of lactotropes emerge later during development, this suggests that they might coincide
169 with the (transcriptomically defined) secondary lactotropes. However, *in situ* hybridization does not
170 support this hypothesis.
171

172 A closer look at the transcriptomic data suggests two alternative explanations. In one scenario, the
173 secondary lactotropes are an artifact of scRNA-seq library preparation. In the other, they represent a
174 developmental stage of lactotropes.
175

176 In the first of these hypotheses, the secondary lactotropes might be the result of a technical artifact.
177 These cells express more genes and have higher read counts (Figure 3), suggesting that the secondary
178 lactotropes were caused by the droplet-based microfluidic devices used to perform scRNA-seq library
179 preparation. During the loading, individual cells are co-encapsulated in each droplet in the microfluidics
180 scRNA-seq process. Due to the random distribution of cells within droplets, droplets are filled with two
181 cells at a frequency depending on cell concentration, resulting in technical artifacts referred to as
182 doublets³³. Doublets are undesirable when characterizing populations at the single-cell level. In

183 particular, they might be mistaken for non-existent transitional populations or transient phases. It is
184 therefore crucial to detect and eliminate doublets from the scRNA-seq data. During the initial data
185 analysis in our earlier study ²⁶, we applied a standard doublet detection protocol, which assumes
186 independent and random stochastic loading of cells. Such a protocol would therefore not remove a
187 single, large population of doublets formed by the specific co-encapsulation of only two (out of 15) cell
188 types, and in fact such an extreme scenario is hard to reconcile with 10x Genomics loading. In other
189 words, if loading were to blame, we would expect many large, hybrid cell populations (between e.g.,
190 gonadotropes and lactotropes), which we do not observe. Alternatively, such specific doublets could be
191 the result of incomplete cell dissociation, or strong and specific *in vitro* affinities between two
192 constituent cell types.

193
194 As a second hypothesis, even if the secondary lactotropes do not coincide with the newly emerging
195 ‘patches’, they might still represent a stage in lactotrope development. We observed the co-expression
196 of *mala*, *sox2* and *pit1* genes in the secondary lactotropes. In mammals, it has been reported that the
197 five hormone-producing populations in the mature anterior pituitary gland originate from a *sox2*, *prop1*-
198 progenitor population and diverge during development to become distinct cell types ³⁴. Together with
199 the trajectory-like placement in the UMAP visualization, this suggests that the secondary lactotropes
200 are developmental intermediates between progenitor cells and primary lactotropes.

201
202 To evaluate these hypotheses (artifact or developmental stage), we used RNAscope *in situ* hybridization
203 to determine the spatial distribution patterns of *prl*, *sox2* and *mala* gene expression in the medaka
204 pituitary. We discovered a high level of *sox2* expression in the brain, whereas only a few cells expressed
205 *sox2* in the adult pituitary. These are mostly located in the dorsal part of the PPD with very few cells
206 spread in the PPD, which is in agreement with a previous study investigating Sox2 protein location in
207 the medaka pituitary ³⁵. However, *sox2* labeling was never observed in *prl*-expressing cells, as suggested
208 by the transcriptomics data. Furthermore, we also investigated *mala* and *sox2* co-expression and could
209 never observe colocalization. These results are in disagreement with the scRNA-seq data, in which these
210 genes are co-expressed in both secondary lactotropes and stem-cell-like cells. As a possible explanation,
211 the relative concentration of *sox2* expression in the pituitary compared to the brain could render it below
212 the detection limit of RNAscope.

213
214 We did observe co-expression of *mala* and *prl* in the pituitary, which is consistent with the expression
215 profile of the secondary lactotropes in our transcriptomics data. As the markers are co-expressed within
216 individual cells, this invalidates our first hypothesis on artifactual hybrids, and demonstrates that the
217 secondary lactotropes are an actual distinct population of cells in the medaka pituitary. They appear to
218 be located in the core of all lactotrope cell clusters, with the primary lactotropes (which have higher
219 expression of *prl*) located at the edges. This spatial and transcriptomic heterogeneity of *prl*-producing
220 clusters is consistent with the second (developmental) hypothesis outlined above. Interestingly, both the
221 RPD cluster and non-RPD patches exhibit this heterogeneity, even though only the latter develop later
222 in life (Figure 4E). Our results therefore suggest that pituitary lactotrope clusters, in general, are plastic
223 and capable of adapting to changing demands. What conditions trigger the formation of additional
224 cluster remains unclear.

225
226 Numerous studies ³⁶⁻⁴³ have demonstrated that prolactin gene expression and/or plasma prolactin levels
227 increase when environmental salinity is reduced. In future experiments, it would therefore be interesting
228 to investigate the effect of salinity on lactotrope development and heterogeneity.

229

230 **Materials and methods**

231 **Animals**

232 Medaka (*Oryzias latipes*) from the d-rR genetic background were raised in the laboratory in a
233 recirculating system (28 °C; pH 7.6; conductivity 800 µS) with 14 hours light and three feedings a day
234 (once with live brine shrimp and twice with dry food). Experiments were performed according to the
235 recommendations of the care and welfare of research animals at the Norwegian University of Life
236 Sciences, and under the supervision of authorized investigators.

237

238 **Single cell transcriptomics analysis (scRNA-seq)**

239 We used processed scRNA-seq datasets for male and female pituitaries from our previous study ²⁶ in
240 which two separate lactotrope clusters were identified in both sexes. Firstly, we investigated the *prl*
241 gene expression using the *FeaturePlot* and *VlnPlot* functions in the Seurat ⁴⁴ R toolkit (v 3.1.5) to
242 identify the differences on expression level among these two lactotropes populations. We selected the
243 top ten genes by differential expression from each sex and visualized them by using the *DoHeatmap*
244 function of Seurat.

245

246 **Integration and differentially expressed genes**

247 We combined the raw datasets from both male and female pituitaries to increase the number of cells by
248 using the merge function in Seurat with default settings. This function combines the raw count matrices
249 of two Seurat objects and returns the resulting combined raw count matrix as a new Seurat object. After
250 merging the data, normalization was done by using the *LogNormalize* method in Seurat. Highly variable
251 genes were identified by using the *vst* method. Subsequently, we used these variable genes (n = 2000)
252 to identify significant principal components (PCs) based on the *jackStraw* function and used ten
253 informative PC dimensions as the input for uniform manifold approximation and projection (UMAP).

254

255 As the study's focus was not on all 16 clusters, four clusters (two lactotrope and two uncharacterized
256 populations) were extracted using Seurat's *subset* function. To identify the differences between these
257 four populations, we utilized Seurat's *FindMarker* function to identify genes whose expression differs
258 by an average of 0.5-fold (log-scale) between the two (lactotropes vs. three other clusters), with at least
259 0.6% of cells in either population expressing the genes.

260

261 **Whole mount fluorescence *in situ* hybridization (FISH)**

262 Medaka fish (1, 3, and 8-months old) from both sexes were euthanized using ice water immersion and
263 directly decapitated thereafter. The pituitary was fixed overnight at 4 °C in 4% paraformaldehyde (PFA,
264 Electron Microscopy Sciences, Hatfield, Pennsylvania) diluted in phosphate-buffered saline with
265 Tween (PBST: PBS, 0.1%; Tween-20). The tissue was processed through a serial dehydration and
266 rehydration in ethanol (25, 50, 75, 96%) and methanol (100%) before use. FISH for *prl* was performed
267 as described in ⁴⁵ with probe sequence obtained from NCBI (XM_004071867.4) as previously
268 performed in ⁴⁶ with a confirmed specificity (F: GAAAGACCGAGGAGGAACTG, R:
269 TTGCAGAGTTGGACAGGACC). After tagging with fluorescein-12-UTP (FITC, Roche
270 Diagnostics), the probe (1.5 ng/µl) was used to hybridize the tissue for 18 h at 55 °C. Subsequently, the
271 tissue was incubated in anti-FITC-conjugated antibody (1:200, Roche Diagnostics) overnight at 4 °C,
272 followed by incubation in FITC-conjugated tyramide (1:200, Sigma) for 30 minutes at room
273 temperature (RT), and nuclei staining with DAPI (1:1000, 4', 6-diamidino-2-phenylindole
274 dihydrochloride; Sigma) for 6 hours at RT, with extensive washing with PBST in between.

275 RNAscope

276 Adult (6-months old) fish were euthanized with an overdose of tricaine (MS222, Sigma). Tissues were
277 fixed and blood was removed by cardiac perfusion with 4% PFA (PBST) as previously described ⁴⁷.
278 Brain and pituitary were dissected and fixed overnight at 4 °C. Tissues were then incubated in 25%
279 sucrose solution (diluted in PBS) for cryoprotection and then mounted in block with OCT (Tissue-Tek,
280 Sakura) and stored at -80 °C until use. Tissues were later parasagittally sectioned with a CM3050 Leica
281 cryostat (10 µm sections). RNAscope was performed as described by the supplier using *prl*, *sox2*
282 (ENSORLG00000001780) and *mala* (ENSORLG00000003048) probes and combined with opals 520,
283 570 and 690 (Akoya Bioscience).

284

285 Imaging and cell volume measurement

286 Pituitary cryostat sections were mounted between glass slide and coverslip with Vectashield (H-1000,
287 Vector, Eurobio/Abcys), while whole pituitaries were mounted with Vectashield and coverslip with
288 spacers (Reinforcement rings, Herma) added in between. Fluorescent images were obtained using either
289 an LSM710 Confocal Microscope (Zeiss) with 25× (for adult pituitary) and 40× (for younger pituitary)
290 objectives and lasers with wavelength of 405 (DAPI), 555 (opal 570), 633 (opal 690) and 488 (FITC;
291 opal 520) nm, or with a Thunder microscope (Leica) with a 20× objective and the appropriate filters.
292 Images were processed using ImageJ (1.52p; <http://rsbweb.nih.gov/ij/>). The prolactin cell number was
293 counted using built-in cell counter plug-in in ImageJ software while the volume analysis was performed
294 using the 3D analyzing tools on the Thunder microscope software Las X (Leica).

295

296 References

297

- 298 1 Weltzien, F. A., Andersson, E., Andersen, O., Shalchian-Tabrizi, K. & Norberg, B. The brain-
299 pituitary-gonad axis in male teleosts, with special emphasis on flatfish (Pleuronectiformes).
300 *Comp Biochem Physiol A Mol Integr Physiol* **137**, 447-477,(2004).
- 301 2 Bole-Feyssot, C., Goffin, V., Edery, M., Binart, N. & Kelly, P. A. Prolactin (PRL) and its
302 receptor: actions, signal transduction pathways and phenotypes observed in PRL receptor
303 knockout mice. *Endocr Rev* **19**, 225-268,(1998).
- 304 3 Pickford Grace, E. & Phillips John, G. Prolactin, a Factor in Promoting Survival of
305 Hypophysectomized Killifish in Fresh Water. *Science* **130**, 454-455,(1959).
- 306 4 Manzon, L. A. The Role of Prolactin in Fish Osmoregulation: A Review. *General and*
307 *Comparative Endocrinology* **125**, 291-310,(2002).
- 308 5 Shima, A. & Mitani, H. Medaka as a research organism: past, present and future. *Mechanisms*
309 *of Development* **121**, 599-604,(2004).
- 310 6 Wittbrodt, J., Shima, A. & Schartl, M. Medaka--a model organism from the far East. *Nature*
311 *Reviews Genetics* **3**, 53-64,(2002).
- 312 7 Inoue, K. & Takei, Y. Diverse Adaptability in Oryzias Species to High Environmental
313 Salinity. *Zool Sci* **19**, 727-734,(2002).
- 314 8 Inoue, K. & Takei, Y. Asian medaka fishes offer new models for studying mechanisms of
315 seawater adaptation. *Comparative Biochemistry and Physiology Part B: Biochemistry and*
316 *Molecular Biology* **136**, 635-645,(2003).
- 317 9 Kang, C. K., Tsai, S. C., Lee, T. H. & Hwang, P. P. Differential expression of branchial
318 Na⁺/K⁺-ATPase of two medaka species, *Oryzias latipes* and *Oryzias dancena*, with
319 different salinity tolerances acclimated to fresh water, brackish water and seawater. *Comp*
320 *Biochem Physiol A Mol Integr Physiol* **151**, 566-575,(2008).

- 321 10 Sakamoto, T., Kozaka, T., Takahashi, A., Kawauchi, H. & Ando, M. Medaka (*Oryzias*
322 *latipes*) as a model for hypoosmoregulation of euryhaline fishes. *Aquaculture* **193**, 347-
323 354,(2001).
- 324 11 Ogoshi, M. *et al.* Growth, energetics and the cortisol-hepatic glucocorticoid receptor axis of
325 medaka (*Oryzias latipes*) in various salinities. *General and Comparative Endocrinology* **178**,
326 175-179,(2012).
- 327 12 Miya, M. *et al.* Major patterns of higher teleostean phylogenies: a new perspective based on
328 100 complete mitochondrial DNA sequences. *Mol Phylogenet Evol* **26**, 121-138,(2003).
- 329 13 Setiamarga, D. H. *et al.* Interrelationships of Atherinomorpha (medakas, flyingfishes,
330 killifishes, silversides, and their relatives): The first evidence based on whole mitogenome
331 sequences. *Mol Phylogenet Evol* **49**, 598-605,(2008).
- 332 14 Sinha, Y. N. & Gilligan, T. A. A Cleaved Form of Prolactin in the Mouse Pituitary Gland:
333 Identification and Comparison of in Vitro Synthesis and Release in Strains with High and
334 Low Incidences of Mammary Tumors*. *Endocrinology* **114**, 2046-2053,(1984).
- 335 15 Corbacho, A., Martinez De La Escalera, G. & Clapp, C. Roles of prolactin and related
336 members of the prolactin/growth hormone/placental lactogen family in angiogenesis. *Journal*
337 *of Endocrinology* **173**, 219-238,(2002).
- 338 16 Rentier-Delrue, F., Swennen, D., Prunet, P., Lion, M. & Martial, J. A. Tilapia Prolactin:
339 Molecular Cloning of Two cDNAs and Expression in *Escherichia coli*. *DNA* **8**, 261-
340 270,(1989).
- 341 17 Specker, J. L. *et al.* Isolation and partial characterization of a pair of prolactins released in
342 vitro by the pituitary of a cichlid fish, *Oreochromis mossambicus*. *Proceedings of the*
343 *National Academy of Sciences* **82**, 7490,(1985).
- 344 18 Yamaguchi, M. *et al.* Electron microscopy of hepatitis B virus core antigen expressing yeast
345 cells by freeze-substitution fixation. *Eur J Cell Biol* **47**, 138-143,(1988).
- 346 19 Kuwana, Y. *et al.* Cloning and Expression of cDNA for Salmon Prolactin in *Escherichia coli*.
347 *Agricultural and Biological Chemistry* **52**, 1033-1039,(1988).
- 348 20 Song, S. *et al.* Molecular cloning and expression of salmon prolactin cDNA. *European*
349 *journal of biochemistry* **172**, 279-285,(1988).
- 350 21 Soukup, S. W. Evolution by gene duplication. S. Ohno. Springer-Verlag, New York. 1970.
351 160 pp. *Teratology* **9**, 250-251,(1974).
- 352 22 Venkatesh, B. Evolution and diversity of fish genomes. *Current Opinion in Genetics &*
353 *Development* **13**, 588-592,(2003).
- 354 23 Volff, J. N. Genome evolution and biodiversity in teleost fish. *Heredity* **94**, 280-294,(2005).
- 355 24 Power, D. M. Developmental ontogeny of prolactin and its receptor in fish. *General and*
356 *Comparative Endocrinology* **142**, 25-33,(2005).
- 357 25 Huang, L. & Specker, J. L. Growth Hormone- and Prolactin-Producing Cells in the Pituitary
358 Gland of Striped Bass (*Morone saxatilis*): Immunocytochemical Characterization at Different
359 Life Stages. *General and Comparative Endocrinology* **94**, 225-236,(1994).
- 360 26 Siddique, K., Ager-Wick, E., Fontaine, R., Weltzien, F.-A. & Henkel, C. V. Characterization
361 of hormone-producing cell types in the teleost pituitary gland using single-cell RNA-seq.
362 *Scientific Data* **8**, 279,(2021).
- 363 27 García-Hernández, M. P., García-Ayala, A., Elbal, M. T. & Agulleiro, B. The
364 adenohypophysis of Mediterranean yellowtail, *Seriola dumerilii* (Risso, 1810): an
365 immunocytochemical study. *Tissue and Cell* **28**, 577-585,(1996).
- 366 28 Saga, T., Yamaki, K.-i., Doi, Y. & Yoshizuka, M. Chronological study of the appearance of
367 adenohypophysial cells in the ayu (*Plecoglossus altivelis*). *Anatomy and Embryology* **200**,
368 469-475,(1999).

- 369 29 Sánchez Cala, F., Portillo, A., Martín del Río, M. P. & Mancera, J. M. Immunocytochemical
370 characterization of adenohypophyseal cells in the greater weever fish (*Trachinus draco*).
371 *Tissue and Cell* **35**, 169-178,(2003).
- 372 30 Naito, N., Takahashi, A., Nakai, Y., Kawauchi, H. & Hirano, T. Immunocytochemical
373 identification of the prolactin-secreting cells in the teleost pituitary with an antiserum to chum
374 salmon prolactin. *General and Comparative Endocrinology* **50**, 282-291,(1983).
- 375 31 Breves, J. P., McCormick, S. D. & Karlstrom, R. O. Prolactin and teleost ionocytes: new
376 insights into cellular and molecular targets of prolactin in vertebrate epithelia. *General and*
377 *comparative endocrinology* **203**, 21-28,(2014).
- 378 32 Shu, Y. *et al.* The basal function of teleost prolactin as a key regulator on ion uptake
379 identified with zebrafish knockout models. *Scientific Reports* **6**, 18597,(2016).
- 380 33 Bloom, J. D. Estimating the frequency of multiplets in single-cell RNA sequencing from cell-
381 mixing experiments. *PeerJ* **6**, e5578,(2018).
- 382 34 Cheung, L. Y. M. *et al.* Single-Cell RNA Sequencing Reveals Novel Markers of Male
383 Pituitary Stem Cells and Hormone-Producing Cell Types. *Endocrinology* **159**, 3910-
384 3924,(2018).
- 385 35 Fontaine, R., Ager-Wick, E., Hodne, K. & Weltzien, F.-A. Plasticity of Lh cells caused by
386 cell proliferation and recruitment of existing cells. *Journal of Endocrinology* **240**, 361-
387 377,(2019).
- 388 36 Yada, T., Hirano, T. & Grau, E. G. Changes in Plasma Levels of the Two Prolactins and
389 Growth Hormone during Adaptation to Different Salinities in the Euryhaline Tilapia,
390 *Oreochromis mossambicus*. *General and Comparative Endocrinology* **93**, 214-223,(1994).
- 391 37 Shepherd, B. S. *et al.* Is the primitive regulation of pituitary prolactin (tPRL177 and
392 tPRL188) secretion and gene expression in the euryhaline tilapia (*Oreochromis mossambicus*)
393 hypothalamic or environmental? *Journal of Endocrinology* **161**, 121-129,(1999).
- 394 38 Lee, K. M., Kaneko, T. & Aida, K. Prolactin and prolactin receptor expressions in a marine
395 teleost, pufferfish *Takifugu rubripes*. *General and Comparative Endocrinology* **146**, 318-
396 328,(2006).
- 397 39 Liu, N.-A. *et al.* Prolactin Receptor Signaling Mediates the Osmotic Response of Embryonic
398 Zebrafish Lactotrophs. *Molecular Endocrinology* **20**, 871-880,(2006).
- 399 40 Fuentes, J., Brinca, L., Guerreiro, P. M. & Power, D. M. PRL and GH synthesis and release
400 from the sea bream (*Sparus auratus* L.) pituitary gland in vitro in response to osmotic
401 challenge. *General and Comparative Endocrinology* **168**, 95-102,(2010).
- 402 41 Sage, M. Responses to osmotic stimuli of Xiphophorus prolactin cells in organ culture.
403 *General and Comparative Endocrinology* **10**, 70-74,(1968).
- 404 42 Seale, A. P., Watanabe, S. & Grau, E. G. Osmoreception: Perspectives on signal transduction
405 and environmental modulation. *General and Comparative Endocrinology* **176**, 354-
406 360,(2012).
- 407 43 Kwong, A. K. Y., Ng, A. H. Y., Leung, L. Y., Man, A. K. Y. & Woo, N. Y. S. Effect of
408 extracellular osmolality and ionic levels on pituitary prolactin release in euryhaline silver sea
409 bream (*Sparus sarba*). *General and Comparative Endocrinology* **160**, 67-75,(2009).
- 410 44 Satija, R., Farrell, J. A., Gennert, D., Schier, A. F. & Regev, A. Spatial reconstruction of
411 single-cell gene expression data. *Nature Biotechnology* **33**, 495-502,(2015).
- 412 45 Fontaine, R. *et al.* Dopamine inhibits reproduction in female zebrafish (*Danio rerio*) via three
413 pituitary D2 receptor subtypes. *Endocrinology* **154**, 807-818,(2013).
- 414 46 Royan, M. R. *et al.* 3D Atlas of the Pituitary Gland of the Model Fish Medaka (*Oryzias*
415 *latipes*). *Frontiers in Endocrinology* **12**,(2021).

416 47 Fontaine, R. & Weltzien, F.-A. Labeling of Blood Vessels in the Teleost Brain and Pituitary
417 Using Cardiac Perfusion with a Dil-fixative. *Journal of Visualized Experiments*,
418 e59768,(2019).
419

420 **Figure. legends**

421
422 **Fig. 1: *prl* gene expression.** Shown are the *prl* gene expression at UMAP level in female (left panel,
423 A), in male (left panel, B), and merged (left panel, C); and in violin plot in female (right panel, A) and
424 in male (right panel, B). C, right panel represents the top 10 differentially expressed genes in female
425 and male. Yellow represents high expression and purple represents low expression. Cell cluster numbers
426 refers to our original scRNA-seq classifications: 3 for the ‘primary’ lactotropes, and 4 for the
427 ‘secondary’ population.

428
429 **Fig. 1: Characterization of four clusters.** (A) describes the differentially expressed genes in merged
430 scRNA-seq data in four clusters. The red text indicates the expression of *prl*, *sox2*, and *mala* in all
431 clusters (B) represents the expression levels of *sox2*, *mala* and *pit1* in UMAP dimension.

432
433 **Fig. 2: Transcriptomic profiles.** (A) Boxplots showing the number of genes detected per four cell
434 types in merged dataset. Boxes correspond to the interquartile range (IQR), whiskers indicate $1.5 \times$ the
435 IQR. (B) Boxplots showing the number of reads detected per four cell population for merged dataset.

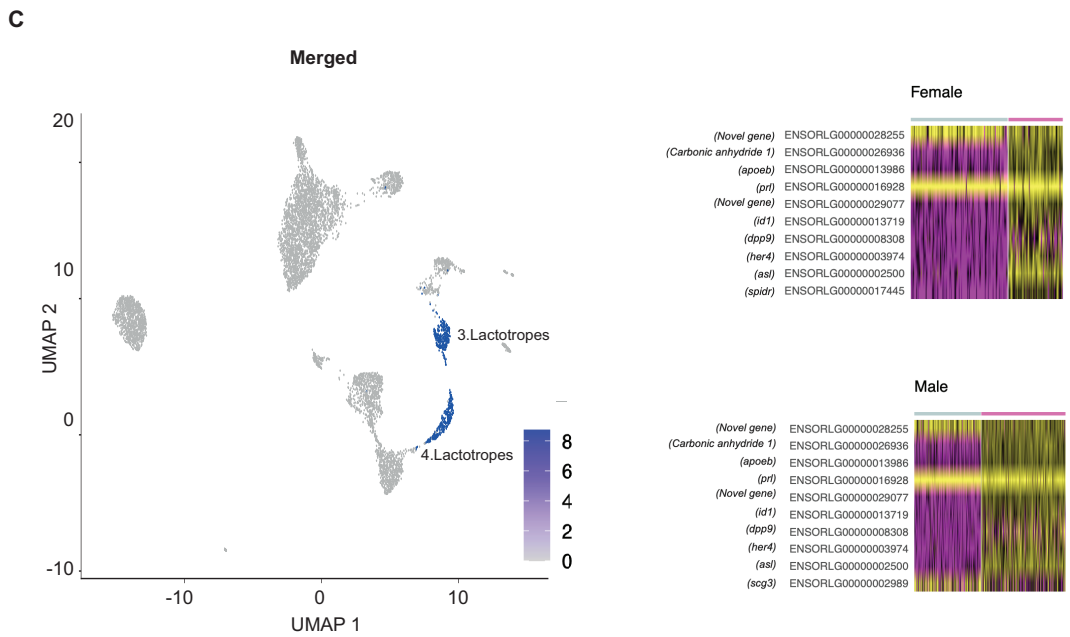
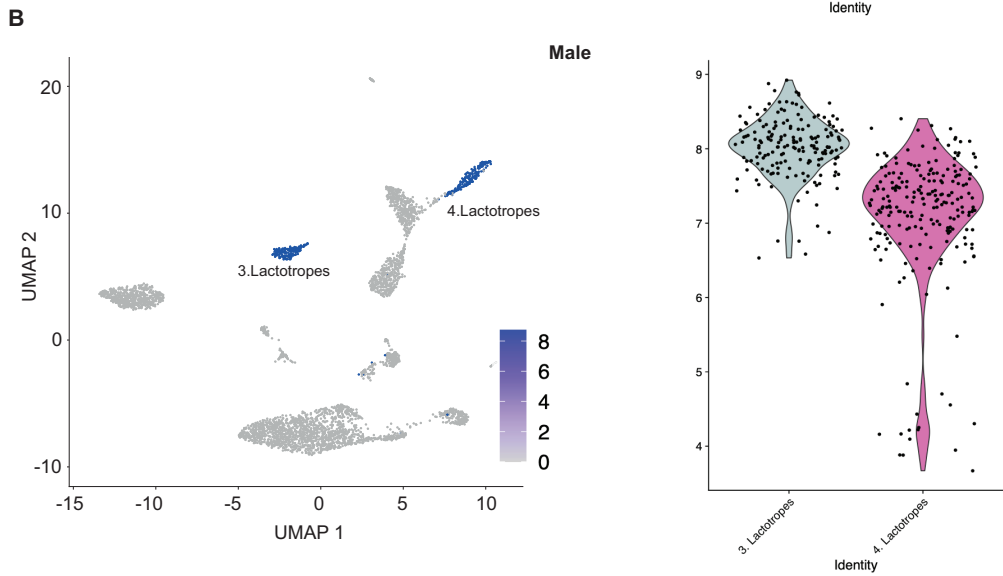
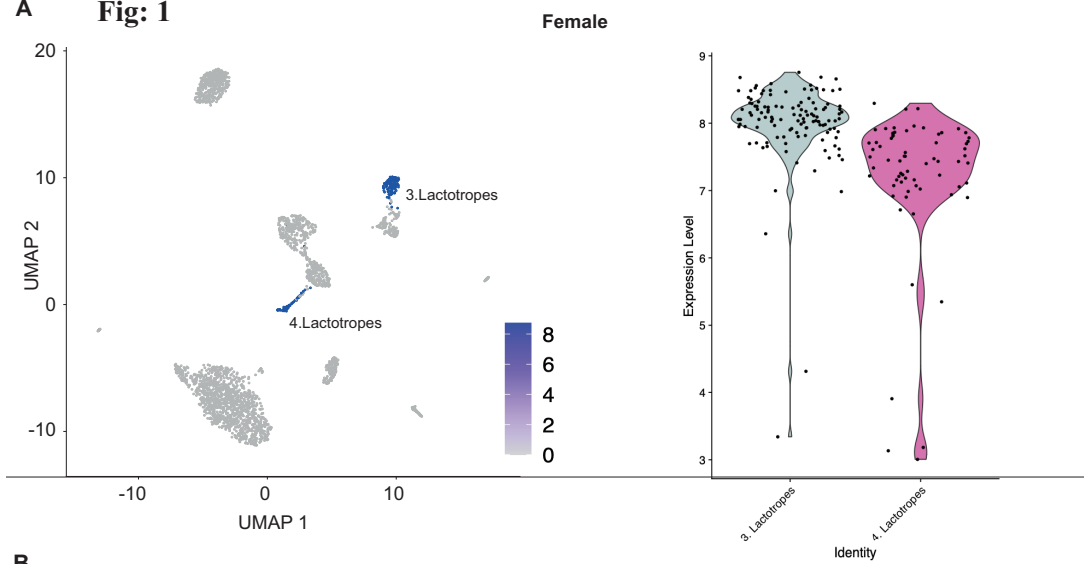
436 **Fig. 3: *In situ* images:** (A) shows the fluorescent *in situ* hybridization images for *prl* expression. Green
437 circles indicate the presence of Prl-populations in two different regions of the medaka pituitary. (B) bar
438 plots represent the percentages of non-RPD Prl cells in the different stages of development of the
439 medaka pituitary. (C) represents the *prl* and *mala* co-expression in the adult medaka pituitary (D)
440 represents the *prl* and *sox2* co-expression in the adult medaka pituitary. (E) shows the co-expression of
441 *prl* and *sox2*.

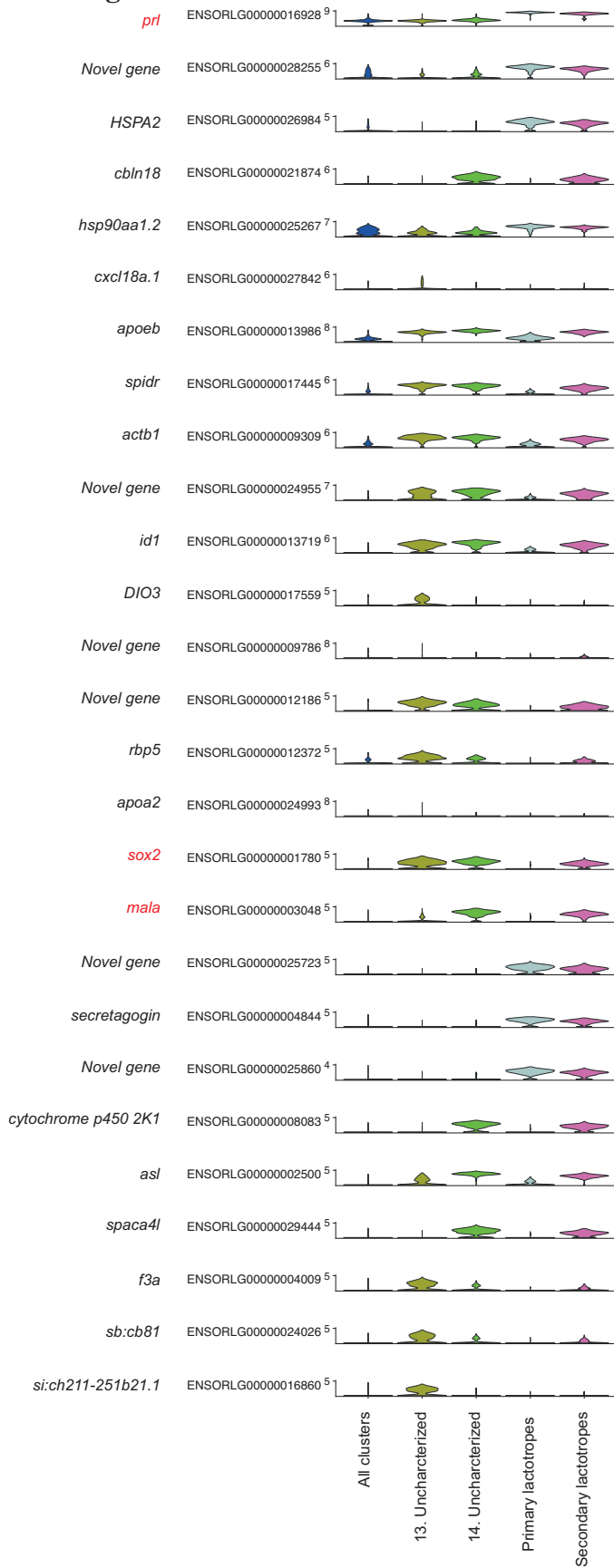
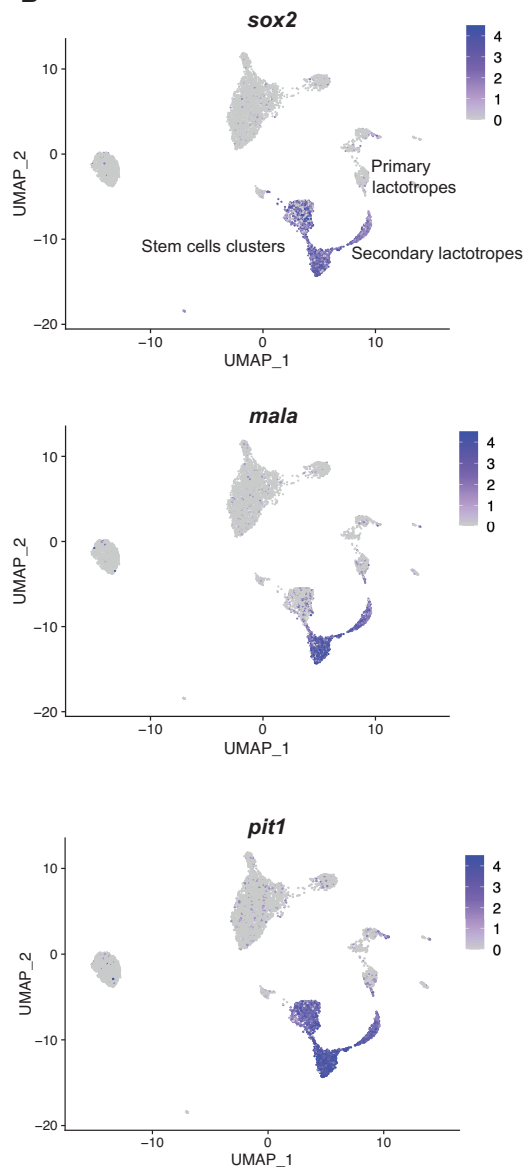
442 **Funding**

444 This study was funded by the Norwegian University of Life Sciences (to RF) and the Norwegian
445 Research Council grants No. 251307, 255601, and 248828 (to FAW).
446

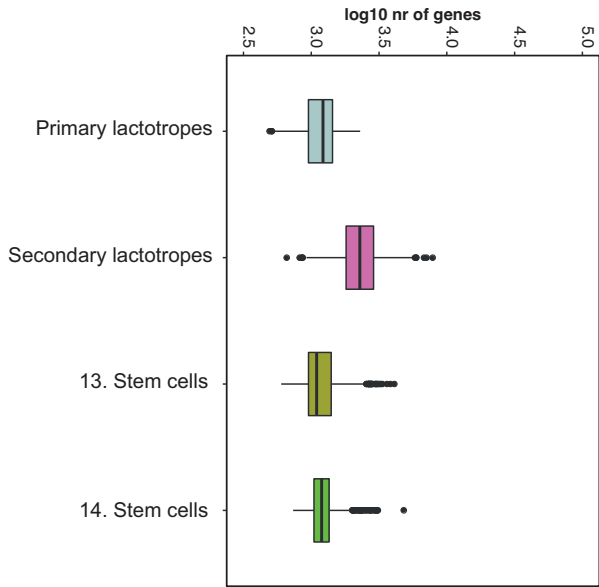
447 **Acknowledgments**

448 The authors are grateful Anthony Peltier and Lourdes Carreon G Tan for fish facility maintenance
449 during the experiments.
450

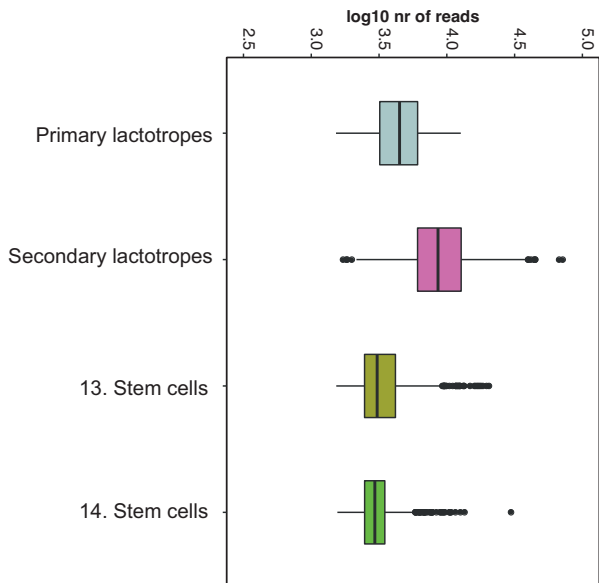
Fig: 1

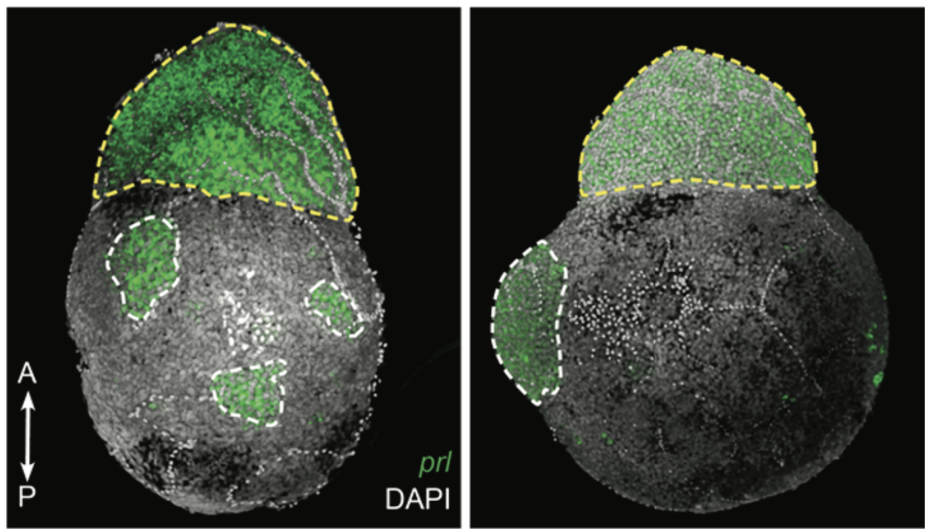
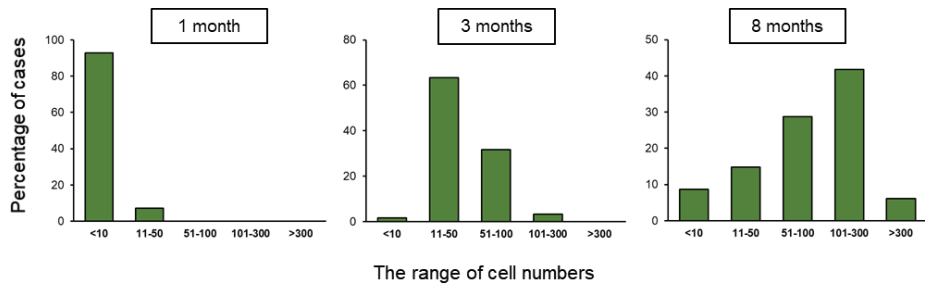
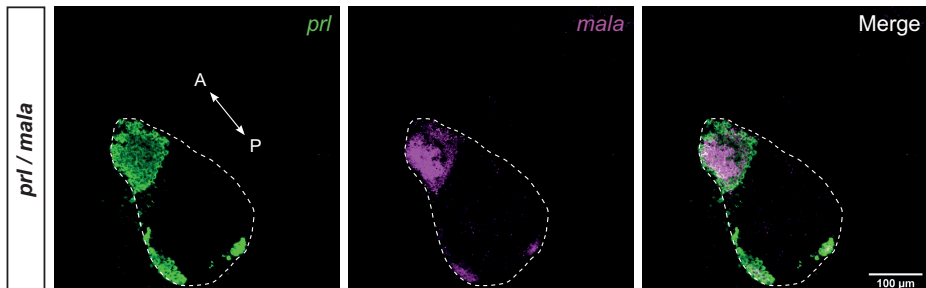
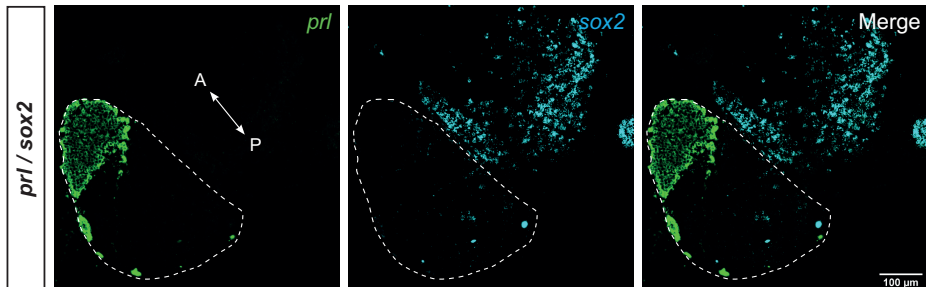
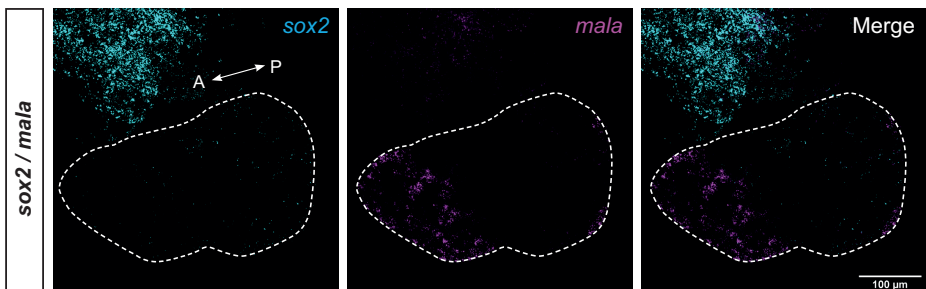
A Fig: 2**B**

A **Fig: 3**



B



A**B****C****D****E****Fig: 4**

ISBN: 978-82-575-1895-0

ISSN: 1894-6402



Norwegian University
of Life Sciences

Postboks 5003
NO-1432 Ås, Norway
+47 67 23 00 00
www.nmbu.no